NOTE TO USER

The original manuscript received by UMI contained pages with broken print. All efforts were made to acquire the highest quality manuscript from the author or school. The manuscript was microfilmed as received.

Pages 34, 35, & 36

This reproduction is the best copy available.

UMI

UNIVERSITY OF ALBRETA

GEOCHEMICAL ASPECTS OF CRUSTAL ACCRETION IN ICELAND

BY

BJARNI GAUTASON ©

A thesis submitted to the Faculty of Graduate Studies and Research in partial fulfillment of the requirements for the degree of Doctor of Philosophy.

DEPARTMENT OF EARTH AND ATMOSPHERIC SCIENCES

Edmonton, Alberta

Fall 2000

National Library of Canada
Acquisitions and Bibliographic Services
395 Wellington Street
Ottawa ON K1A 0N4
Canada

Bibliothèque nationale du Canada
Acquisitions et services bibliographiques
395, rue Wellington
Ottawa ON K1A 0N4
Canada

Your file Votre référence

Our file Notre référence

The author has granted a non-exclusive licence allowing the National Library of Canada to reproduce, loan, distribute or sell copies of this thesis in microform, paper or electronic formats.

L'auteur a accordé une licence non exclusive permettant à la Bibliothèque nationale du Canada de reproduire, prêter, distribuer ou vendre des copies de cette thèse sous la forme de microfiche/film, de reproduction sur papier ou sur format électronique.

The author retains ownership of the copyright in this thesis. Neither the thesis nor substantial extracts from it may be printed or otherwise reproduced without the author's permission.

L'auteur conserve la propriété du droit d'auteur qui protège cette thèse. Ni la thèse ni des extraits substantiels de celle-ci ne doivent être imprimés ou autrement reproduits sans son autorisation.

0-612-59591-9

Canada

UNIVERSITY OF ALBERTA
LIBRARY RELEASE FORM

NAME OF AUTHOR: Bjarni Gautason

TITLE OF THESIS: Geochemical Aspects of Crustal Accretion in Iceland

DEGREE: Doctor of Philosophy

YEAR THIS DEGREE GRANTED: 2000

Permission is hereby granted to the University of Alberta Library to reproduce single copies of this thesis and to lend or sell such copies for private, scholarly or scientific research purposes only.

The author reserves all other publication and other rights in association with the copyright in the thesis, and except as hereinbefore provided neither the thesis nor any substantial portion thereof may be printed or otherwise reproduced in any material form whatever without the author's prior written permission.

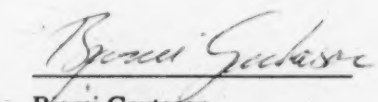

Bjarni Gautason
Grundargerdi 6E, 600 Akureyri
ICELAND

Date: Aug 6, 2000

University Of Alberta

Faculty of Graduate Studies and Research

The undersigned certify that they have read, and recommend to the Faculty of Graduate Studies and Research for acceptance a thesis entitled *Geochemical Aspects of Crustal Accretion in Iceland* submitted by Bjarni Gautason in partial fulfillment of the requirements for the degree of Doctor of Philosophy

K. Muehlenbachs – Supervisor

T. Chacko

R. A. Creaser

M. R. Gray

R. W. Luth

H. Sigurdsson – External Examiner

Date: Oct 2, 2000

ABSTRACT

The low-^{18}O lavas of Iceland provide a unique window into crustal accretion processes at a rifting plate boundary. In this locality reactions between surface-derived fluids, juvenile crust and mantle-derived magmas result in the magmas acquiring a fingerprint of the precipitation, even though the magmas themselves contain little water. A significant flux of ^{18}O to the hydrosphere results from these reactions. Calculations reveal that the rift zones in Iceland are efficient in transferring ^{18}O to the hydrosphere, releasing up to five times the amount of ^{18}O as does an equivalent length of mid-ocean ridge.

I argue that most of the depleted ^{18}O-signature is a result of exchange processes (including solution-recrystallization) operating in the crust. A model of isotopic exchange between magma and crust in a magma mush reservoir in the deep crust is proposed. Oxygen transfer to the magma is efficient due to a large surface area between crust and magma. The model specifically suggests that surface-derived fluids infiltrate the lower crust (> 8 km) during "amagmatic periods."

I also suggest that the most magnesian lavas (MgO > 8 wt. %) may have reacted with an ^{18}O-depleted component in the mantle. This is supported by data on mineral separates from Tertiary lavas associated with the Iceland mantle plume. The parental magmas were depleted in ^{18}O relative to the common mid-ocean ridge basalts, suggesting that the mantle plume contains a ^{18}O-depleted component.

ABSTRACT (CONTINUED)

On the basis of textural evidence and trace major- and trace-element data, I propose that melt-mantle reactions played a role in the generation of the Dagmálafell picrite. Apparently incompatible element enriched and depleted magmas are closely associated at some point in their evolution, and may be in a genetic relationship. Abundant evidence for melt-rock reaction provides a possible link between enriched and depleted melts. I hypothesize that Icelandic picrites are derived from enriched (E-MORB like) high-MgO basalts through melt-rock reactions.

ACKNOWLEDGMENTS

First and foremost, very warm thanks to my wife, Thorbjorg, and our three children for their loving support over the years. Thanks also to my parents for their constant encouragement.

A very deep thank you to my supervisor Karlis Muehlenbachs for his enthusiasm, support and patience. I am grateful also to the Muehlenbachs family for their friendship and encouragement.

During my Doctoral studies I have come to know and work with a large number of people, this is one of the big upsides of graduate work and academic life. I'd like to thank my fellow graduate students who overlapped with me at the U of A. Special thanks to fellow isotope- and coffee enthusiasts Paul Blanchon, Al Brandon, Suman De, James Farquhar, Chris Holmden, Ted Little, Devon Rowe, James Steer, Serguey Arkadakskiy, Steve Talman and Taro Yamashita. Thanks also to the many good friends and neighbors from Michener Park and the Malmo area.

Sincere thanks to the members of my advisory- and defense committees Tom Chacko, Robert A. Creaser, Murray Gray, Robert Luth, and Haraldur Sigurdsson, for careful reviews and many helpful comments at various stages of this work.

In Iceland, very warm thanks to my good friend Astthor Johannsson for being my field companion in Iceland. Thanks also to Arnthor Bjarnason, Gauti Arnthorsson, Björn Bjarnason and Ingvar Atli Sigurdsson, who helped in various ways with fieldwork. Thanks to Sveinn Jakobsson and Haukur Jóhannesson at the Museum of Natural History for supplying samples. Thanks to Vigdis Hardardottir, Martin Heinesen, Regin Waagstein and Reidar Trönnes who also helped with obtaining samples.

Thanks to U of A technical staff members George Braybrook, Olga Levner, Lang Shi and Paul Wagner and non-academic staff Anette Bell, Judith Enarson and Sherry Gobeil for their generous help.

TABLE OF CONTENTS

Chapter 1.

Introduction

1.1 Mantle Derived Magmas, Crustal Fluids and Country Rocks p. 1
1.2 A Note on Standards 3
1.3 References 5

Chapter 2.

Oxygen Isotope Ratios of Silicate and Oxide Minerals in Tertiary Basalts from the Faeroe Islands and NW-Iceland: Evidence for an Anomalous Component in the Mantle

2.1 Introduction 6
2.2 A note on Geology 8
2.3 Analytical Methods 9
2.4 Results 8
2.5 Discussion 11
2.6 Conclusions 12
2.7 References 14

Chapter 3.

Oxygen Isotope Systematics in Gabbro-Nodules and Volcanic Glasses from the Western Rift-Zone in SW-Iceland. Implications for Fluid Infiltration into the Deep Crust

3.1 Introduction 22
3.2 Analytical Techniques 23
3.3. Results 24
3.3.1 $\delta^{18}O$ of Gabbro Nodules 25
3.3.2 $\delta^{18}O$ of Hengill Area Volcanics 26
3.3.3 Petrography of Nodules 27
3.3.4 Chemical Composition of Nodule 28

TABLE OF CONTENTS (CONTINUED)

3.3.5 Unusual Nodules 29
3.4 Discussion 30
3.4.1 Depth of Origin 30
3.4.2 Implications of the $\delta^{18}O$ Systematics 31
3.4.3 Regional Systematics 32
3.4.4 Towards a New Model 33
3.4.5 Mantle Processes 34
3.5 Conclusions 35
3.6 References 37

Chapter 4.
Oxygen Isotopic Fluxes Associated With High Temperature Processes in the Rift Zones of Iceland
4.1 Introduction 52
4.2 Geologic Setting 53
4.3 ^{18}O-Flux Through the Rift Zones 54
4.4 Oxygen Isotopic Composition of the Icelandic Crust. 55
4.4.1 Unaltered Crust 55
4.4.2 Hydrothermally Altered Crust 56
4.4.3 The Lower Crust 58
4.4.5 Oxygen Isotopic Composition of The Mantle Source 59
4.5 Model Results 60
4.6 Comparison to Oceanic Rifts 61
4.7 Discussion. 62
4.7.1 ^{18}O of Seawater 63
4.7.2 Low ^{18}O Magmas 64
4.8 Conclusions 65
4.9 References 66

TABLE OF CONTENTS (CONTINUED)

Chapter 5.

Melt-Mantle Reactions as a Possible Link Between Enriched and Depleted Mafic Melts: Evidence from Reaction Textures and Trace-Element Concentrations in Clinopyroxene Bearing Nodules and Megacrysts in the Dagmálafell Picrite, SW Iceland

5.1 Introduction 75

5.2 Occurrence, Texture and Mineralogy of the Micro-Nodules, Megacrysts and Gabbro-Nodules 77

5.3 Major and trace Element Chemistry 79

5.3.1 Clinopyroxene 79

5.3.2 Cr-Spinel 80

5.3.3 Plagioclase and Olivine 81

5.4 Melt-Rock Reaction and the Origin of the Dagmálafell Picrite 82

5.4.1 Textural Evidence for Melt-Rock Reaction 82

5.4.2 Trace Elements in Clinopyroxene: Implications for Magma Composition 83

5.4.2 Major Element Variation in Cr-Spinel 84

5.4.4 Melts: Bulk Samples and Glass Inclusions Revisited. 85

5.4.5 Modeling Melt-Rock Reactions 86

5.4.6 Melt Mantle Reaction: What is Known What is Not 87

5.5 High-MgO Basalts from the Rift Zones 88

5.5.1 Relationship Between Magma Volume, Incompatible Element Variation and Spatio-Temporal Factors. 90

5.5.2 Melt Rock Reaction and Nd Isotope Ratios 92

5.5.3 Effect on Mineral-Liquid Equilibria 93

5.5.4 High MgO Basalts: Major Element Variations 94

5.6 Summary 96

5.7 References 97

TABLE OF CONTENTS (CONTINUED)

Chapter 6.
Thesis Conclusions
6.1 Summary 122
6.2 Future Research Projects 122
6.3 Final Speculative Remarks 123
6.4 References 124

Appendices
Appendix A (127-146)

List Of Tables

2-1. Chemical composition of olivine from Faeroese basalts p. 17

2-2. $\delta^{18}O$ values of minerals separated from Faeroese and Icelandic basalts 18

2-3. Major element composition of olivine in Faeroese basalts 19

3-1. $\delta^{18}O$ values of consituent minerals in gabbro nodules 42

3-2. $\delta^{18}O$ values of volcanic glasses and whole rocks from Hengill region 43

4-1. Summary of flux calculations 71

5-1. Major element composition of clinopyroxene from the Dagmálafell picrite 102

5-2. Cation proportions in clinopyroxene from the Dagmálafell picrite 103

5-3. Rare-Earth element abundances in clinopyroxene from the Dagmálafell picrite 104

5-4. Trace element abundances in clinopyroxene from the Dagmálafell picrite 105

5-5. Composition of pillow rim glass from the Dagmálafell picrite 106

A-I. Composition of clinopyroxene from gabbro nodules 128

A-II. Composition of olivine from gabbro nodules 133

A-III. Composition of plagioclase from gabbro nodules 134

A-IV. Composition of Cr-spinel from Dagmálafell 137

A-V. Composition of Cr-spinel from Dagmálafell micronodules 145

List Of Figures

2-1. $\delta^{18}O$ values of minerals from Faeroese and Icelandic basalts p. 21

3-1. Location map showing gabbro nodule localities 44

3-2. Histogram of $\delta^{18}O$ values of minerals from gabbro nodules 45

3-3. $\delta^{18}O$ values of coexisting plagioclase and clinopyroxene 46

3-4. $\delta^{18}O$ values of volcanic glasses from Hengill area 47

3-5. Mg# -range in clinopyroxene in nodules vs. MgO content of host lava 48

3-6. TiO_2 versus Mg# in clinopyroxene 49

3-7. Cr_2O_3 versus Mg# in clinopyroxene 50

3-8. Comparison of $\delta^{18}O$ values of basalts from Hengill and Krafla area 51

4-1. Schematic map outlining the volcanic zones in Iceland 72

4-2. Cartoon illustrating model used for estimating ^{18}O fluxes in the rift zones 73

4-3. Histogram of $\delta^{18}O$ values of lavas from the Icelandic roft zones 74

5-1. Backscatter-image of micronodule and associated reaction textures 107

5-2. REE patterns of clinopyroxenes occuring in Dagmálafell picrite 108

5-3. La/Sm vs. Sm normalised values of clinopyroxenes from Dagmálafell 109

5-4. Ti vs. Zr content of clinopyroxenes from Dagmálafell 110

5-5. TiO_2 vs. Cr# in Cr-spinel from Dagmálafell 111

5-6. REE abundances of model magmas compared to natural magmas 112

5-7. Variation in Cr-spinel chemistry in Dagmálafell compared to Cr-spinel in an enriched lava and gabbroic selvages in mantle harzburgites 113

5-8. A and B: Comparison of melts produced by magma mixing and fractional melting to natural variation observed in glass inclusions and bulk samples in Ti/Zr vs. $(La/Sm)_N$ space 114

LIST OF FIGURES (Continued)

5-9. Comparison of REE abundances in natural magmas to model magmas 116

5-10. Relationship between volume and trace element abundance ratios for lavas and olivine hosted glass inclusions 118

5-11. $^{143}Nd/^{144}Nd$ values plotted against 10/La abundance for high MgO lavas in the rift zones 119

5-12. A, B and C: Harker diagrams showing TiO_2, FeO and CaO/Al_2O_3 respectively vs. MgO 120

Chapter 1

THESIS INTRODUCTION

1.1 Mantle-Derived Magmas, Crustal Fluids and Country Rocks.

This thesis is the culmination of several years of research, driven primarily by the author's desire to understand better the interplay between mantle-derived magmas, crustal fluids and the enveloping crust in a rifting environment. A starting point is the fundamental observation that basaltic magmas from the Icelandic rift zones are depleted in ^{18}O relative to basaltic magmas in other rifting environments (Muehlenbachs et al., 1974). This anomaly is generally considered to be linked to the ^{18}O-depleted local precipitation, which also is the fluid source of most high-temperature geothermal systems. However, the exact mechanism of transferring O from fluid to magma is poorly understood. Several mechanisms have been proposed in the literature. They include: 1) Assimilation-Fractional-Crystallization where the latent heat of crystallization allows a mafic magma to assimilate hydrothermally altered crust. 2) Mixing of mantle-derived magmas with hydrous silicic magmas formed by fusion of the hydrothermally altered crust. 3) Isotopic exchange between country rock and magma. 4) Isotopic exchange between fluids and magma (without hydration). The lack of consensus on this issue points to a lack of understanding. Any study that sheds some light on this process in Iceland also promises to increase our understanding of the general process of crust formation in a rifting environment.

This thesis follows the "paper format" meaning that each of the subsequent chapters represents an independent scientific contribution. Of the following four chapters, one (Chapter 4) has already been published and the other three (Chapters 2, 3 and 5) will be submitted at a later date.

In Chapter 2, oxygen isotope data from whole rocks and mineral separates from basalts in NW Iceland and the Faeroe Islands are presented. The data are taken to indicate that basalts derived from the Iceland mantle plume in early and late Tertiary times were slightly depleted in ^{18}O relative to common Mid-Ocean-Ridge basalts. This data is consistent with a small contribution ($\approx$ 0.5‰) to the ^{18}O anomaly from a component in the mantle. It is proposed that this component may be recycled oceanic crust contained within

the Iceland mantle plume. Several investigators have suggested similar models for other plumes based on stable- and radiogenic isotope data and/or major- and trace-element data.

In Chapter 3, oxygen isotope and major-element data on gabbro nodules, their constituent minerals and a set of roughly coeval magmas from the rift zone in SW Iceland are presented. In light of this data, comparisons with previous studies, and the regional distribution of the ^{18}O anomaly a number of inferences may be made. The isotopic fractionation between plagioclase and clinopyroxene in a number of nodules indicates that they were exposed to and exchanged oxygen with an external reservoir. This exchange probably took place at very high temperatures (>700°C). The lack of retrograde hydrated phases argues against interaction with hydrothermal fluids in the fluid dominated shallow (<3km) high temperature (200-400°C) geothermal systems. The regional distribution of the ^{18}O anomaly correlates broadly with the large scale hydraulic features of the volcanic zones. It is an indication that recharge during magmatism is necessary to maintain the anomaly. Otherwise the flux of ^{18}O from the mantle quickly exhausts the ^{18}O anomaly in the crust. It is argued that magma mush reservoirs, similar to those inferred to exist in the mid-ocean ridge crust, also exist in the deep Icelandic crust. If this is the case, a key characteristic of these mush zones is the very large surface area between magma and crust. In such a reservoir exchange processes are very effective at modifying the isotopic composition of the magma. The exchange of oxygen between magma and crust could be greatly enhanced if the rise of magma through this mush zone is aided by a dissolution-reprecipitation process. It is proposed that during amagmatic periods some porosity is maintained in this mush zone allowing fluids to infiltrate and exchange oxygen with the crust.

In Chapter 4 the published oxygen isotope data on Icelandic lavas are summarized. This summary allows estimates to be placed on the average isotopic composition of the crust. In turn, these estimates allow constraints to be placed on the flux of ^{18}O from the mantle through the rift zone to the hydrosphere. This flux is compared to equivalent high temperature fluxes on the mid ocean ridges. The results have implications for models dealing with the ^{18}O history of seawater through time.

Chapter 5 is an outgrowth of Chapter 3 in that it is initiated by the discovery of some unusual nodules in one of the picrites sampled in relation to the study in Chapter 3. Textural relationships in this picrite, major element variation in Cr-spinel and REE and trace element variation in diopside is interpreted in terms of a melt-rock reaction model. It is suggested that an initially REE enriched magma reacts with a clinopyroxene-bearing lithology resulting in the production of a magma depleted in REE abundances. It is

tempting to suggest that this clinopyroxene-bearing lithology is the "eclogitic component" proposed to exist in the plume in Chapter 2. However, the evidence at the present time does not allow such an inference to be made with confidence.

This thesis is in a broad sense concerned with the process of building oceanic crust (albeit a very thick one) in a rifting environment. All of the Recent and late Quaternary samples come from the rift zone in SW-Iceland. There the rift has been in "steady state" rift production for the last 7 Ma. This implies that any solid material brought to the surface must be related to the general process of crust production, regardless of its relationship to the immediate host lava (i.e. pheno-, auto-, xenocryst).

1.2 A Note on Standards

The ratios of light stable isotopes in geological materials are reported in the δ notation. δ was originally defined by McKinney et al. (1953) as follows:

$$\delta_{A\text{-}B}\ (‰) = (R_A/R_B - 1) \times 10^3 \quad (1\text{-}1)$$

R denotes the $^{18}O/^{16}O$ ratio and subscripts A and B refer to phases A and B. δ is customarily reported in units of per mille (‰).

In practice the δ value of some sample X is measured relative to an in house working standard (WS). From the definition above it is clear that:

$$\delta_{X\text{-}WS} = (R_X/R_{WS} - 1) \times 10^3 \quad (1\text{-}2)$$

where R_X and R_{WS} are the $^{18}O/^{16}O$ ratios of the sample and working standard respectively. It is customary to report the oxygen isotopic composition of minerals and rocks relative to the international reference standard SMOW (Standard Mean Ocean Water) originally defined by Craig (1961). Again, $\delta_{X\text{-}SMOW}$ should satisfy the relationship:

$$\delta_{X\text{-}SMOW} = (R_X/R_{SMOW} - 1) \times 10^3 \quad (1\text{-}3)$$

Isolating R_X in (2) and substituting into (3):

$$(\delta_{X\text{-}WS}/10^3 + 1) \times R_{WS} = (\delta_{X\text{-}SMOW}/10^3 + 1) \times R_{SMOW}$$

$$(\delta_{X\text{-}WS}/10^3 + 1) \times R_{WS}/R_{SMOW} = \delta_{X\text{-}SMOW}/10^3 + 1$$

$$(\delta_{X\text{-}WS}/10^3 \times R_{WS}/R_{SMOW} + R_{WS}/R_{SMOW} - 1) \times 10^3 = \delta_{X\text{-}SMOW}$$

$$\delta_{X\text{-}SMOW} = \delta_{X\text{-}WS} \times R_{WS}/R_{SMOW} + (R_{WS}/R_{SMOW} - 1) \times 10^3 \qquad (1\text{-}4)$$

The second term is by definition equal to $\delta_{WS\text{-}SMOW}$ and recalling the definition of $\alpha = R_A/R_B$ (which may also be written as $\alpha_{A\text{-}B} = \delta_{A\text{-}B}/10^3 + 1$). We can rewrite (4) as follows:

$$\delta_{X\text{-}SMOW} = \delta_{X\text{-}WS} \times \alpha_{WS\text{-}SMOW} + \delta_{WS\text{-}SMOW} \qquad (1\text{-}5)$$

This is an equation of a straight line on a plot of $\delta_{X\text{-}WS}$ versus $\delta_{X\text{-}SMOW}$. Equation (1-5) may be manipulated to give Equation (1-3) again.

To calibrate the Oz Tech 427 working gas a small amount of CO_2 gas was equilibrated with water (O'Neil and Epstein 1966) standards SLAP and SMOW (reference material RM). After correcting for small amounts of ^{18}O in the added CO_2 and correcting for the fractionation between water and CO_2 ($\alpha_{CO2\text{-}H2O} = 1.0407$ Compston and Epstein, 1958) $\delta_{RM\text{-}Oz}$ was plotted versus $\delta_{RM\text{-}SMOW}$, the recommended values for SLAP (= -55.5‰) and SMOW (=0‰). An equation of the form of Equation (5) was obtained, with the goal of minimizing, by trial and error, the sum of differences squared (($\delta_{RM\text{-}SMOW}$ (measured) – $\delta_{RM\text{-}SMOW}$ (defined))^2) for the reference materials

It is important to note that the CO_2 -H_2O fractionation factor used is 1.0407 rather than the now commonly used 1.0412. This is done to ensure that the reported δ values are comparable to the early work on Iceland (Muehlenbachs et al. 1974) and Mid-Ocean Ridge basalts (Muehlenbachs and Clayton, 1972).

1.3 References

Compston, W., Epstein, S., 1958. A method for the preparation of carbon dioxide from water vapor for oxygen isotope analysis. Trans. Am. Geophys. Un. 39, 511-512.

Craig, H., 1961. Standard for reporting concentrations of deuterium and oxygen-18 in natural waters. Science 133, 1833-1834.

McKinney, C. R., McCrea, J. M., Epstein, S., Allen, H. A., Urey, H. C., 1950. Improvements in mass spectrometers for the measurement of small differences in isotope abundance ratios. Rev. Sci. Instrum. 21, 724-730.

Muehlenbachs, K., Clayton, R. N., 1972. Oxygen isotope studies of fresh and weathered submarine basalts. Can. J. Earth Sci. 9, 172-184.

Muehlenbachs, K., Anderson, A. T., Sigvaldason, G. E., 1974. Low-O^{18} basalts from Iceland. Geochim. Cosmochim. Acta 38, 577-588.

O'Neil, J. R., Epstein, S., 1966. Method for oxygen isotope analysis of milligram quantities of water and some of its applications. J. Geophys. Res. 71, 4955-4961.

Chapter 2

OXYGEN ISOTOPE RATIOS OF SILICATE AND OXIDE MINERALS IN TERTIARY BASALTS FROM THE FAEROE ISLANDS AND NW-ICELAND: EVIDENCE FOR AN ANOMALOUS COMPONENT IN THE MANTLE.[1)]

2.1 Introduction

Tracer studies employing radioactive isotopes and their daughter nuclides in oceanic basalts provide strong evidence for a geochemically heterogeneous mantle. The origins of isotopic heterogeneity in the mantle are in many instances related to elemental fractionations associated with past melting episodes, i.e. a residual mantle or recycling of crustal material back into the mantle (e.g. Zindler and Hart, 1986). Confirmation of the return of subducted material to the Earth's surface has been sought utilizing oxygen isotope data. This stems from the influence of hydrosphere-crust interactions at the Earth's surface on the oxygen isotopic ratio ($\delta^{18}O$) of crustal rocks. These interactions (e.g. weathering, hydrothermal alteration) can lead to a significant increase or decrease in the $\delta^{18}O$ value of the crust relative to the $\delta^{18}O$ of the mantle (see below). Oxygen is a major element constituting 45 to 50% (wt.) of most silicate minerals, therefore the surface isotopic signature in subducted crust may prevail for long periods of time after subduction. As a case in point, oxygen isotope data demonstrate that many eclogite nodules, brought to the surface in kimberlites, are fragments of subducted oceanic crust (Garlick et al., 1971; McGregor and Manton, 1984; Jacob et al., 1994). Similarly, some workers have, on the basis of oxygen isotope data, suggested that basaltic magmas were derived from mantle sources containing recycled crust (Cartwright and Valley, 1991;

1) A version of this chapter will be submitted to a peer reviewed journal for consideration, with Dr. K. Muehlenbachs as second author.

Woodhead et al., 1991). However, interactions between magma and crust during emplacement and evolution of magma in the lithosphere have also been invoked (Eiler et al., 1995, 1996; Thirwall et al., 1997; Garcia et al., 1998).

The homogeneity of the MORB source with respect to its oxygen isotopic composition ($\delta^{18}O$ = 5.7±0.3‰ SMOW) is well established (Muehlenbachs and Clayton 1972; Pineau et al., 1976; Ito et al., 1988). Lunar basalts are identical in their oxygen isotopic composition to MORB´s and this observation points to the existence of a large homogeneous reservoir early in Earth's history (Clayton et al., 1973). As mentioned before, deviation from this mantle value in crustal rocks is related to interaction with the hydrosphere (e.g. weathering and hydrothermal alterations). For example, seawater-rock interaction at Mid-Ocean Ridges leads either to an enrichment in ^{18}O in the upper part (≈ Layer 2) of the oceanic crust or a depletion in ^{18}O in the lower part the crust (≈ Layer 3) (Muehlenbachs and Clayton, 1976; Gregory and Taylor, 1981). Consequently, subduction and delamination of oceanic crust could lead to the development of reservoirs with anomalous $\delta^{18}O$ (Cartwright and Valley, 1991).

The mantle $\delta^{18}O$ for a particular basalt province may be difficult to establish, because of magma-lithosphere interaction. This is particularly true for the Iceland mantle plume and its present-day products. Holocene basalts in Iceland are anomalously low in $\delta^{18}O$ when compared to MORBs (Muehlenbachs et al., 1974)). The origin of this isotopic signature has been linked to assimilation and/or exchange processes in the crust (e.g. Óskarson et al., 1982; Condomines et al., 1983; Hémond et al., 1988 and others). The magma may inherit it´s low ^{18}O-signature from the hydrothermally altered and depleted crust. Thus it is a formidable challenge to look beyond this veil of hydrothermal alteration and determine the primary mantle signature.

In this paper we present oxygen isotope data on mineral separates and host rocks, from the Paleocene basalts of the Faeroe Islands and from Miocene basalts from NW Iceland. We demonstrate that the original basaltic liquids were relatively low in $\delta^{18}O$ compared to MORB. Given that the Faeroese basalts were emplaced on top of continental crust and do show evidence of minor contamination by continental material, a

model were the oxygen isotopic signature is derived from mantle lithologies containing recycled and depleted oceanic crust is proposed.

2.2 A note on geology

The basaltic successions in the Faeroe Islands and Iceland represent early (≈50 Ma) and late (≈11Ma) Tertiary outpourings of the Iceland mantle plume, respectively. There are many similarities between the successions but also some important differences. The Faeroese lava pile rests on continental lithosphere (Bott et al., 1974) in contrast to the lava pile in NW Iceland which is anchored by oceanic lithosphere. In the successions in NW Iceland, several central volcanoes have been located where locally dacitic and rhyolitic rocks crop out. Such silicic centers have not been found in the Faeroe Islands.

Samples for this study were selected to be as fresh as possible. However, the Tertiary basalt piles in both the Faeroe Islands and NW Iceland have suffered (low-temperature) alteration. Low-temperature alteration is more prevalent in the Faeroe Islands and fresh olivine phenocrysts are rare in the these basalts (Heinesen, pers. comm. 1995). The three main startigraphic sections are represented in the samples from the Faeroe Islands (Table 2.1). The samples from NW Iceland were collected in stratigraphic sections above the zeolite-zones at relatively high altitude. They are quite fresh and contain phenocrysts of olivine, plagioclase and clinopyroxene. The samples from NW Iceland were collected by Dr. H. Sigurdsson (Univ. of Rhode Island) and the previously unpublished isotope data presented here were obtained by Dr. K. Muehlenbachs.

2.3 Analytical methods

Olivine, pyroxene and plagioclase (grain size 35-80 mesh) were separated from the crushed whole rocks using magnetic methods, and hand-picking under the binocular microscope. The mineral separates were washed with dilute hydrochloric acid to remove any surface alteration. Purity of separates is estimated to be > 95%. Pure olivine separates were crushed in an agate mortar to a grain size of ≤10 microns. Oxygen was liberated by reacting silicates and whole rocks with BrF_5 using the method described by Clayton and Mayeda (1963). To ensure complete reaction of the refractory olivine a large excess of reagent was used and the temperature maintained at approximately

670±10°C. Whole rock powders, pyroxene and plagioclase were reacted at ≈600°C. Oxygen yields are 95% or better. Repeated analysis of olivine separate F-13, gave an average of 4.48 ± 0.13 ‰ (1σ, n=7).

The oxygen isotope data is reported relative to SMOW assuming a fractionation factor of 1.0407 between CO_2 gas and water at 25°C (Compston and Epstein, 1958; O'Neil and Epstein, 1966). The aim is to have the data directly comparable to the early work done on Mid-Ocean Ridge basalts (Muehlenbachs and Clayton, 1972) and on Iceland (Muehlenbachs et al., 1974). To confirm comparability, selected samples from these early studies were successfully re-analyzed.

The mineral separates from the Faeroe Islands were analyzed for major elements on the JEOL 8900 electron microprobe in the Department of Earth and Atmospheric Sciences at the University of Alberta. An accelerating voltage of 15kV and a sample current of 20na was employed. Both natural and synthetic compounds were used as standards. The electron microprobe operating software employs the ZAF scheme for reduction of raw data. Counting times were typically 20 seconds on peak and 10 seconds on background.

2.4 Results

The $\delta^{18}O$ values for the basalts from the Faeroe Islands cluster at +4.5 to +6.0‰ (SMOW) with a few values scattered between +6.0 and +8.5 (Table 2.2). These higher values are characteristic of low-temperature weathering. The Icelandic basalts show a smaller variation in $\delta^{18}O$ from 4.7 to 6.7‰ (SMOW), consistent with being almost free of secondary alteration. Because all the rocks have undergone low-temperature weathering to some extent, we cannot infer the original magmatic $\delta^{18}O$ values from whole rock analyses. Phenocrysts in basalts are relatively resistant to alteration at such conditions; in particular pyroxene is known to retain its isotopic composition up to at least greenschist-facies metamorphism (Stakes and O'Neil, 1982). Olivine retains its original oxygen isotopic composition provided it survives the hydrothermal event. Plagioclase is more susceptible to low-temperature alteration and isotopic modification than either olivine or pyroxene.

The variation in $\delta^{18}O$ values of olivine, pyroxene and plagioclase is small (Table 2.2). Olivines (all but one from the Faeroes) range from +4.5 to +5.0‰ (SMOW). The pyroxene and plagioclase analyses cover a wider range than olivine from +4.4 to +5.4 and +4.7 to +5.4‰ (SMOW) respectively. The wider range of values among the latter probably reflects the larger sample size. The range of values for each mineral type is shown graphically in Fig. 2.1, where for comparative purposes we also plot analysis of the same minerals from MORB. It is clear that the mineral separates from the Faeroese and NW Iceland basalts are systematically displaced to lower values than their MORB counterparts.

From consideration of empirical data (i.e. mineral and whole rock/glass $\delta^{18}O$ data from fresh volcanic rocks), one can establish approximate relationships for oxygen isotope fractionation between the minerals olivine, pyroxene and plagioclase on the one hand, and basaltic magma on the other. These minerals form solid solutions at high temperatures, between two or more end members, and the isotopic behavior differs between these end members. The composition of the minerals changes with changing chemistry of the parental magma and one cannot therefore expect to establish singular values for the fractionation factor between the minerals and the magma. In general, analysis of fresh MORBs and Lunar basalts have shown that the $\delta^{18}O$ value of olivine is about 0.5 to 1.0‰ lower than the host whole rock value (where we assume the whole rock represents the magma) whereas clinopyroxene typically is the same to about 0.5 ‰ lower than the host whole rock and plagioclase is typically the same to about 0.3‰ higher than the whole rock in $\delta^{18}O$ (Clayton et al., 1971; Onuma et al., 1970, 1972; Muehlenbachs and Clayton, 1972).

Given these considerations, we can estimate the oxygen isotopic composition of the parental magmas from the mineral data in Fig 2.1. Two boxes are shown at the bottom of the figure. The filled box indicates the narrow range of the overwhelming majority of MORB basalts. The other box represents parental liquid oxygen isotopic compositions that we infer from the mineral data. The conclusion drawn from these diagrams is that the magmas forming the Tertiary basalts in the Faeroe Islands and NW Iceland were lower in $\delta^{18}O$ than MORB.

Forsterite (Fo) content of olivines in the Faroese basalt range from Fo_{80} to Fo_{90} (Table 2.3). With reference to the empirical data of Hald and Waagstein (1991) Mg# numbers between 0.57 and 0.80 in the parental basalts are implied. The Mg# number in most of the basalts from NW Icelandic is close to 0.60±0.06 with two samples having significantly lower Mg# number at ≈0.35 and finally two with higher Mg# number at ≈67 and 0.73 (H. Sigurdsson pers. comm.).

2.5 Discussion

The $\delta^{18}O$ composition of the olivine, pyroxene, and plagioclase clearly indicates that the parental magmas were significantly displaced from the $\delta^{18}O$ values of MORBs and Lunar basalts (5.7±0.3‰). Two contrasting hypotheses may be forwarded to explain the data. Both involve interaction of magma with ^{18}O-depleted crust; one at shallow levels involving juvenile crust, the other in the mantle involving subducted crust. First we look at the "shallow interaction" hypothesis.

This hypothesis requires that relatively depleted crust be first produced at the ridge axis during magmatism. Three key factors come into play here. Hydrothermal fluids have to be sufficiently depleted in ^{18}O, the permeability of the crust has to be high and crustal level intrusions should also be present to drive hydrothermal convection. Several investigators have shown that precipitation in the North-Atlantic area was relatively depleted (i.e. -8 to -14 ‰) in early Tertiary times (e.g. Brandriss et al., 1995). If we assume this holds true for the N-Atlantic area through the Tertiary period then the first condition is met. The second condition is also met because the extensional tectonics involved in rifting almost certainly provided similar hydraulic conditions to those in the present-day Icelandic rift zones. It is not clear, however, that the third condition is met in both Iceland and the Faeroe Islands. In the case of Iceland a number of silicic centers crop out in the Tertiary succession in NW Iceland and intense hydrothermal alteration is associated with them. However, such centers have not been recorded in the Faeroe Islands. Shallow level basic or silicic intrusions capable of driving hydrothermal convection cells in the Faeroe Islands are apparently absent. This could simply be a result of poor exposure or perhaps the basalt pile represents basalts flowing far away

from the contemporaneous ridge axis (distal facies) We conclude that the conditions for producing juvenile crust depleted in ^{18}O because of meteoric-hydrothermal systems appear to have been present in Late Tertiary times during the formation of the successions in NW Iceland but it is unlikely that this holds true for the Early Tertiary basalts in the Faeroe Islands.

The "deep interaction" hypothesis assumes that subducted oceanic crust is present in the mantle (plume?) during generation and/or evolution of the magmas. The magmas could either be generated by melting lithologies containing recycled oceanic crust (eclogite) or they might interact with (assimilate) such lithologies enroute to the surface. A complication of this model is that it requires that the subducted oceanic crust is delaminated during or subsequent to subduction. The mantle source has to be enriched preferentially in recrystallized equivalents of Layer 3 (the depleted Mid-Ocean Ridge gabbros). Cartwrigth and Valley (1991) proposed such a model to explain the origin of the low $\delta^{18}O$ Scourie dikes.

In choosing between the two hypotheses the following observations are of particular importance. Seismic evidence indicates that the Faeroese plateau rests on continental lithosphere (Bott et al., 1974). Isotopic evidence (Nd, Pb and Sr) suggests minor contamination of basalt magmas by continental material (Gariépy et al., 1983). This is consistent with trace-element studies that indicate that the Faeroese basaltic magmas fractionated at high pressures (garnet stability) at the base of the continental lithosphere (Bernstein, 1994). The younger portions of the Iceland-Faroe ridge, including presumably NW Iceland, is in contrast anchored by oceanic mantle lithosphere (Bott, 1983). Therefore, although assimilation and exchange processes between magma and hydrothermally altered wall-rock could be invoked to explain the depleted basalts in NW Iceland, it seems that in the case of the Faeroe Islands, the assimilant is of "continental origin" and therefore probably higher in $\delta^{18}O$ than the MORB reservoir. Minor assimilation of the continental lithosphere is not likely to affect the $\delta^{18}O$ of the magmas at all. If large quantities are assimilated the $\delta^{18}O$ of the magma will probably rise to $\geq$+6‰ as is seen in Andean magmatism (e.g. review by Taylor, 1986). These observations and the apparent lack of shallow-level intrusions that are capable of driving

hydrothermal cells that lead to the depletion of the crust lead us to prefer the "deep interaction" model.

The small $\delta^{18}O$ anomaly in Tertiary basalts from the Faeroe Islands and Iceland most likely result from processes or components in the mantle. Takahashi et al. (1998) suggest that in a mixed eclogite/peridotite lithology, the eclogite would melt preferentially in the early stages of melting and the peridotite contribute more to the melt with increasing degree of melting. If this is true and the peridotite and eclogite have different isotopic composition (e.g. +5.5 and +4.5‰ (SMOW), respectively), the $\delta^{18}O$ of the magmas should vary with degree of melting. It follows then that the oxygen isotopic data cannot be used to constrain the proportion of eclogite in the source.

2.6 Conclusions

Oxygen isotope ratios of olivine, pyroxene and plagioclase phenocrysts from Paleocene and Miocene basalts in the Faeroe Islands and Iceland, respectively, prove that the parental magmas were depleted in $\delta^{18}O$ compared to MORB. Two opposing models may be forwarded to explain the data. One involving assimilation and exchange with juvenile, hydrothermally-altered crust. The other involving melting of or interaction with recycled oceanic crust in the mantle. Both models can successfully explain the present data, but the latter is favored because the Faeroese lavas have probably interacted with continental lithospheric material, and significant assimilation of or isotopic exchange with such material would have lead to an increase in the ^{18}O-content of the magma, raising rather than lowering the $\delta^{18}O$ value.

2.7 References

Bernstein, S., 1994. High pressure fractionation in rift-related basaltic magmatism: Faeroe plateau basalts. Geology 22, 815-818.

Bott, M. H. P., 1983. The crust beneath the Iceland Faeroe ridge. In Bott, M. H. P., Saxov S., Talwani, M., Thiede, J. (Eds.). Structure and development of the Greenland-Scotland ridge. New York/London, Plenum Press pp. 63-76.

Bott, M. H. P., Sunderland, J., Smith, P. J., Casten, U., Saxov, S., 1974. Evidence for continental crust beneath the Faeroe Islands. Nature 248, 202-204.

Brandriss, M. E., Nevle, R. J., Bird, D. K., O'Neil, J. R., 1995. Imprint of meteoric water on the stable isotope compositions of igneous and secondary minerals, Kap Edvard Holm Complex, East Greenland. Contrib. Mineral. Petrol. 121, 74-86.

Cartwright, I., Valley, J. W., 1991. Low-^{18}O Scourie dike magmas from the Lewisian complex, northwestern Scotland. Geology 19, 578-581.

Clayton, R. N., Mayeda, T. K., 1963. The use of bromine pentafluoride for the extraction of oxygen from oxides and silicates for isotopic analysis. Geochim. Cosmochim. Acta 27, 43-52

Clayton, R. N., Hurd, J. M., Mayeda, T. K., 1973. Oxygen isotope compositions of Apollo 15, 16 and 17 samples, and their bearing on lunar origin petrogenesis. Geochim. Cosmochim. Acta, Suppl. 4, 1535-1542

Clayton, R. N., Onuma, N., Mayeda, T. K., 1971. Oxygen isotope fractionation in Apollo 12 rocks and soils. Geochim. Cosmochim. Acta Suppl. 2, 2, 1417-1420.

Compston, W., Epstein, S., 1958. A method for the preparation of carbon dioxide from water vapor for oxygen isotope analysis. Trans. Am. Geophys. Un. 39, 511-512.

Condomines, M., Grönvold, K., Hooker, P. J., Muehlenbachs, K., O'Nions, R. K., Óskarsson, N., Oxburgh, E. R., 1983. Helium, oxygen, strontium and neodymium isotopic relationships in Icelandic volcanics. Earth Planet. Sci. Lett. 66, 125-136.

Eiler, J. M., Farley, K. A., Valley, J. W., Stolper, E. M., Hauri, E. H., Craig H., 1995. Oxygen isotope evidence against bulk recycled sediment in the mantle sources of Pitcairn Island lavas. Nature 377, 138-141.

Eiler, J. M., Farley, K. A., Valley, J. W., Hofman, A. W., Stolper, E. M., 1996. Oxygen isotope constraints on the sources of Hawaiian volcanism. Earth Planet. Sci. Lett. 144, 453-468.

Garlick, G. D., MacGregor, I. D., Vogel, D. E., 1971. Oxygen isotope ratios in eclogites from kimberlites. Science 172, 1025-1027.

Gariépy, C., Ludden, J., Brooks, C., 1983. Isotopic and trace element constraints on the genesis of the Faeroe lava pile. Earth Planet. Sci. lett. 63, 257-272.

Garcia M. O., Ito, E., Eiler, J. M., Pietruszka, A. J., 1998. Crustal contamination of Kilauea Volcano magmas revealed by oxygen isotope analyses of glass and olivine from Puu Oo eruption lavas. J. Petrol. 39, 803-817.

Garcia, M. O., Muenow, D. W., Aggrey, K. E., O'Neil, J. R., 1989. Major element, volatile, and stable isotope geochemistry of Hawaiian submarine tholeiitic glasses. J. Geophys. Res. 94, 10525-10538.

Gregory, R. T., Taylor, H. P., 1981. An oxygen isotope profile in a section of Cretaceous oceanic crust, Samail ophiolite, Oman: Evidence for d ^{18}O buffering of the oceans by deep (> 5 km) seawater hydrothermal circulation at mid-ocean ridges. J. Geophys. Res. 86, 2737-2755.

Hald, N., Waagstein, R., 1991. The dykes and sills of the Early Tertiary Faeroe Island basalt plateau. Trans Roy. Soc. Edinburgh: Earth Sci. 82, 373-388.

Hémond, C., Condomines, M., Fourcade, S., Allégre, C., Óskarsson, N., Javoy, M., 1988. Thorium, strontium and oxygen isotopic geochemistry in recent tholeiites from Iceland: crustal influence on mantle-derived magmas. Earth Planet. Sci. Lett. 87, 273-285.

Ito, E., White, W. M., Göpel, C., 1987. The O, Sr, Nd and Pb isotope geochemistry of MORB. Chem. Geol. 62, 157-176.

Jacob, D., Jagoutz, E., Lowry, D., Mattey, D., Kudrjavtseva, G., 1994. Diamondiferous eclogites from Siberia: remnants of Archean oceanic crust. Geochim. Cosmochim. Acta 58, 5191-5207.

MacGregor, I. D., Manton, W. I., 1986. Roberts Victor eclogites: ancient oceanic crust. J. Geophys. Res. 91, 14063-14079.

Muehlenbachs, K., Clayton, R. N., 1972. Oxygen isotope studies of fresh and weathered submarine basalts. Can. J. Earth Sci. 9, 172-184.

Muehlenbachs, K., Clayton, R. N., 1976. Oxygen isotopic composition of the oceanic crust and its bearing on seawater. J. Geophys. Res. 81, 4365-4369.

Muehlenbachs, K., Anderson, A. T. and Sigvaldason, G. E., 1974. Low-O^{18} basalts from Iceland. Geochim. Cosmochim. Acta 38, 577-588.

O'Neil, J. R., Epstein, S., 1966. Method for oxygen isotope analysis of milligram quantities of water and some of its applications. J. Geophys. Res. 71, 4955-4961.

Onuma, N., Clayton, R. N., Mayeda, T. K., 1970. Oxygen isotope fractionations between minerals, and an estimate of the temperature of formation. Geochim. Cosmochim. Acta Suppl. 1, 2, 1429-1434.

Onuma, N., Clayton, R. N., Mayeda, T. K., 1972. Oxygen isotope cosmothermometer. Geochim. Cosmochim. Acta 36, 169-188.

Óskarsson, N., Sigvaldason, G. E., Steinthórsson, S., 1982. A dynamic model for the rift zone petrogenesis and the regional petrology of Iceland. J. Petrol. 23, 28-74.

Pineau, F., Javoy, M., Hawkins, J. W., Craig, H., 1976. Oxygen isotope variations in marginal basin and ocean-ridge basalt. Earth Planet. Sci. Lett. 28, 299-307.

Takahashi, E., Nakajima, K., Wright, T. L., 1998. Origin of the Columbia River Basalts: Melting model of a heterogeneous plume head. Earth Planet. Sci. Lett.162, 63-80.

Taylor, H. P., 1986. Igneous rocks: Isotopic case studies of circumpacific magmatism. In J. W. Valley, H. P. Taylor, J.R. O'Neil, (Eds.). Stable isotopes in high temperature geological processes. Reviews in Mineralogy 16, Mineralogical Society of America, 273-317.

Thirlwall, M. F., Jenkins, C., Vroon, P. Z., Mattey, D. P., 1997. Crustal interaction during construction of ocean islands: Pb-Sr-Nd-O isotope geochemistry of the shield basalts of Gran Canaria, Canary Islands. Chem. Geol. 135, 233-262

Woodhead, J. D., Greenwood, P., Harmon, R. S., Stoffers, P., 1991. Oxygen isotope evidence for recycled crust in the source of EM-type ocean island basalts. Nature 362, 809-813.

Zindler, A., Hart, S. R., 1986. Chemical Geodynamics. Ann. Rev. Earth Planet. Sci.14, 493-571.

Table 2.1 Stratigraphic location and oxygen isotopic composition ($\delta^{18}O$ (‰ SMOW)) of basalts from the Faeroe Islands.

Sample Id.	Sample Location	Elev.[1]	Form.[2]	Type[3]	$\delta^{18}O$[4]	Sep.[5]
RW 19880531-28	Knúkur, Mykines	555	L	BL	4.5	F13
RW 19850902-08	Tindur, Sandoy	475	U	BL	5.5	F11
RW 19890601-10A	Bustin, Suduroy	310	M	BL	7.9	F10
JR 200655-01	Nevtangi, Víkar, Vágoy		(L)	BD	5.4	F6
JR 110668-04	Tjörnuvík, Streymoy		(M)	BD	4.7	F3
RW 19890608-13*	Ryggvíkstangi, Vágar	260	M	BL	5.7	F7
RW 19890524-08	Skardsá, Vágar	220	M	BL	5.1	n. o.
RW 19880519-09	Villingadalsfjall, Vidoy	190	U	BL	8.6	n. o.
JR 200650-07	Selvík, Vágoy	173	M	BL	7.9	F5
RW 19880519-06	Villingadalsfjall, Vidoy	165	U	BL	5.4	F9
JR 190757-01	Creek by Kirkjug., Tjörnuvík, Streymoy	77	M	BL	7.4	F4
JR 170650-03	Rættará, Sörvágur, Vágoy	42	M	BL	5.9	n. o.
VM1-199	DDV[7]	-199	M	BL	5.5	F2
VM1-484	DDV[7]	-484	M	BL	6.6	F1

1) Elevation: meters above sealevel.
2) Stratigraphic Formation: U=Upper; M=Middle; L=Lower.
3) Type of rock: L= Basaltic Lava; D=Basaltic Dike.
4) Oxygen isotopic composition in per mille (‰) relative to SMOW.
6) Sample Id of mineral separates from respective hosts (n.o. not obtained)
7) Deep Drilling in Vestmanna, 1980.

Table 2.2 Oxygen isotopic composition ($\delta^{18}O$ ‰(SMOW)) of mineral separates and host basalts, from the Faeroe Islands (F-#) and NW-Iceland (S*-# and J*-#).

Sample Id	Ol	Cpx	Plg	Mt	Wr
F-6	4.75				5.4
F-4	4.66				7.4
F-3	4.80				4.7
F-1	4.56				6.6
F-7	4.48				5.7
F-5		5.25			7.9
F-10		5.01			7.9
F-13		4.28			4.5
F-11			5.28		5.5
SU-87				2.64	4.99
JD-8			4.83	2.94	4.73
JE-10		4.39	4.68	2.37	4.67
JB-7			5.26	2.66	5.07
JD-45		4.62	4.90	2.06	4.60
JC-6		4.71	5.16	2.73	4.94
SB-23		4.71	5.21		6.41
JB-20			5.05		4.98
SL-57		4.72			5.04
JD-10		4.77	5.11	2.51	5.14
SL-32	4.51	5.25			6.74
SB-25		4.85	5.36	2.63	4.95

Abbreviations: Ol=olivine; Cpx=clinopyroxene; Plg=plagioclase; Mt=titaniferous magnetite; Wr=wholerock;

Table 2.3 Electron microprobe analysis of major elements (wt %) in olivine phenocrysts in basalts from the Faeroe Islands

Sample	F-8		F-1	F-2	F-3	F-3
	Average	St. Dev.	G-1	G-5	G-3	G-1
Oxides	n=8	1σ	n=2	n=2	n=3	n=3
SiO2	39.8	0.3	40.9	39.2	41.1	40.2
Al2O3	0.07	0.03	0.12	0.26	0.16	0.16
FeO	15.3	0.3	14.9	17.9	10.6	12.8
MnO	0.22	0.04	0.22	0.26	0.11	0.18
MgO	44.8	0.3	45.7	42.7	48.6	46.9
CaO	0.38	0.02	0.35	0.34	0.34	0.40
NiO	0.30	0.05	0.32	0.32	0.36	0.33
Total	100.9		102.5	101.0	101.2	100.9
Cations						
Si	0.994		1.001	0.991	0.999	0.993
Al	0.002		0.003	0.008	0.005	0.005
Fe	0.320		0.305	0.378	0.215	0.263
Mn	0.005		0.004	0.006	0.002	0.004
Mg	1.668		1.667	1.608	1.762	1.724
Ca	0.010		0.009	0.009	0.009	0.010
Ni	0.006		0.006	0.007	0.007	0.007
O	4		4	4	4	4
fo	84		84	81	89	87
fa	16		16	19	11	13
CATS	3.004		2.995	3.007	2.999	3.006

Table 2.3 (Continued) Electron microprobe analysis of major elements (wt %) in olivine phenocrysts in basalts from the Faeroe Islands

Sample	F-5		F-1		F-9	
	Average	St. Dev.	Average	St.Dev.	Average	St.Dev.
Oxides	n=3	1σ	n=2	1σ	n=3	1σ
SiO2	39.8	0.1	40.9	0.3	39.8	0.1
Al2O3	0.11	0.03	0.12	0.08	0.08	0.05
FeO	16.8	0.3	14.9	0.2	15.6	0.8
MnO	0.23	0.03	0.22	0.02	0.23	0.02
MgO	43.4	0.6	45.7	0.2	44.4	1.0
CaO	0.32	0.01	0.35	0.03	0.43	0.06
NiO	0.26	0.02	0.32	0.02	0.24	0.04
Total	100.9		102.5		100.85	
Cations						
Si	0.9997		1.0013		0.9956	
Al	0.0032		0.0033		0.0025	
Fe	0.3535		0.3053		0.3268	
Mn	0.0050		0.0044		0.0049	
Mg	1.6237		1.6674		1.6571	
Ca	0.0085		0.0093		0.0114	
Ni	0.0052		0.0063		0.0048	
O	4		4		4	
fo	82		84		83	
fa	18		16		17	
CATS	2.999		2.997		3.003	

Abbreviations: n=number of analysis; St Dev =standard deviation; fo=Forsterite, fa=Fayalite; CATS=Summ of cations;

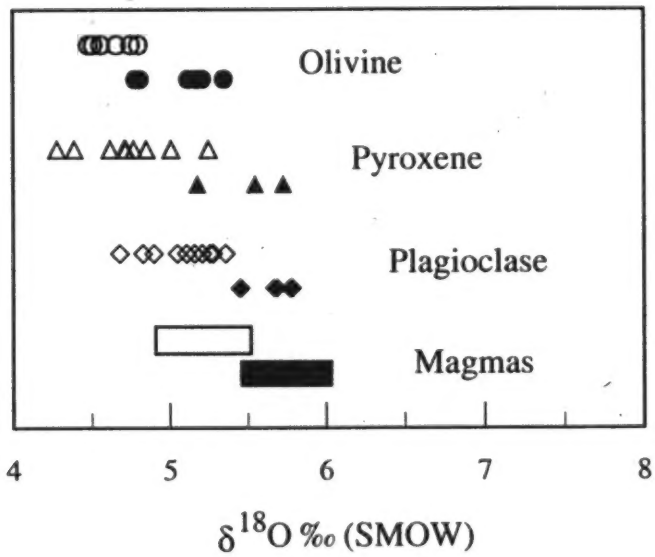

Figure 2-1. $\delta^{18}O$ (‰ SMOW) of mineral separates from basalts in NW Iceland and the Faeroe Islands (open symbols). Isotopic composition of the same phases from MORB (filled symbols) shown for comparison (Muehlenbachs and Clayton, 1972). Symbols: Circles =olivine, triangles=pyroxene; diamonds=plagioclase. Implied $\delta^{18}O$ of parental magmas (boxes) are also indicated.

Chapter 3

OXYGEN ISOTOPE SYSTEMATICS IN GABBRO NODULES AND VOLCANIC GLASSES FROM THE WESTERN RIFT-ZONE IN SW-ICELAND. IMPLICATIONS FOR FLUID INFILTRATION INTO THE DEEP CRUST[1)]

3.1 Introduction

The oxygen isotope ratios of terrestrial basaltic magmas show little variation worldwide. Most basalts have $\delta^{18}O$ values between +5 and +6 ‰ relative to SMOW (Standard Mean Ocean Water) (e.g., Taylor, 1986; Harmon and Hoefs, 1995). Mid-ocean ridge basalts, in particular, are homogeneous with over 90% of analyzed samples between 5.5 and 6.0 ‰ (Muehlenbachs and Clayton, 1972; Pineau et al, 1978; Ito et al., 1987). Basaltic magmas that deviate from these averages do occur, and are often associated with either ^{18}O-enriched (high $\delta^{18}O$) continental crust, or ^{18}O-depleted hydrothermally altered crust. The occurrence of ^{18}O-depleted (low $\delta^{18}O$) basalts in Iceland is well known, where $\delta^{18}O$ values of +3 to +5 (‰ SMOW) are common. Muehlenbachs et al. (1974) demonstrated that these low $\delta^{18}O$ values represent true magmatic values. In several subsequent petrochemical studies, the oxygen isotope systematics played an important role in the development of regional and local models, many of which emphasized the influence of the crust on mantle-derived melts (Sigurdsson and Sparks, 1980; Óskarsson et al, 1982; Condomines et al., 1983; Hémond et al. 1988; Sigmarsson et al., 1992; Gunnarsson et al., 1998; and many others). There is agreement in the literature that ^{18}O-depletion is related to processes operating within the Icelandic crust; however, a general consensus on the mechanism of oxygen transfer is lacking. Due to the high latitude, the precipitation in Iceland is depleted in ^{18}O. Alteration and re-crystallization of basaltic rocks in hydrothermal systems involving meteoric-derived fluids leads to significant subsolidus lowering in the $\delta^{18}O$ of the altered rocks (e.g. Hattori and Muehlenbachs, 1982).

1) A version of this chapter will be submitted to a peer reviewed journal for consideration, with Dr. K. Muehlenbachs as second author.

Interaction between magma and country rocks and/or geothermal fluids may lead to the ^{18}O-depletion (supersolidus) of the magma. The depleted magmas have inherited their oxygen isotopic signature from the precipitation. Yet the basaltic magmas contain little water ($\leq$ 1% wt.). Thus, while the magma carries the "fingerprint" of meteoric water, it is essentially anhydrous.

Five mechanisms, have been proposed to explain this anomaly (e.g., Muehlenbachs et al., 1974; Taylor, 1986; Sheppard, 1986): 1) magmas are derived from an anomalous ^{18}O-depleted mantle under Iceland; 2) magmas assimilate hydrothermally-altered crust; 3) mantle-derived magmas mix with magmas formed by melting of hydrothermally-altered crust; 4) magmas exchange oxygen with hydrothermally-altered crust; 5) magma exchange oxygen with hydrothermal fluids. The scenarios that attribute the anomaly to near-surface processes may be divided into two categories. Those that assume significant mass-transfer of oxygen and other elements from the crust to the magma, and those that assume only exchange of oxygen. In the debate over the last 25 years, attention has focused on assimilation-type scenarios and magma mixing (cases 2 and 3) or isotopic exchange between crust and magma (case 4). However, a general consensus on the exact mechanism or the relative importance of the various processes is lacking. This is unsatisfactory, because the existence of low-^{18}O magmas in Iceland may well point to a globally important process (e.g. Muehlenbachs, 1974; Taylor, 1986), that is only revealed in places such as Iceland which have a distinctive meteoric water composition.

In an attempt to constrain processes operating within the Icelandic crust, in particular the exchange or transfer of oxygen from crustal fluids to magma, we have measured the oxygen isotope ratios of gabbro nodules, their constituent minerals, and coeval basaltic liquids. The underlying rationale is to understand better the interaction between magma, fluids and crust anywhere in the global rift system. We propose two end-member models, that essentially constitute variations on familiar themes, one of isotopic exchange between crust and magma, the other re-crystallization of the solid portion of a magma mush, during magma ascent in the lower crust.

The nodules come from five different localities in SW Iceland (Fig. 3-1). Two of the localities are within the Hrómundartindur volcanic system (a subsystem in the Hengill volcanic region). Two other localities, on the rift proper, belong to the Krísuvík and Grindavík volcanic system. Nodules from Seydishólar, a system located off the main rift, represent the fifth locality. Mantle nodules from Iceland have not been recorded in the literature to date. However, gabbroic nodules do occur, and some investigators have attempted to use these crustal samples to constrain the magmatic processes, and the environment attendant to magmatic differentiation (P, T, fO_2) . The petrography of

gabbro-nodules, from SW-Iceland in particular, have been studied by a number of researchers. These include; Jónsson (1963) who recorded and described gabbroes from several localities, Tryggvason (1957) described the gabbro bombs at Graenavatn and Jakobsson (1966) studied some nodules from Seydishólar in his work on the Grímsnes lavas. More recently, the petrological studies on gabbro nodules from Dagmálafell (Risku-Norja 1985), Maelifell (Hardardóttir 1983; Hansteen, 1991), Hraunsvík (Sigurdsson, 1989) and Krísuvík area (Høj, 1993) have been carried out.

3.2 Analytical Techniques

The nodules were crushed to grain sizes between 35 and 80 mesh, and then sieved and cleaned. Minerals were separated by hand-picking under the binocular microscope. Whole-rocks and separated minerals and glasses were reacted with BrF_5 in a vacuum extraction system similar to that described by Clayton and Mayeda (1963). Results are reported relative to SMOW, assuming a 1.0407 fractionation of oxygen isotopes between CO_2-gas and water at 25°C (Compston and Epstein, 1958; O'Neil and Epstein, 1967).

Thin sections of nodules, and probe mounts with mineral separates, were prepared for petrographic and chemical analysis. Minerals were analyzed for major elements on the JEOL JXA 8900 electron microprobe at the Department of Earth and Atmospheric Sciences at the University of Alberta. Analysis were performed in WDS mode, with a 15kV acceleration potential and 20 nA sample current. The microprobe operating software reduces the analytical data using the ZAF correction scheme. A large number of natural and synthetic standards were used for calibration, and calibrations were checked against alternate standards not employed in the calibration scheme.

3.3. Results

3.3.1 $\delta^{18}O$ of Gabbro Nodules

The variation in $\delta^{18}O$ in the nodules is limited (Table 3-1) Plagioclase separates range from 3.7 to 5.7 ‰. Ignoring the lowest value reduces the variation by almost 1 ‰. The clinopyroxene separates range from 4.6 to 5.3 ‰ (Fig. 3-2). Greater variation in $\delta^{18}O$ of plagioclase than clinopyroxene is consistent with plagioclase being more susceptible to post-crystallization isotopic exchange (see below). No evidence can be found in the current data set, for ultra-depleted material (i.e. -5 to -10 ‰) similar to the evolved nodules in the Askja 1875 rhyolite (Muehlenbachs et al., 1974).

The partitioning of oxygen isotopes between two phases is temperature dependent, but insensitive to pressure over the range of pressure applicable to the Earth's crust (e.g. Clayton et al. 1989). The fractionation of oxygen isotopes between major silicate minerals

has been calibrated in experimental studies (Clayton et al., 1989; Chiba et al., 1989) and theoretical calculations (Kieffer, 1982; Kieffer and Clayton, 1991). At magmatic temperatures (≈1000-1200°C) fractionations between major silicate minerals in gabbroic rocks are about 1per mille or less. Most of the plagioclase-pyroxene pairs show fractionations indicative of high-temperature equilibrium (Fig. 3-3). For reference two isotherms are shown in Figure 3-3 indicating isotopic fractionation between plagioclase (An_{80}) and clinopyroxene at 1000 and 1200 °C, respectively (Clayton et al., 1989; Chiba et al., 1989). These are labeled solidus and liquidus, respectively. Plagioclase-pyroxene pairs that precipitated from a basaltic magma should plot within this band, with the exact location, a function of the $\delta^{18}O$ of the magma.

Two pairs plot significantly off the high-temperature band. One to the left, the other to the right. The plagioclase-pyroxene pair plotting to the left of the line shows a fractionation opposite to what is possible at equilibrium. That is, plagioclase in SH-1 is lower in $\delta^{18}O$ than the coexisting pyroxene. It indicates that plagioclase has exchanged oxygen with an external reservoir while the $\delta^{18}O$ of the pyroxene did not change appreciably. This occurs because the rate of oxygen diffusion in plagioclase is about 1 to 3 orders of magnitude faster than that in pyroxene at the same temperature. This relationship holds at high-temperatures (≈1000 °C) under both "dry" (Muehlenbachs and Kushiro, 1974; Connolly and Muehlenbachs, 1988) and "hydrothermal" (Giletti et al., 1978; Farver 1988)) experimental conditions, thus it probably true for a variety of geological conditions. The most likely candidate for the low-^{18}O external reservoir is a hydrothermal fluid of meteoric origin.

The nodule plotting to the right of the trend is from Seydisholar locality. Its position to the right of the magmatic band is consistent with retrograde closed system isotopic exchange, between plagioclase and pyroxene and other phases in the rock (e.g. olivine, oxides and glass), during slow cooling. During cooling the phases will exchange oxygen and re-equilibrate at progressively lower temperatures, resulting in this case, in an increase in the $\delta^{18}O$ of the plagioclase and a decrease in the $\delta^{18}O$ of the pyroxene. The magnitude of this shift in each phase is dependent on their modal abundance. In general, phases with low modal abundance are more sensitive to the effect of cooling and show larger shifts in isotopic composition.

Three pairs plot to the left of the 1200°C (≈ liquidus) isotherm. All, however, plot to the right of the $\delta^{18}O_{plg} = \delta^{18}O_{cpx}$ line. Theoretically, this line represent equilibrium at infinite temperature ($1/T^2 = 0$). Obviously temperatures significantly above 1200°C are unlikely, and hence there is the possibility that the plagioclase in these pairs has partially exchanged oxygen with an external reservoir at high temperatures.

3.3.2 $\delta^{18}O$ of Hengill Area Volcanics

To complement the data on the gabbro nodules, we have analyzed the $\delta^{18}O$ of volcanic glasses and whole rocks from Hengill volcanic area (Table 3-2). The whole rocks and glasses were previously described by Hardardóttir (1983) and Trønnes (1991), respectively. The erupted magmas span the complete range in composition from picrites to dacite/rhyolite which is reflected in their MgO content (Table 3-2).

In Figure 3-4 the variation in $\delta^{18}O$ is examined as a function of MgO (wt. %) content. The compositional spectrum is divided into three fields. They are: 1) "Picrites" at MgO > 8.9 wt. %; 2) Basalts at 5.0 < MgO < 8.9 wt. %; 3) Evolved basalts and silicic rocks at MgO < 5.0 wt. %. Trønnes (1991) noted that glasses in the Hengill area, with MgO > 8.9 wt. %, contain olivine, plagioclase and minor resorbed Cr-Al-rich diopside and used MgO value of 8.9 wt. % to separate piciritic formations from basaltic formations. There are only three data points in the "picrite" field. Interestingly, these hint at a negative correlation between MgO and $\delta^{18}O$ at MgO contents above 8.9%. Within the basalt field, the $\delta^{18}O$ of glass and whole rocks correlates well with MgO content. At lower MgO contents (intermediate and silicic rocks) there is significant scatter in the data. Some of this scatter is probably the result of mixing of magmas derived from anatexis of a heterogeneous crust and mantle-derived basaltic melts. However, this paper is primarily concerned with the basalts and their $\delta^{18}O$ systematics.

3.3.3 Petrography of Nodules

The gabbro nodules are anorthositic, gabbroic, olivine-gabbroic and troctolitic (Table 3-3). All the nodules are small, ranging from several centimeters to a few decimeters in maximum diameter. In the larger nodules, centimeter-scale heterogeneity in the mineral proportions or mode is observed in places.

The nodules derive from Recent or late Quaternary flows or subglacial formations (Tuyas). They are free of low-temperature weathering and alteration. Deuteric oxidation of olivine is observed in nodules from all the localities except Dagmálafell and Graenavatn. Olivine in nodule 9377 from Seydishólar is pervasively oxidized to iddingsite. Olivine in nodules from both Hraunsvík and Tjarnarhnúkshraun is slightly oxidized. Oxidation is apparent from a light red-brown or deep red "coating" on the grains. In the Hraunsvik lava this oxidation is exclusively on olivine crystals that are adjacent to vesicles and often only on the crystal faces terminating toward the vesicle.

Olivine in nodules SH-1 from Graenavatn is often lined with titaniferous-magnetite along grain boundaries and cracks in the crystals. This may be the result of re-

crystallization of olivine to a more Fo-rich variety and formation of magnetite, resulting in the release of SiO_2 to form either orthopyroxene or amorphous silica (or quartz). Orthopyroxene has, however, only been found as exsolution lamellae in clinopyroxene and amorphous silica or quartz has not been identified.

Nodule SH-1 from Graenavatn, also contains minor biotite. Microprobe analyses show that the biotite is high in MgO (22 wt. %) and fluorine (1.9 wt. %) and poor in TiO_2 (< 0.2 wt.%) and chlorine (< 0.2 wt.%). The high MgO and low TiO_2 content is difficult to reconcile with crystallization from a late-stage magma. The biotite may form during hydrothermal re-crystallization at high temperatures, involving surface-derived fluids perhaps mixed with a late-stage magmatic fluid. The absence of other hydrous minerals such as epidote and chlorite indicates that low-temperature retrograde re-equilibration did not take place. Tryggvason (1957) found evidence of hornblende in nodules from Graenavatn. We have not, however, observed this mineral in our thin sections.

It seems logical to assume that the ^{18}O-depleted fluid originally derives from meteoric water. The data, however, does not rule out contributions from seawater. The fluid circulating at present in the western-most hydrothermal systems on the Reykjanes Peninsula is of seawater origin (Arnórsson, et al. 1983). Reactions between a modified seawater and basaltic rocks at high temperatures would presumably produce similar isotopic effects in the Icelandic crust as in Mid-ocean ridge gabbros. Some gabbroic rocks from the oceanic rift systems show evidence of seawater-derived fluids infiltrating at temperatures up to and above 700°C (Mével and Cannat, 1991; Vanko and Stakes 1991, Dick et al., 1992; Gillis, 1995). In the temperature range between about 500 to above 700°C and at low water/rock ratios, this fluid causes a shift in the $\delta^{18}O$ of plagioclase to lower values and the formation of small amounts of brown or green hornblende. These effects are similar to what we observe in the Graenavatn nodule. Therefore contribution from seawater-derived fluid cannot be excluded, particularly in the alteration of the Graenavatn nodule.

Clinopyroxene in the nodules from Seydishólar and Graenavatn contain lamellae of exsolved orthopyroxene. Exsolution lamellae are absent in clinopyroxene in the nodules from Dagmálafell, Tjarnarhnúkshraun and Hraunsvík, there are, however, commonly quench textured inclusions in plagioclase and pyroxenes. This may reflect slower and more substantial cooling, prior to eruption, experienced by the nodules from the Seydisholar and Graenavatn localities compared to the other three. On the basis of their blocky appearance, several investigators argued that nodules from Seydisholar and Graenavatn were ripped or plucked out of the country rock during the eruption (Tryggvason, 1957; Jakobsson, 1967; Ragnarsdóttir et al., 1982; Høj, 1993). The

presence of patchy biotite in the nodule SH-1 supports this notion, as heating to magmatic temperatures would result in breakdown of this phase.

In the Dagmalafell nodules, groundmass is commonly present along grain boundaries between clinopyroxene and plagioclase causing the nodules to be friable. The nodules from Hraunsvik appear more consolidated, and are often surrounded by reaction rims of fine-grained plagioclase and pyroxene. They are, however, vesicular and plagioclase in the nodules is commonly riddled with inclusions. The nodules from Tjarnarhnúkshraun are again more consolidated than the ones mentioned above, and do not contain vesicles. Large olivine crystals, poikilitically enclosing plagioclase, display kink-banding which probably result from near-solidus deformation.

On the basis of these observations we suggest that the primitive nodules from Dagmálafell, Hraunsvík and Tjarnarhnúkshraun resided in the region between the "rigidus" and the solidus prior to eruption. We assume that the magma plumbing system in Iceland may be similar in some respects to that of the mid-ocean ridges (Sinton and Detrick, 1992), and that the primitive nodules come from a magma mush zone in the deep crust. The reaction rims or coronas on the nodules from Hraunsvik indicates that replenishment of the magma mush before eruption plays a role in stirring up the region containing the nodules. The nodules from Graenavatn and Seydisholar, on the other hand, have been cooled below the solidus prior to being brought to the surface, as indicated by the presence of exsolution lamellae in clinopyroxene and reversed isotopic fractionation in the Graenavatn nodule.

Studies of gabbros from the oceanic crust and ophiolites show that the crust is chemically stratified with a refractory base overlying ultramafic rocks. A reasonable assumption is that the Icelandic crust, although much thicker (Bjarnason et al., 1993), is stratified in an analogous way.

3.3.4 Chemical Composition of Nodules

There is a broad correlation between the Mg# in clinopyroxene in the nodules and the composition of the host lava (Fig. 3-5). The most primitive nodules are brought to the surface by the most primitive magmas. This indicates that the nodules are related to the magmas, although there is not necessarily a direct parental relationship between host and nodules. If it is assumed that the lower crust in Iceland is compositionally zoned similar to the oceanic crust then the most refractory (MgO-rich) nodules must come from the greatest depth.

The chemistry of the clinopyroxene in the nodules reflects the chemistry of the parental liquids. The TiO_2 content in clinopyroxene increases steadily with decreasing Mg# in clinopyroxene (Fig. 3-6) from Mg# 90 to Mg# 75. Below about Mg# 75, the TiO_2

content drops with further decrease in Mg#. The trend of TiO_2 versus Mg# trend forms a type of "liquid line of descent." The inflection in this trend at about Mg# 75 probably reflects the appearance of ilmenite-hematite and magnetite-ulvöspinel solid solutions, as co-fractionating phases in the magma.

There is a positive correlation between Cr_2O_3 and Mg# in clinopyroxene at Mg# > 80 (Fig. 3-7). Below Mg# 80, the basaltic liquids have lost almost all of their Cr_2O_3 as reflected in the composition of the clinopyroxene. Cr_2O_3 content in clinopyroxene is positively correlated with Al_2O_3 content for the nodules from Hraunsvik, Dagmalafell and Tjarnarhnúkshraun. The correlation suggests substitution of a Cr-Tschermak's component ($CaCrAlSiO_6$) in the clinopyroxene.

The plagioclase in the gabbro-nodules from Dagmálafell, Tjarnarhnúkshraun and Hraunsvík is anorthitic. The anorthite content of most nodule plagioclase is between An_{86} and An_{88} at all localities (Sigurdsson, 1989; Risku-Norja, 1985; this work). A few "outliers" extend the compositional range to An_{81} and An_{90}. Plagioclase phenocrysts display a similar compositional range, however An content in phenocrysts of up to An_{94} was recorded in Dagmálafell lava by Risku-Norja (1985). Anorthite content of plagioclase in SH-1 from Graenavatn ranges from An_{80} to An_{84}.

Olivine in the Dagmálafell-nodules is the most refractory of these samples ranging from Fo_{88} to Fo_{84}. The Hraunsvík-nodules are slightly more fayalitic ranging from Fo_{87} to Fo_{80} (this work and Sigurdsson, (1989)). The nodules from Tjarnarhnúkshraun are again more fayalitic with a average of Fo_{80}.

3.3.5 Unusual Nodules

The Hraunsvik lava contains two types of nodules that are unusual in texture and composition. One type are the large (up to 15 cm long) plagioclase xenocrysts that Karlsson and Jones (1982) mentioned previously. Samples 1987 and 1989 are fragments of such xenocrysts that were provided by the Museum of Natural History in Iceland. To our knowledge the other type has not been recorded previously in basaltic lavas from Iceland. These are olivine phenocrysts that due to oxidation appear to be in the process of breaking down to a more Fo-rich olivine and an Fe-rich spinel phase. The olivines often include what we interpret to be originally Cr-spinel crystals which have re-equilibrated to form a more Fe-rich spinel similar in composition to "ferrit chromit" that has been described from metamorphosed ultramafic rocks (Wylie, et al., 1987; Liipo et al., 1995). A detailed account of these nodules is outside the scope of this paper and will be presented later. However, the breakdown of olivine in these nodules and the common occurrence of

oxidized olivine in the nodules indicates that gabbroic rocks forming the lower crust may be exposed to oxidizing conditions during or shortly after their formation.

3.4 Discussion

3.4.1 Depth of Origin

Previous investigators have attempted to place some constraints on the depth of origin of the gabbro nodules. For the relatively evolved nodules from Graenavatn, Høj (1993) suggested a depth of 4 to 7 km based on extrapolating the results of oxide and pyroxene thermometry onto an assumed geothermal gradient.

Hansteen (1991) used fluid inclusions in olivine phenocrysts to argue that the Maelifell picrite resided in a magma reservoir at a minimum depth of 7 to 10 km prior to eruption. He concluded that the gabbro nodules in the Maelifell picrite were derived from the same reservoir. The Maelifell picrite is similar in age and composition to the Dagmálafell picrite and both are from the Hrómundartindur volcanic system in the Hengill region (Saemundsson 1967, Risku-Norja 1985, Hansteen 1991). The results of Hansteen (1991), therefore, probably apply to the Dagmálafell picrite as well. Based on experiments on natural basalts (Bender et al., 1979; Maaloe and Jakobsson, 1980; Elthon and Scarfe, 1984), a maximum pressure of approximately 7 to 8 kbars (≈20 to 25 km) can be inferred from the presence of plagioclase in the nodules.

From the above discussion it is clear that only loose constraints can be placed on the depth of origin of these nodules. We assume a minimum depth of 4 to 5 kilometers for the most evolved nodules and depth range of ≈10 to ≈20 kilometers for the most primitive nodules. Inherent in this view is our assumption that a compositional gradient exists in the crust. The chemistry of the nodules, and the chemical correspondence of host and nodules further supports this view. As mentioned above the pyroxenes from the five localities form a coherent "liquid line of descent" trend in TiO_2 vs. Mg# space. This is an important observation because it is consistent with the assumption that the nodules sample a chemically stratified section of crust, that may be up to 15 km in thickness, with a refractory base.

3.4.2 Implications of the $\delta^{18}O$ Systematics

In the material analyzed for the present study, no strongly ^{18}O-depleted (e.g. $\delta^{18}O$ = -5 to –10 ‰) samples have been found. However, this should not be taken as evidence for complete absence of highly ^{18}O-depleted crystalline material in the lower crust. The origin and constitution of any ^{18}O-depleted (i.e. -5 to –10 ‰) material, however, remains elusive. I suggest here that the positioning of the Tjarnarhnúkshraun nodules to the left of the high-temperature fractionation band, and the prevalent evidence for oxidation of olivine, is an indication that fluids (C-O-H) containing relatively ^{18}O-depleted oxygen may be present in the immediate vicinity of the magma.

The correlation between the $\delta^{18}O$ and MgO content of the basaltic liquids (Fig.3-4) is of interest. The same type of relationship between $\delta^{18}O$ and MgO (wt. %) was observed for whole rocks from the Krafla area (Nicholson et al., 1991). The two data sets (basalts and picritic rocks only) are compared in Figure 3-8. Two arrows are drawn through the data sets. These are not true "best fit" lines, but rather two parallel lines, drawn to highlight the similarity in the "slope" of the two sets of data. The lower line (or arrow) is a reasonable "eyeball" best fit for the whole Krafla data set whereas the upper line is only a reasonable fit if the picritic magmas are ignored. The two arrows are offset by a little less than 1 per mille in the y-direction, with the basalts from the Eastern rift zone being more depleted than correspondingly evolved basalts from the Western rift zone. Similarly, the intermediate and silicic rocks in the Krafla region (not shown) are more depleted (i.e. lowest $\delta^{18}O \approx +2$ ‰) than their Hengill area counterparts (lowest $\delta^{18}O \approx +3.4$ ‰). As we are comparing data-sets from two different labs this offset could be influenced by different standardization procedures. However, we note that in the original study by Muehlenbachs et al. (1974) the basalts in the Eastern rift zone were generally more depleted than the ones from the Western rift zone. The difference between the Krafla and Hengill region is therefore probably real although the exact magnitude may be slightly smaller or greater than indicated here.

Although fractional crystallization of olivine may be responsible for the change in MgO, crystal fractionation cannot cause the observed change in the $\delta^{18}O$ of the magmas. Nicholson et al. (1991) suggested that the correlated MgO and $\delta^{18}O$ were directly linked through an AFC process, where olivine crystallizes and basaltic crust is assimilated. As an alternative, we suggest that the variables are not directly linked, but that both are a function of magma residence time and are therefore correlated. For instance, if the ^{18}O-depletion is due to an isotopic exchange process, the degree of exchange is time dependent. Similarly, if the major-element variation of the magma is controlled by crystal-fractionation, then the MgO content of the magma varies with time. If this is true, then the processes that produces

the ^{18}O-depletion, and the change in major-element chemistry, are operating on the same time-scale. We suggest that the rate of the $\delta^{18}O$ depletion ($d\delta^{18}O/dt$) is proportional to the rate of change of magma chemistry (dMgO/dt) in other words:

$$(d\delta^{18}O/dt) = \kappa\,(dMgO/dt) \qquad (3\text{-}1)$$

where κ is a constant of proportionality. The slope of the lines in Figure 3-8 suggests that $\kappa_{WRZ} \approx \kappa_{ERZ}$, and that κ has a value of ≈ 0.8 (‰/wt.%). However, the rate of the ^{18}O-depletion (i.e. $d\delta^{18}O/dt$) cannot be inferred from the present data.

3.4.3 Regional Systematics

As stated above, the Krafla lavas are more ^{18}O-depleted at a given MgO content than their counterparts in Hengill. This observation is consistent with the lavas in the Eastern rift zone being in general more ^{18}O-depleted than their counterparts in the Western rift zone. The systematic difference in isotopic composition is probably related to difference in the structure of the rift zones (Óskarsson et al. (1982)). Compared to the western rift-zone, the eastern rift-zone is characterized by greater overall width, mature volcanic centers and large caldera structures. The wider eastern rift-zone is able to funnel more meteoric fluids into the crust resulting on average in a greater ^{18}O-depletion of the crust in this area.

The data set produced by Muehlenbachs et al. (1974) showed that the magnitude of the oxygen isotope anomaly decreased southwards along the South Iceland volcanic zone. Subsequent studies have confirmed this general trend. This zone represents a propagating rift, and it differs from the rift zones in that graben type structures are absent and heat flow is relatively low. It is generally believed that volcanic centers on the propagating rift such as Hekla and Torfajökull are reworking (re-melting) crust that was originally formed some 5 to 10 Ma earlier in the Western rift zone (e.g. Sigvaldason, 1974; Sigmarsson et al. 1992; Gunnarsson, 1998). No evidence currently exists regarding the isotopic composition of the local precipitation at the time of formation of these protoliths. However, we note that Eocene precipitation in the North Atlantic Area, i.e. Greenland and Scotland was depleted ($\delta^{18}O \approx -8$ to -14 ‰ SMOW) (Brandriss et al., 1995) and hence it is possible that precipitation in this area was similarly depleted for most of the Tertiary period. If this is true, then the protoliths to the rhyolites erupted in Hekla and Torfajökull should have been low in $\delta^{18}O$ similar to the protoliths forming the rhyolites at volcanic centers on the rift zones today. This is not the case, however. In particular, the evolved rocks at Hekla show no appreciable depletion of ^{18}O compared to the basalts (Sigmarsson, et al. 1991). We

infer from this that formation of a ^{18}O-depleted protolith is not enough to generate low ^{18}O magmas (basalts or rhyolites). It is suggested that the crust has to allow continual recharge of ^{18}O-depleted oxygen during magmatism for low ^{18}O magmas to form. Otherwise the flux of oxygen from the mantle will quickly exhaust any ^{18}O-depletion in the crustal section it travels through. At Torfajökull, the rhyolites are depleted in ^{18}O relative to coexisting basalts (Gunnarsson, et al. 1998). This is consistent with our suggestion, given the multiple caldera structures that encompass the volcanic center and the fact that the south end of the Veidivötn fissure system cuts into this volcanic center.

The variation in the magnitude of the $\delta^{18}O$ anomaly along the neovolcanic zones is apparently related to the hydraulic properties of the crust. This is an indication that some form of hydrothermal recharge during rifting, i.e. both during and between individual rifting episodes, is necessary to produce the anomaly in the basaltic magmas.

3.4.4 Towards a New Model

We propose that fluids containing surface-derived water infiltrate the deep crust during rifting and that these fluids play a crucial role in generating the $\delta^{18}O$ anomaly. The basaltic magmas must inherit much of their depleted signature during residence in the lower crust. It seems likely that the magma storage area is a melt mush zone, similar to that inferred to exist at Mid-ocean ridges. If some porosity is maintained in the gabbroic residue after magma withdrawal, fluids containing surface-derived water may invade this region and exchange oxygen with the deep-seated rocks. Only the outermost surface of the constituent minerals, however, need to be depleted in ^{18}O. The isotopically exchanged material retains its original mineralogy.

When fresh magma re-invades the region it may exchange oxygen with the gabbroic mush acquiring the depleted signal of the precipitation. This mechanism of transferring oxygen to the magma is possible because of the (inferred) large surface area between the crust and magma. This is a surface enhanced exchange process.

This model has several advantages. Since only oxygen "anions" are exchanged while little or no net transfer of "cations" takes place, the process does not lead to multiple saturation of the magma. The magma mush region that we infer to exist is characterized by large surface area between crust and magma and short diffusion distances within the magma. Hence long residence times are not necessary to equilibrate large volumes of magma by exchange and diffusion. This hypothesis circumvents oft-mentioned problems of exchanging oxygen directly between an H_2O under-saturated magma and surface-derived fluid. Yet the "correlation" between the physical characteristics of the volcanic zones and the magnitude of depletion observed is consistent with the model.

NOTE TO USER

The original manuscript received by UMI contained pages with broken print. All efforts were made to acquire the highest quality manuscript from the author or school. The manuscript was microfilmed as received.

Pages 34, 35, & 36

This reproduction is the best copy available.

UMI

ı infiltrate to
ring periods of
ermost mantle

olution and re-precipitation is a process often called upon to account for fluid nges, and fluid transport in metamorphic rocks. If the rise of basaltic magmas mush region is aided by such a re-crystallization process, it will of course lead epletion of the magma (lower $\delta^{18}O$), provided the solid fraction of the mush a ^{18}O-depleted signature prior to magma infiltration. We propose that this ı result of deep infiltration of surface-derived fluids. It is noted, however, that : and re-crystallization model is not dependent on this deep infiltration of ved fluids. The solid portion of the mush may also represent lithologies that vere hydrothermally altered at higher levels in the crust, and subsequently sank ıg at the ridge axis.

rate of depletion ($d\delta^{18}O/dt$) in our model is related to the difference in the pic composition of the mantle-derived magma and the crust it enters. This turn may be controlled to a large extent by the efficiency of hydrothermal fluid rior to a given rifting episode. Such fluid infiltration is also likely to affect the lition of the crust. The rate of cooling of the magma must be related to the difference between the mantle-derived magma and the crust the magma he greater the difference the more rapid the cooling. If this is correct then it the time required to mature a magma in the Eastern rift zone is shorter than in rift zone. That is $(d\delta^{18}O/dt)_{ERZ} > (d\delta^{18}O/dt)_{WRZ}$ and $(dMgO/dt)_{ERZ} >$ RZ but because both are linked to the conditioning of the crust prior to a rifting nstant of proportionality is similar in both rift zone (i.e. $\kappa_{WRZ} \approx \kappa_{ERZ}$). nportant implication of the model is that fluids must invade the magma-mush nagma-withdrawal. This places fluids containing surface-derived oxygen at r than 8 km and possibly as deep as 15 to 20 km.

Processes

ly, a comment on the most magnesian basalts or picrites is in order. We note tes are depleted in $\delta^{18}O$ relative to common MORB basalts and furthermore ar high-temperature equilibrium with their gabbro nodules and xenocrysts they carry to the surface (Table 3-1 and Fig. 3-3). Because the Al rich diopside crystal in the picrites are in high-temperature equilibrium with is impossible that the depletion of the magma is related to the assimilation of . Similar phenocrysts have been found in oceanic basalts and were originally ıve crystallized at high pressure (P > 7 kbar) (e.g. Bender et al. 1978). More s been suggested that they form as a result of melts interacting with a residual phere (Dick and Natland, 1996). In a separate communication (Gautason in

preparation) we present evidence that indicates that the Icelandic picrites have reacted extensively with a clinopyroxene-bearing lithology in the uppermost mantle. If this lithology represents recycled oceanic crust then it is possible that its oxygen isotopic composition is depleted in ^{18}O relative to bulk mantle. Reactions between mantle melts and this lithology could produce ^{18}O-depleted primitive magmas and Cr-Al-rich diopside that is in near isotopic equilibrium with its host liquid. In Figure 3-4, the data in the picrite field hints at an increase in depletion with increasing MgO, a "trend" that is nearly perpendicular to the trend among the basalts. Gee et al. (1998) analyzed olivine from lavas on the Reykjanes peninsula by laser fluorination and in their data there is similarly a hint of a similar "trend" (their Fig. 6). We suggest therefore that both mantle and crustal processes may contribute to the depletion of $\delta^{18}O$ in mafic Icelandic magmas.

3.5 Conclusions

The oxygen isotopic composition of gabbro nodules from 5 localities in SW Iceland and coeval basaltic lavas have been analyzed. Reversed fractionation between plagioclase and pyroxene is observed only in the most evolved nodule, presumably derived from the shallowest depth. It is a clear sign of hydrothermal fluids infiltrating the solidified rock. If one assumes that Høj's (1993) thermo-barometry on nodules from the same locality also applies to these nodules then one has to conclude that fluids have infiltrated to depths of at least 4 to 7 km in the rift zones.

The range in oxygen isotope composition of the other nodules is only about 1 per mille. The most primitive nodules show plagioclase-pyroxene fractionations consistent with equilibration at magmatic temperatures. There is a suggestion of oxygen re-equilibration in the Tjarnarhnúkshraun nodules in that they plot to the high-temperature side of the "liquidus isotherm." The location of these nodules on the left side of the liquidus isotherm is an indication that plagioclase has exchanged oxygen with high-temperature C-O-H fluids containing surface-derived water.

The oxygen isotopic composition of basalts in the Hengill region correlates with the MgO content of the magma. Hence the $\delta^{18}O$ depletion may be a function of the crustal residence time of the magma. The pattern of depletion in the Hengill area is similar to that in the $\delta^{18}O$ Krafla region (Nicholson et al., 1991), but the magnitude of depletion differs. The differences between the two volcanic centers is probably related to differences in the hydraulic properties of the crust in each region.

We propose a model that is consistent with the current data. It involves isotopic exchange between interstitial magma and crust in a magma mush reservoir in the lower crust, where isotopic exchange is enhanced by the large surface area between melt and

3.6 References

Arnórsson, S., Gunnlaugsson, E., Svavarsson, H., 1983. The chemistry of geothermal waters in Iceland. II. Mineral equilibria and independent variables controlling water compositions. Geochim. Cosmochim. Acta 47, 547-566.

Bender, J. F., Hodges, F. N., Bence, A. E., 1978. Petrogenesis of basalts from the project FAMOUS area: Experimental study from 0 to 15 kbars. Earth Planet. Sci. Lett. 41, 277-302.

Chiba, H., Chacko, T., Clayton, R. N., Goldsmith, J. R., 1989. Oxygen isotope fractionations involving diopside, forsterite, magnetite, and calcite: Application to geothermometry. Geochim. Cosmochim. Acta 53, 2985-2995.

Clayton, R. N., Goldsmith, J. R., Mayeda, T. K., 1989. Oxygen isotope fractionation in quartz, albite, anorthite and calcite. Geochim. Cosmochim. Acta 53, 725-733.

Clayton, R. N., Kieffer S. W., 1991. Oxygen isotopic thermometer calibrations. In H. P. Taylor, J. R. O'Neil, I. R. Kaplan (Eds.) A tribute to Samuel Epstein. The Geochemical Society Spec. Publ. 3, pp.3-10.

Clayton, R. N. and Mayeda, T. K., 1963. The use of bromine pentafluoride in the extraction of oxygen from oxides and silicates for isotopic analysis. Geochim. Cosmochim. Acta 27, 43-52.

Compston, W., Epstein, S., 1958. A method for the preparation of carbon dioxide from water vapor for oxygen isotope analysis (abstract). Trans. Am. Geophys. Union 39, 511-512.

Condomines, M., Grönvold, K., Hooker, P. J., Muehlenbachs, K., O'Nions, R. K., Óskarsson, N., Oxburgh, E. R., 1983. Helium, oxygen, strontium and neodymium isotopic relationships in Icelandic volcanics. Earth Planet. Sci. Lett. 66, 125-136.

Connolly, C., Muehlenbachs, K., 1988. Contrasting oxygen diffusion in nepheline, diopside and other silicates and their relevance to isotope systematics in meteorites. Geochim. Cosmochim. Acta 52, 1585-1591.

Dick, H.J.B., Natland, J.H., 1996. Late-stage melt evolution and transport in the shallow mantle beneath th East Pacific rise. In: Mével, C., Gillis, K. M. and Meyer P. S. (Eds.), Proceedings of the Ocean Drilling Program, Scientific Results, 147. Ocean Drilling Program, College Station, TX, pp. 103-134.

Dick, H. J. B., Robinson, P. T., Meyer, P. S., 1992. The plutonic foundation of a slow-spreading ridge. In: R. A. Duncan, D. K. Rea, R. B. Kidd, U. von Rad, J. K. Weissel (Eds.) Synthesis of results from scientific drilling in the Indian Ocean. American Geophysical union, Geophysical Monograph 70, pp. 1-39.

Eiler, J. M., Farley, K. A., Valley, J. W., Hofman, A. W., Stolper, E. M., 1996. Oxygen isotope constraints on the sources of Hawaiian volcanism. Earth Planet. Sci. Lett. 144, 453-468.

Elthon, D., Scarfe, C. M., 1984. High-pressure phase equilibria of a high-magnesia basalt and the genesis of primary oceanic basalts. Am. Mineral. 69, 1-15.

Farver, J. R., 1989. Oxygen self-diffusion in diopside with application to cooling rate determinations. Earth Planet. Sci. Lett. 92, 386-396.

Gee, M. A. M., Thirlwall, M. F., Taylor, R.N., Lowry, D., Murton, B. J., 1998. Crustal processes: Major controls on Reykjanes peninsula lava chemistry, SW Iceland. J. Petrol. Spec. Iss., 39, 819-803.

Giletti, B. J., Semet, M. P., Yund, R. A., 1978. Studies in diffusion - III. Oxygen in feldspars: an ion microprobe determination. Geochim. Cosmochim. Acta 42, 45-57.

Gillis, K.M., 1993. Controls on hydrothermal alteration in a section of fast-spreading ocenic crust. Earth Planet. Sci. Lett. 134, 473-489.

Gregory, R. T., Taylor, H. P., 1981. An oxygen isotope profile in a section of cretaceous oceanic crust, Samail Ophiolite, Oman: Evidence for $\delta^{18}O$ buffering of the oceans by deep (>5 km) seawater-hydrothermal circulation at mid-ocean ridges. J. Geophys. Res. 86, 2737-2755.

Gunnarsson, B., Marsh, B. D., Taylor, H. P. J., 1998. Generation of Icelandic rhyolites: silicic lavas from the Torfajökull central volcano. J. Volcanol. Geotherm. Res. 83, 1-45.

Hansteen, T. H., 1991. Multi-stage evolution of the picritic Mælifell rocks, SW Iceland: constraints from mineralogy and inclusions of glass and fluid in olivine. Contib. Mineral. Petrol. 109, 225-239.

Hardardóttir, 1983. The petrology of the Hengill volcanic system, southern Iceland. M. Sc., McGill University, Montreal. pp.

Harmon, R. S., Hoefs, J., 1995. Oxygen isotope heterogeneity of the mantle deduced from global ^{18}O sytematics of basalts from different geotectonic settings. Contrib. Mineral. Petrol. 120, 95-114.

Hattori, K., Muehlenbachs, K., 1982. Oxygen isotope ratios of the Icelandic crust. J. Geophys. Res. 87, 6559-6565.

Hémond, C., Condomines, M., Fourcade, S., Allégre, C. J., Óskarsson, N., Javoy, M., 1988. Thorium, strontium and oxygen isotopic geochemistry in recent tholeiites from Iceland: crustal influence on mantle-derived magmas. Earth Planet. Sci. Lett. 87, 273-285.

Høj, J. W., 1993. Gabbro-anorthosite nodules from the Krisuvik fissure system and active zone of rifting, Reykjanes peninsula, SW Iceland. Neues Jb. Miner. Abh. 165, 169-189.

Ito, E., White, W. M., Göpel, C., 1987. The O, Sr, Nd and Pb isotope geochemistry of MORB. Chem. Geol. 62, 157-176.

Jakobsson, S., 1966. The Grimsnes lavas SW-Iceland. Acta Naturalia Islandica II, 5-30.

Jónsson, J., 1963. Hnydlingar í Íslenzku bergi. Náttúrufraedingurinn 33, 9-22.

Karlsson, H. R., Jones, A. P., 1982. Zoned labradorite megacrysts in xenolithic picrite from S.W. Iceland. Annual Meeting of the Geological Society of America, New Orleans.

Kieffer, S, 1982. Thermodynamics and lattice vibrations of minerals: 5. Applications to phase equilibria, isotopic fractionations and high pressure thermodynamics properties. Rev. Geophys.Space Phys. 20, 827-849.

Liipo, J. P. Vuollo, J. I. Nykänen, V. M., Piirainen T. A., 1995. Zoned Zn-rich Chromite from the Näätäniemi serpentinite massif, Kuhmo greenstone belt, Finland. Can. Mineral. 33, 537-545.

Maaløe, S., Jakobsson, S. P., 1980. The PT phase relations of a primary oceanite from the Reykjanes peninsula, Iceland. Lithos 13, 237-246.

Mével, C., Cannat, M., 1991. Lithospheric stretching and hydrothermal processes in oceanic gabbros from slow-spreading center. In: Tj. Peters, A. Nicolas, R. G. Coleman (Eds.) Ophiolite genesis and evolution of the oceanic lithosphere. Kluwer Academic Publishers, Dordrecht, pp.293-312.

Muehlenbachs, K., Anderson, A. T., Sigvaldason, G., 1974. Low-O^{18} basalts from Iceland. Geochim. Cosmochim. Acta 38, 577-588.

Muehlenbachs, K., Clayton, R. N., 1972. Oxygen isotope studies of fresh and weathered submarine basalts. Can. J. Earth Sci. 9, 172-184.

Muehlenbachs, K., Kushiro, I., 1974. Oxygen isotope exchange and equilibration of silicates with CO2 and O2. Cartnegie Inst. Wash. Yearb. 73, 232-236.

Nicholson, H., Condomines, M., Fitton, J. G., Fallick, A. E., Grönvold, K., Rogers, G., 1991. Geochemical and isotopic evidence for crustal assimilation beneath Krafla, Iceland. J. Petrol. 32, 1005-1020.

O'Neil, J. R., Epstein, S., 1966. Method for oxygen isotope ana;ysis of milligram quantities of water and some of its applications. J. Geophys. Res. 71, 4955-4961.

Óskarsson, N., Sigvaldason, G. E., Steinthórsson, S., 1982. A dynamic model of rift zone petrogenesis and the regional petrology of Iceland. J. Petrol. 23, 28-74.

Pineau, F., Javoy, M., Hawkins, J. W., Craig, H., 1976. Oxygen isotope variations in marginal basin and ocean-ridge basalt. Earth Planet. Sci. Lett. 28, 299-307.

Ragnarsdóttir, K. V., Bishop, F. C., Jakobsson, S. P., 1982. Crystalization Processes in a shallow magma chamber beneath Seydisholar, Griímsnes. Int. Ass. Volcanol. Chem. Earth's Int.-Int Ass. Geol. Geophys. Abstarct

Risku-Norja, H., 1985. Gabbro nodules from a picritic pillow basalt, Midfell SW Iceland Nordic Volcanological Institute, Reykjavik, pp. 61.

Saemundsson, K., 1967. Vulcanismus und Tectonik des Hengill Gebietes in Sudwest-Island. Acta Nat. Islandica. 2, 105 pp.

Sheppard, S. M. F., 1986. Igneous Rocks III. Isotopic case studies of magmatism in Africa, Eurasia and Oceanic Islands. In J. W. Valley, H. P. Taylor, J.R. O'Neil, (Eds.) Stable isotopes in high temperature geological processes. Reviews in Mineralogy 16, Mineralogical Society of America, 319-371.

Sigmarsson, O., Condomines, M., Fourcade, S., 1992. A detailed Th, Sr and O isotope study of Hekla: differentiation processes in an Icelandic Volcano. Contrib. Mineral. Petrol. 112, 20-34.

Sigurdsson, H., Sparks, R. S. J., 1980. Petrology of rhyolitic and mixed magma ejecta from the 1875 eruption af Askja, Iceland. J. Petrol. 22, 41-84.

Sigurdsson, I. A., 1989. Gabbrohnydlingar i Hraunsvik a Reykjanesskaga. B.Sc. hon. thesis. University of Iceland, pp. 67.

Sigvaldason, G. E., 1974. The petrology of Hekla and the origin of silicic rocks in Iceland. The eruption of Hekla 1947-1948. Societas Scientarium Islandica 5, pp.1-44

Sinton, J. M., Detrick R. S., 1992. Mid-ocean ridge magma chambers. J. Geophys. Res. 97, 197-216.

Sveinbjörnsdóttir, A. E., Coleman, M. L., Yardley, B. W. D., 1986. Origin and history of hydrothermal fluids of the Reykjanes and Krafla geothermal fields, Iceland. Contrib Mineral Petrol 94, 99-109.

Taylor, H. P., 1986. Igneous rocks II. Isotopic case studies in circumpacific magmatism. In J. W. Valley, H. P. Taylor, J.R. O'Neil, (Eds.). Stable isotopes in high temperature geological processes. Reviews in Mineralogy 16, Mineralogical Society of America, 273-317.

Tryggvason, T., 1957. The gabbro bombs at Lake Graenavatn. Bull. Geol. Univ. Uppsala 38, 1-5.

Trønnes, R. G., 1990. Basaltic melt evolution of the Hengill volcanic system, SW Iceland, and evidence for clinopyroxene assimilation in primitive tholeiitic magmas. J. Geophys. Res.

Vanko, D. A., Stakes, D. S., 1991. Fluids in oceanic layer 3: evidence from veined rocks, hole 735B, Southwest Indian Ridge. In R. P. von Herzen, P.T. Robinson et al. (Eds.) Proc. Ocean Drilling Program, Scientific Results 118, 181-218.

Wylie, A. G., Candela, P. A., Burke, T. M., 1987. Compositional zoning in unusual Zn-rich chromite from the Sykesville district of Maryland and its bearing on the origin of "ferritchromit." Am. mineral. 72, 413-422.

Table 3-1 Oxygen Isotopic composition $\delta^{18}O$ (per mille SMOW) of mineral separates from gabbro nodules and their hosts.

Locality	Id	Plg	n	1σ	Cpx	n	1s	Other	n	1σ
Dagmálafell	Host Lava							5.03 (wr)	2	0.09
	9302 G3	5.20			4.79	2	0.23			
	9302 T1	5.35	2	0.13						
	9302 XA	5.09								
	9302 XB	4.86								
	9302XC	5.34	2	0.11						
	9305 G	5.26	2	0.06	4.68	3	0.07			
	9306 XD	5.18	3	0.07						
	9101 X1				4.83	2	0.05			
	9101 X2									
Tjarnar-	Host Lava							5.20 (wr)	2	0.02
hnúkshraun	9321 G1	5.35	3	0.07	5.28	1				
	9321 G2	5.38	2	0.03	5.01	2	0.09			
	9321 T1	5.15	1							
	9322 C G1	5.47	3	0.06	4.78					
	9323 T1	4.99								
	9324 XA	5.15	3	0.21						
	9324 G1	5.22	2	0.02	5.16	3	0.18			
	9325 G1	4.90	2	0.00						
Seydishólar	Host Lava							5.25 (wr)		
	9377	5.78	2	0.07	4.69	2	0.08			
	9375				4.76	2	0.09			
Graenavatn	S1	3.79			4.96			0.6 (mt)		
Hraunsvík	Host Lava							5.07 (wr)	2	0.00
	5781	5.47	2	0.01						
	7795	5.35	2	0.31	5.21	2	0.08			
	9361	5.37	2	0.02						
	9362 N2	5.10								
	9364 N4 C	4.70	1							
	9364 N4 R	4.54	1							
	9365 N5									
	9363 N6									
	9363 N7	5.12	2	0.07						
	X 1987	4.97	2	0.10						
	X 1989									

Abbreviations; Id=Sample Identification; n=number of analysis; plg=plagioclase; cpx=clinopyroxene; wr=whole rock; mt=titaniferous magnetite.

Table 3-2 Oxygen isotopic composition, $\delta^{18}O$ (per mille SMOW), and MgO content of glasses (He-*) and whole rocks (H-*) from the Hengill area.

Sample	MgO (wt %)	$\delta^{18}O$ (per mille SMOW)
He 5	7.29	4.92
He 9	0.5	3.80
He 11	1.6	3.37
He 22	7.7	5.11
He 32	6.42	4.49
He 46	3.35	4.73
He 51	7.55	4.69
He 53	7.94	4.79
He 66	9.34	5.05
He 72	4.31	4.28
He 73	8.98	4.77
He 79	6.71	4.87
He 88	4.55	3.41
He 89	5.31	4.19
He 90	3.67	4.67
He 91	4.69	4.78
He 100	7.14	4.92
He 109	5.83	4.32
He 111	7.47	5.25
H-1	10.01	4.65
H-2	6.75	4.59
H-6	7.8	5.12
H-7	7.88	4.98
H-13K	2.84	4.54
H-17	7.75	4.83
H-20K	5.73	4.18

1. MgO data for He-* and H-* samples from Trønnes (1991) and Hardardóttir (1983) respectively. Standard deviation on pooled data 1σ = per mille0.12 for n=40.

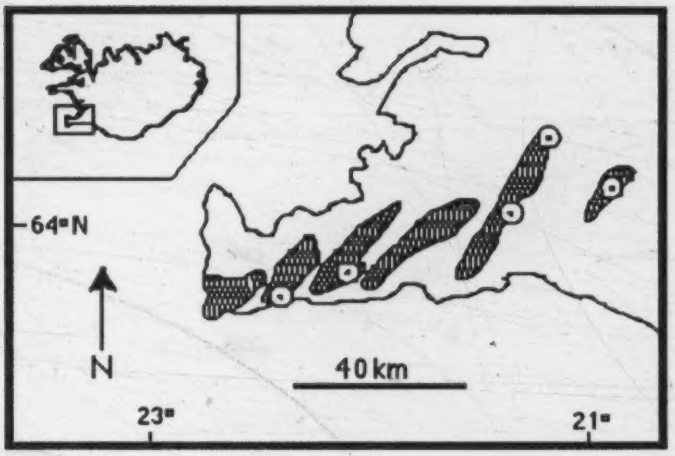

Figure 3-1 Simple map showing the approximate outline of the volcanic systems in SW-Iceland. Points indicate localities where gabbro nodules were collected. Volcanic systems from West to East are; Reykjanes: Grindavík; Krísuvík; Bláfjöll; Hengill and Grímsnes (following Jakobsson et al., 1978). Nodule localities form West to East are: Hraunsvík (N63°51'05", W22°20'56"); Graenavatn (N63°53', W22°03'); Tjarnarhnúkshraun (N64°06'14", W21°09'49"); Dagmálafell (N64°10'32", W21°02'48") and Seydishólar (N64°05', W20°51'). Geographic location, in degrees, minutes and seconds, given in paranthesis (Horizontal datum: Hjörsey-1955).

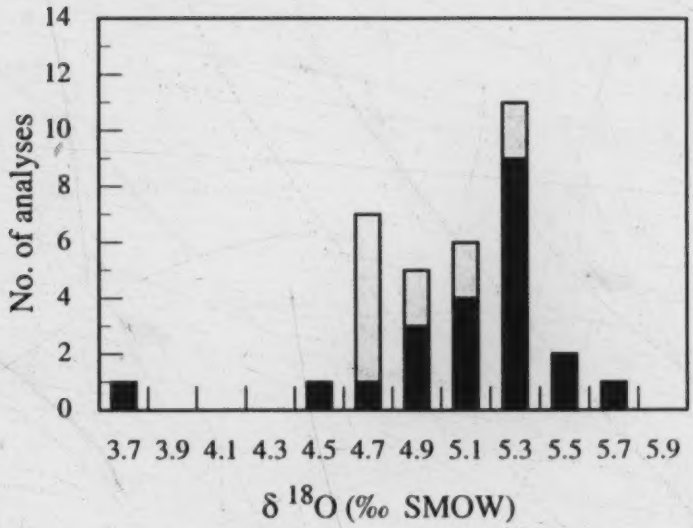

Figure 3-2 Histogram showing oxygen isotopic composition ($\delta^{18}O$) of plagioclase (dark) and clinopyroxene (light) from gabbro-nodules and phenocrysts.

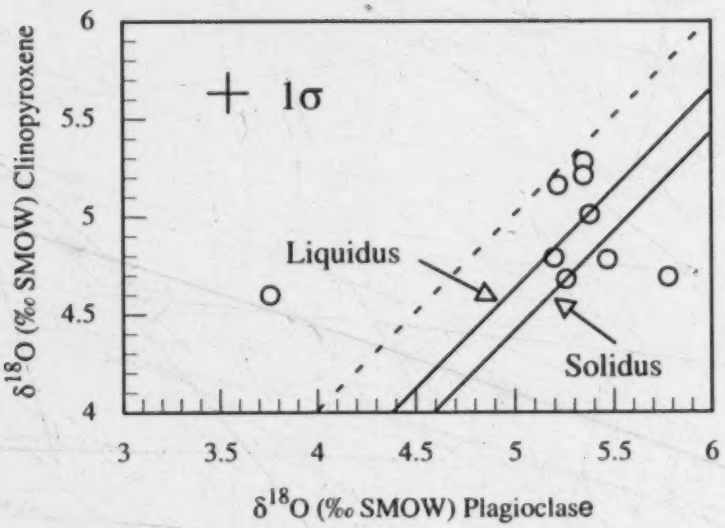

Figure 3-3 Oxygen isotopic composition ($\delta^{18}O$) of plagioclase and pyroxene pairs from gabbro nodules in SW Iceland. Solidus and liquidus lines are the 1000 and 1200°C isotherms. Broken line indicates infinite temperature

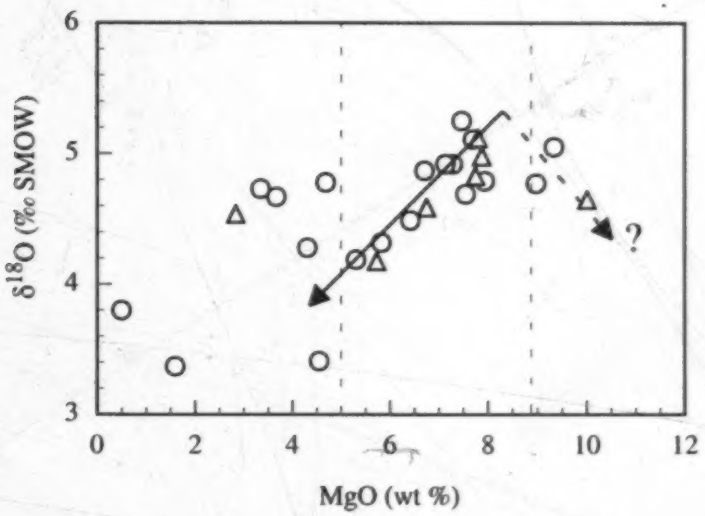

Figure 3-4 Oxygen isotopic composition ($\delta^{18}O$) of volcanic glasses (circles) and whole rocks (triangles) from the Hengill area in SW-Iceland plotted against MgO content

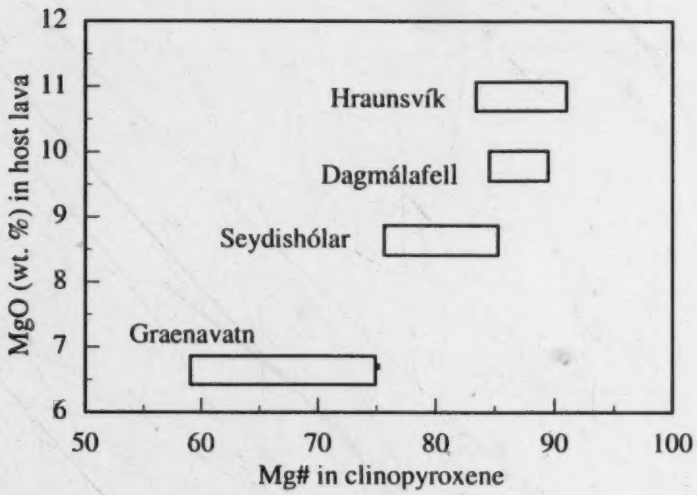

Figure 3-5 MgO (wt %) in host lava plotted against the range in Mg# observed in clinopyroxene from gabbro nodules in the same host.

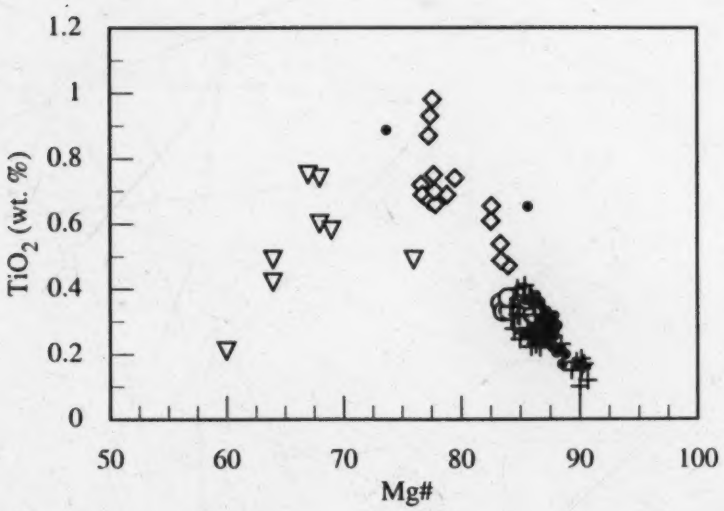

Figure 3-6 TiO_2 (wt %) in clinopyroxene plotted against Mg# in clinopyroxene from Dagmálafell (solid dots), Hraunsvík (crosses), Tjarnahnúkshraun (open circles), Seydishólar (diamonds), Graenavatn (triangles).

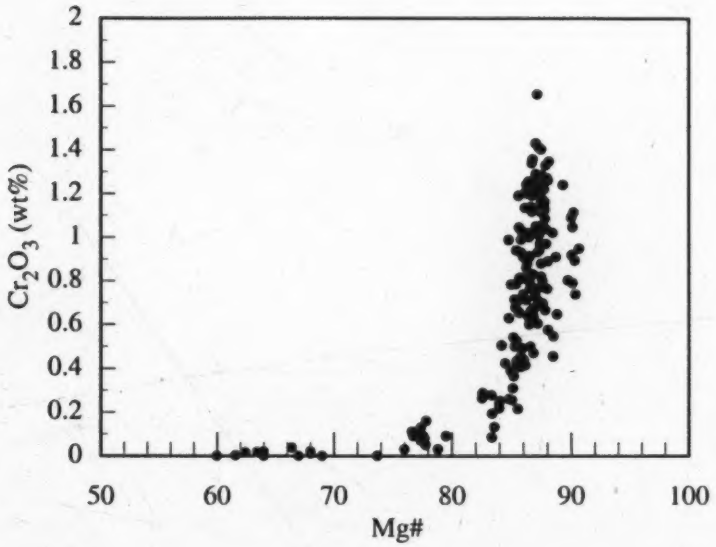

Figure 3-7 A plot of Cr_2O_3 (wt %) in clinopyroxene against Mg# in clinopyroxene from gabbros.

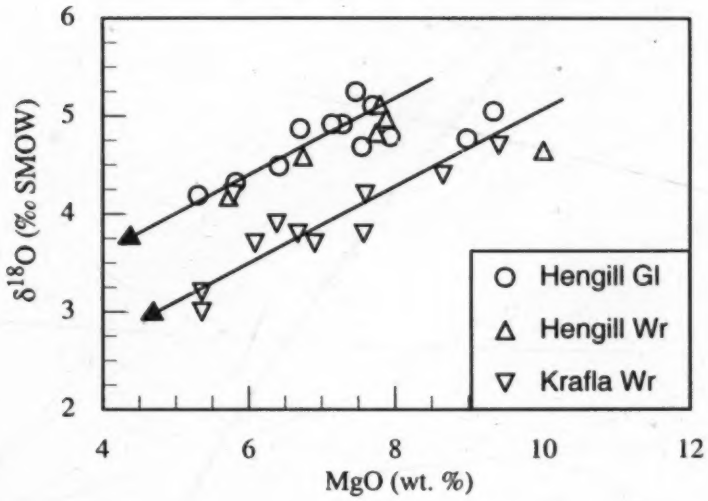

Figure 3-8 Oxygen isotopic composition ($\delta^{18}O$) of volcanic glasses (circles) and whole rocks (triangles) from the Hengill area in SW-Iceland (basalts and picrites only) compared to whole rocks from Krafla in NE-Iceland (data from Nicholson et al., 1991).

Chapter 4

OXYGEN ISOTOPIC FLUXES ASSOCIATED WITH HIGH TEMPERATURE PROCESSES IN THE RIFT-ZONES OF ICELAND.

4.1 Introduction

Reactions between seawater and juvenile crust at mid-ocean ridges play an important role in controlling the chemical composition of the oceans and atmosphere. Mass and heat fluxes associated with these reactions have been described in some detail in the literature (e.g., Elderfield and Schultz (1996), and references therein). Similar reactions between subaerial rift-zones and hydrosphere and the concomitant fluxes have, on the other hand, received relatively little attention. In this paper we summarize the ^{18}O-flux associated with high temperature processes in the rift-zones in Iceland.

It is well known that unaltered volcanic rocks from Iceland are lower in $\delta^{18}O$ and isotopically more variable than extrusives in any other oceanic setting (Muehlenbachs et al., 1974; Condomines et al., 1983; Hémond et al., 1988, 1993; and many others). Published $\delta^{18}O$ analyses of recent basalts range from +1.8 to +6.3‰ (SMOW). This variability is in sharp contrast to the very narrow range, +5.7 ± 0.3‰, displayed by unaltered mid-ocean ridge basalts (Muehlenbachs and Clayton 1972; Pineau et al., 1976; Ito et al., 1987; see also Harmon and Hoefs, 1995).

The oxygen isotope anomaly is commonly ascribed to assimilation and/or exchange processes within the Icelandic crust (e.g. Óskarsson et al., 1982, 1985; Hattori and Muehlenbachs, 1982; Taylor, 1986; Steinthórsson et al., 1987; Macdonald et al., 1987; Hémond et al., 1988; Nicholson et al., 1991; Sigmarsson et al., 1991a). Scenarios that have been suggested to account for this anomaly call for the following steps. Magma rising through the crust interacts with and assimilates hydrothermally altered basalt.

---

1) A version of this chapter has been published in Chemical Geology (1998, Vol. 145, pp. 275-286) with Dr. K. Muehlenbachs as second author.

Assimilation in this context, is either direct melting of stoped blocks of country rock, or formation of near eutectic melts from the crust and subsequent mixing of these into the magma. The altered basaltic pile is highly depleted with respect to ^{18}O due to the depleted character of meteorically-derived hydrothermal fluids. Thus, the ^{18}O anomaly in Icelandic basalts is ultimately related to the isotopic composition of the local precipitation.

This contribution summarizes published oxygen isotope data relevant to high temperature processes in the rift-zones in Iceland. The purpose is to estimate the oxygen isotopic composition of the crust. This in turn allows us to place constraints on the ^{18}O-flux from the mantle through the rift-zones to the hydrosphere. The flux through the rift-zones may be compared to a corresponding flux at mid-ocean ridges.

On the basis of our findings, we argue that: 1) High temperature processes in the rift-zone are efficient in transferring ^{18}O to the hydrosphere; 2) The ^{18}O-flux from the rift-zones in Iceland to the hydrosphere is up to 5 times that of an equivalent length of mid-ocean ridge gabbros; 3) In spite of the large contribution of ^{18}O to the hydrosphere, the net depletion of the crust in the rift-zone is only about 1 to 3‰.

4.2 Geologic Setting

Iceland is an oceanic island resulting from a mantle plume situated at a ridge. The rift-zones in Iceland (Fig. 4-1) are extensions of the Mid Atlantic Ridge. The mantle plume under Iceland has been imaged seismically (Tryggvason et al., 1983; Wolfe et al., 1997). The southward continuation of the Eastern rift-zone (the South Iceland volcanic zone, Fig. 4-1) is a propagating rift. In this region extensional features are poorly developed and heat flow is relatively low compared to the rift-zones (Saemundsson, 1979; Pálmason and Saemundsson, 1979). Recent volcanic products in the rift-zones are tholeiitic, in contrast to the South Iceland volcanic zone where volcanics are dominated by transitional and alkalic rock types (Jakobsson, 1972, 1979).

The rift-zones are subdivided into volcanic systems, which are the surface expression of foci of magmatic ascent from the mantle (Jakobsson, 1979; Saemundsson, 1979). Each consists of spatial groupings of eruptive vents and associated fissure swarms. Early in the evolution of a volcanic system, extrusives are characterized by primitive tholeiitic material, e.g. picrites and olivine tholeiites, commonly forming small and large shields, respectively (Jakobsson et al., 1978). With the maturation of a volcanic system a shallow magma reservoir may develop. The shallow magma chambers provide heat that drives geothermal systems in the rift-zone. Extrusives are dominated by more evolved tholeiites and quartz normative tholeiites. Finally, explosive eruption of dacitic and

rhyolitic material and concomitant formation of caldera structures (e.g., Askja 1875, see Sigurdsson and Sparks, 1981) is an important feature in the latter stages of the evolution of volcanic systems (Saemundsson, 1978).

A natural consequence of the loading of eruptive material on the rift-zones is the isostatic subsidence of the volcanic pile. Subsidence rates on the order of 0.4 to 1 cm/a were measured in three sections across the volcanic zone by Tryggvason (1974). This subsidence and potential reworking of the lava pile in the rift-zone is a key feature in many petrological models (e.g. Óskarsson et al., 1982), crustal accretion models (Pálmason, 1986) and the overall mass balance of the crust (Steinthórsson, 1987). It also provides a mechanism for bringing low ^{18}O, hydrothermally-altered rocks deeper into the crust.

The Icelandic crust is a natural laboratory to study major-element fluxes associated with the formation and evolution of rift-zones. A comparison of the ^{18}O-fluxes in Iceland to well documented ^{18}O-fluxes associated with hydrothermal metamorphism at mid-ocean ridges has implications for models dealing with the $\delta^{18}O$ history of seawater.

4.3 ^{18}O-flux Through the Rift-Zones

We consider the ^{18}O-fluxes in the rift-zone in terms of a simple box model (Fig. 4-2). The reservoir of interest is a cross section of the rift-zone. We consider three fluxes that transfer ^{18}O to and from this reservoir. The first, F_i, is the flux into the reservoir from the mantle and is equal to the product of the rate of transfer of mass from the mantle times the ^{18}O concentration in the Icelandic plume. The second, F_o, is due to the removal of material from the reservoir by advective transport due to seafloor spreading and erosion. Again, F_o is simply the rate of material removal times the concentration of ^{18}O in the mature Icelandic crust. The third flux F_{hs} is the consequence of isotopic exchange between the crust and the hydrosphere.

The ^{18}O-fluxes are calculated by multiplying the amount of oxygen introduced into each reservoir annually by its ^{18}O concentration in $\mu g/g$. That ^{18}O concentration is calculated from the definition of δ and SMOW having 2005 ppm ^{18}O (Baertschi, 1976). The amount of oxygen involved is given by the annual volume flux (i.e. the volume of rock involved), its density and the proportion of oxygen in the crust.

Oxygen is exchanged between the cooling crust and hydrosphere because of reactions between magma, crust and hydrothermal fluids. Due to the lower ^{18}O concentration of precipitation relative to the mantle these interactions result in a net transfer

or flux of ^{18}O to the hydrosphere (F_{hs}). F_{hs} is equal to $F_o - F_i$, if the reservoir has achieved a steady state. We therefore wish to determine first the oxygen isotopic composition of the crust subsequent to the high temperature interactions that deplete the crust. In this we distinguish between a domain of the crust which is depleted in ^{18}O through supersolidus reactions only, and another domain where the crust suffers further depletion of ^{18}O due to subsolidus reactions. We then proceed to estimate the oxygen isotopic composition of the mantle source under Iceland (the plume) and thereby the $\delta^{18}O$ of liquids that are extracted from it and enter the rift-zones.

Our calculations are scaled to a 20 km thick rift-zone crust (Bjarnason et al., 1993; Brandsdóttir et al., 1997). The full spreading rate is taken to be 2.1 cm/a (Sigmundsson et al., 1995). The rift-zones in Iceland are approximately 300 km long. The volume flux required to fill the crustal reservoir, integrated across the full length of the rift-zone, is ≈ 0.13 km^3/a. For comparison the total (i.e. in both rift-zones and flank zones) average rate of extrusion of volcanic material over the last 10 ky has been estimated to be 0.042 km^3/a (Thorarinsson and Saemundsson, 1979; Jakobsson, 1979).

4.4 Oxygen Isotopic Composition of the Icelandic Crust.

4.4.1 Unaltered Crust

One can estimate the average $\delta^{18}O$ value of volcanic rocks of Iceland from a compilation of all analyses to date. In Figure 4-3 we present a histogram of over 140 analyses of $\delta^{18}O$ in extrusive products from the rift-zones. These analysis include recent basalts and fresh glass from late Quaternary subglacial eruptions. Quaternary and Holocene samples, which are suspected to have suffered low temperature weathering (e.g. Hémond et al., 1988) are not shown. An effort was made to have each basalt lava or formation represented only once in the histogram, however, some "duplication" may still exist. The $\delta^{18}O$ values in the histogram are as recorded in the original references. The value of NBS 28 standard reported in the sources ranges from +9.4 to +9.7 ‰ (SMOW) we have however, not normalized the data to a single value for NBS 28.

Fresh basaltic rocks (MgO > 4 % wt.) range in $\delta^{18}O$ from +5.8 to +1.8 (Fig.4-3). It is clear from inspection of the figure that the distribution is bell-shaped and has a maximum at +4.4 ‰ (SMOW). We take +4.4 ‰ as a conservative estimate of the average unaltered crust in the rift-zone and assign an uncertainty of ± 0.5‰ to this value. The low $\delta^{18}O$ values of basalts in Iceland are the result of isotopic exchange and/or mass transfer

processes taking place in the crust at supersolidus temperatures. The exact mechanism of exchange is not key to the present study but it is discussed briefly below.

It has been established that in any given area (i.e. within a particular volcanic system) the evolved basalts are in general, lower in $\delta^{18}O$ than the primitive ones (e.g., Muehlenbachs et al., 1974; Nicholson et al., 1991). This suggests that the $\delta^{18}O$ of basaltic rocks is broadly related to the crustal residence time of the liquid. Our average might be slightly biased towards high $\delta^{18}O$ values if the crust is dominantly made up of highly evolved basalts which are lower in $\delta^{18}O$ than the primitive ones.

4.4.2 Hydrothermally Altered Crust

A significant portion of the rift-zone crust is subjected to subsolidus hydrothermal interaction in addition to the supersolidus exchange/assimilation mentioned above. High temperature geothermal fields (T≈200°C at 1 km depth) in the rift-zones are intimately associated with the volcanic systems. Shallow magma reservoirs and conduits provide the heat that drives convection in the geothermal systems. Hattori and Muehlenbachs (1982) published oxygen isotope analyses on altered rocks and mineral separates from the geothermal fields at Krafla and Svartsengi. Whole rock samples from the geothermal drill cores display a range of values from -3 ‰ to -10 ‰ (SMOW). Clearly the alteration process in the uppermost part of the geothermal fields leads to an isotopically heterogeneous crust. The net depletion within these hydrothermal systems is a function of the integrated water-rock ratios, composition of the fluids attendant to the alteration process, temperature of interaction, and the abundance and isotopic fractionation properties of the minerals involved. Rather than attempting to integrate these parameters with the necessary assumptions inherent to such an approach, we take a simpler route.

The proportion of rhyolitic and dacitic rocks in Iceland is high compared to other oceanic islands. Dacites and rhyolites in the rift-zones are commonly thought to form as a result of anatexis of hydrothermally altered crust. There is strong evidence to support this claim e.g. from major and trace elements, and from radiogenic isotope systematics (Óskarsson et al., 1982, 1985; Thy et al., 1990; Jónasson 1994). In part by analogy with experimental studies on dehydration melting of basaltic rocks, and based on petrological criteria, the pressure and temperature conditions of melting are approximately 1 to 2 kbars and 800 to 950 °C (Thy et al., 1990; Jónasson, 1994). The $\delta^{18}O$ of the liquids produced by this anatexis probably reflect closely the $\delta^{18}O$ of the protolith (see below), since the potential isotopic fractionations between the liquid, restites and any external fluids, are small at the temperature of melting.

Two scenarios of crustal melting are considered here from the standpoint of oxygen isotope geochemistry. On the one hand the protolith may have become relatively homogeneous at the time of melting. If melting proceeds in isotopic equilibrium, we can calculate the $\delta^{18}O$ of the protolith provided we know the abundance and identity of the phases participating in the melting reaction and the appropriate fractionation factors. Approximate fractionation factors between rhyolite liquid and major restite phases may be obtained from the normative content of quartz and feldspar in glasses (Palin et al., 1996) and experimental calibrations on silicates and oxides (Clayton et al., 1989; Chiba et al., 1989). As an example we take rhyolite glass from the Askja 1875 eruption (analysis no 1, Table 8, in Sigurdsson and Sparks 1981). Assuming this rhyolite formed by fluid absent melting and produced a restite of plagioclase and clinopyroxene as the dominant phases, with minor amounts of oxides and low Ca pyroxene (Spulber and Rutherford, 1983; Thy et al., 1990), we estimate the fractionation between the liquid and restite ($\Delta_{liq\text{-}rest}$) to be approximately 1 ‰ at 1000°C.

On the other hand the homogenization prior to melting may be minimal. The protolith then is heterogeneous with respect to $\delta^{18}O$. In this case the melting would probably be initiated in the most altered and hydrated domains and therefore lowest $\delta^{18}O$ parts of the crust. The $\delta^{18}O$ of the resulting liquids would then be lower than that of the bulk protolith.

At this time it is not possible to say unequivocally which of these two scenarios is more appropriate. We use the $\delta^{18}O$ composition of the rhyolites and dacites as a first approximation to the composition of the protolith (hydrothermally altered crust). Thus rhyolites and dacites are essentially oxygen isotope probes into the history and conditions of the hydrothermally altered crust.

The isotopic composition of siliceous and intermediate rocks span a wider range of $\delta^{18}O$ values (Fig. 4-3) from 0 to +5 ‰ (SMOW) than do the basalts. For the evolved rocks we have included all the data available. Hence products of some eruptions are represented more than once, for example there are several analyses of various phases of the Askja 1875 eruption. This is done in an attempt to get a true reflection of the potential heterogeneity of the protolith. Most of the data come from the volcanic systems of Krafla and Askja. In general, evolved rocks from Askja have the lowest $\delta^{18}O$ from about 0 to +2‰, while those from rocks Krafla have $\delta^{18}O$ values between +1 and +3 ‰. Our unpublished data on evolved rocks from Hengill and published data on rocks from the Kerlingarfjöll region fall between +3 and +5 ‰. The data shows that the depletion

process in the Western rift-zone is much less efficient than in the wider Eastern rift-zone, as pointed out by Óskarsson et al. (1982). It is also clear that the variation among evolved rocks in a given volcanic system is much smaller than the variation along the rift-zone.

There are two samples of icelandite ($\delta^{18}O$ = 4.1 and 3.5 ‰ , respectively) represented among the siliceous and intermediate rocks in Figure 4-3. The icelandites have often been inferred to reflect the process of crystal fractionation (Carmichael 1964) or magma mixing (e.g. Jónasson 1994) or a combination of these two, rather than direct fusion of crust. We therefore limit ourselves only to dacites and rhyolites, for estimating the $\delta^{18}O$ of the average hydrothermally altered crust. Taking the average of the evolved rocks in Figure 4-3 and rounding off we get $\delta^{18}O$ = +2 (± 1) ‰ (SMOW) as a crude estimate of the hydrothermally altered domain in the rift-zones.

Crustal xenoliths from the rift-zones have been analysed for $\delta^{18}O$ only rarely. Muehlenbachs et al. (1974) and Macdonald et al. (1987) presented $\delta^{18}O$ of analysis on crustal xenoliths from the Askja 1875 eruption. The xenoliths display a wider range yet in oxygen isotopic composition. $\delta^{18}O$ whole rock values range from ≈ +3 to -10 ‰ in these samples. The large variation in $\delta^{18}O$ and presence of quartz veins in some xenoliths (Macdonald et al., 1987) suggests that the xenoliths were subjected to subsolidus alteration. Therefore the $\delta^{18}O$ values of the xenoliths should not be taken as proxies for the siliceous liquids generated within the crust. Rather they probably represent material that subsequent to crystallization suffered further depletion in $\delta^{18}O$ due to hydrothermal activity.

4.4.3 The Lower Crust

Gabbroic nodules have been recovered from a number of localities within the rift-zones. In SW- Iceland gabbroic nodules have been described from Hengill, Hraunsvik and the Krisuvik area. Petrological studies on nodules from these localities indicate that they crystallized in magma chambers in the lower crust (Risku-Norja, 1985; Sigurdsson, 1989; Høj, 1993). Pressure constraints are rather poor but pressure of 1 to 3 kbars with an upper limit of 7 to 8 kbars due to presence of plagioclase have been inferred (Risku Norja, 1985; Sigurdsson, 1989; Høj, 1993). These nodules are brought to the surface by late Quaternary or Recent flows and therefore represent samples of zero age crust or the solid fraction of the magma mush. The data available indicate that the more primitive nodules are brought to the surface by the more primitive magmas. The nodules therefore probably do not represent fragments of country rocks unrelated to the magma, but are intimately

associated with the evolution of the host magma at depth. Preliminary work in our laboratory indicates that most of the gabbro nodules show only minor ^{18}O depletion. Plagioclase in the nodules is typically between +4.6 and +5.2 (±0.1)‰ (SMOW). Analyses of clinopyroxene from three nodules give values of +4.4, +4.8 and +5.1 (±0.1)‰ (SMOW).

It seems reasonable to assume that the Icelandic crust becomes more mafic with depth. If most of the basaltic rocks are derived from magma reservoirs in the deep crust, then their isotopic composition must reflect the gabbroic rocks crystallizing in those reservoirs. The $\delta^{18}O$ of the basalts, and the isotopic data gathered from the nodules to date, show that the depletion of the lower crust is relatively small and that a value of +4.4 (±0.5)‰ is also reasonable for the lower crust.

4.4.5 Oxygen Isotopic Composition of the Mantle Source

A direct way to determine the $\delta^{18}O$ of the mantle under Iceland would be to analyze mantle material brought to the surface in Iceland. To date however no mantle nodules have been found on Iceland. Therefore an indirect approach has to be taken.

Among the recently erupted basalts $\delta^{18}O$ values within the range of MORB are rare. Many but not all primitive basalts from the rift-zones have $\delta^{18}O$ values between +5.0 and 5.5 ‰ (SMOW). These basalts may represent the $\delta^{18}O$ value of the mantle under Iceland or alternatively reflect exchange and assimilation processes in the crust.

Gautason et al. (1995) presented $\delta^{18}O$ data on olivine and pyroxene separates from basalts in the Faeroe Islands and NW Iceland. The host basalts derive from successions that respectively represent early and late Tertiary products of the Iceland mantle plume. Olivines from the Faeroe Islands and pyroxenes from basalts in NW-Iceland have $\delta^{18}O$ values from +4.4 to + 4.9‰ and +4.6 to +5.3‰ (SMOW), respectively (Gautason and Muehlenbachs in preparation). Mineral-melt fractionations in basaltic systems are not well constrained. However a direct comparison of the Icelandic and Faeroe data with $\delta^{18}O$ values of the same phases from MORB and Lunar basalts indicates the $\delta^{18}O$ of the original liquids. Lunar basalts and MORBs display the same relatively narrow range of $\delta^{18}O$ values (e.g. Onuma et al., 1972). Olivines and clinopyroxenes separated from MORB basalts range from +4.78 to +5.35 (7 analyses) and +5.18 to +5.73 ‰ (3 analyses), respectively (Muehlenbachs and Clayton 1972). Oxygen isotope data presented by Onuma et al. (1970) and Clayton et al. (1971) on these same phases separated from crystalline

Lunar rocks give +5.05 to +5.25 ‰ for olivine (6 analyses) and +5.33 to +5.77 ‰ for clinopyroxene (18 analyses). The data from NW Iceland and the Faeroe Islands therefore suggests that the melts erupted from the Iceland mantle plume over the last 50 Ma have a $\delta^{18}O$ possibly as low as +4.9 and as high as +5.5 ‰. While this range overlaps slightly the observed range in MORBs, it is displaced to lower values.

Unusually high $\delta^{18}O$ values of +6.25‰ for a picrite from Reykjanes peninsula and 6.30‰ for a picrite from Theistareykir in north Iceland were reported by Hémond at al., (1988; 1993). Originally Hémond et al. (1988) considered subsolidus weathering to be responsible for the very high $\delta^{18}O$ (+6.25‰) value of sample RSG 54. We suggest this may be true for both picrites. Notably Muehlenbachs and Jakobsson (1979) gave 5.53 ± 0.06 as an average for four small picrite shields from the Reykjanes peninsula.

Together the above arguments indicate that either the mantle source under Iceland, and thereby the plume, differs from that of MORB with respect to its oxygen isotopic composition and the plume is possibly heterogeneous with respect to $\delta^{18}O$. Alternatively it suggests that assimilation and exchange processes are very effective in overprinting even the most primitive lavas, and that assimilation and exchange processes similar to those operating presently, were also at work in the past.

Studies on basalts from other oceanic islands such as Hawaii (Kyser et al., 1982; Garcia et al., 1989; Eiler et al., 1996) and the Canary Islands (Thirlwall et al., 1997) have identified low-^{18}O basalts ($\delta^{18}O \approx +4.9$ to + 5.5 ‰) on these Islands. In the case of Hawaii, Eiler et al.(1996) advocate oxygen isotopic exchange between the plume derived magmas and the overriding Pacific oceanic crust or assimilation of this crust into the magma. In contrast Kyser et al. (1982) and Garcia et al. (1989) had previously interpreted the $\delta^{18}O$ signal to be primary. Thirlwall et al. (1997) on the other hand suggested the presence of recycled oceanic crust in the Canary Islands plume.

It is difficult to establish unequivocally the origin of moderate ^{18}O depletions that have been reported on some oceanic islands. For Iceland specifically this is problematic given the massive overprinting by the present-day hydrothermal signal. For the purpose of the calculations that follow we use a value $\delta^{18}O = +5.2 \pm 0.3$ ‰, for primary mantle derived liquids entering the Icelandic rift-zone. We also discuss the effect of choosing a different initial $\delta^{18}O$ value.

4.5 Model Results

To summarize: Basaltic liquid with isotopic composition of $\delta^{18}O = +5.2 \pm 0.3‰$ intrudes into the crust at the base of the rift-zone. Isotopic exchange processes involving fluids, magma, and country rock, result in a lowering of the $\delta^{18}O$ of the magma. The average composition of basalts that have been subjected to this exchange/assimilation process is $\delta^{18}O = +4.4 \pm 0.5‰$, with amount of depletion correlating roughly with the residence time of the basaltic liquid. Subsolidus hydrothermal alteration further depletes a portion of the crust. The average composition of this altered crust is taken to be $\delta^{18}O = +2 \pm 1‰$.

The net depletion of the crust of ^{18}O depends on the proportion of crust that is subjected to the subsolidus hydrothermal alteration. This is difficult to estimate. Questions that have to be answered first are, to what depth does the hydrothermally altered package sink before it leaves the rift-zone and how thick is the crust? It is clear, however, that the average $\delta^{18}O$ of the crust will lie between the $\delta^{18}O$ composition of the two crustal domains discussed above.

The hydrothermally altered package probably makes up about half of the upper crust. This is supported by the observations that rhyolites and dacites constitute close to 10% of the Tertiary lava pile (Walker, 1959) and approximately 20% of Tertiary central volcanoes (e.g. Carmichael, 1964). Given the assumption that all evolved material is associated with central volcanoes then these centers must make up about 50% of the upper crust. Models of crustal accretion along the rift axis indicate that surface material may be brought down to depths of 10 to 12 kilometers (Pálmason, 1986). If we assume that the near surface hydrothermally altered package, or its re-crystallized equivalent, is not brought down much below this depth (below 10 km) then we have 1/2 and 1/4 as upper and lower limits respectively, on the amount of hydrothermally altered material in the crust. In light of these simple arguments we estimate the net flux F_{hs} assuming that 1/3 of the crust is subjected to some degree of hydrothermal subsolidus alteration.

The net flux is obtained from the product of the mass of oxygen in the crust that is available for exchange with the hydrosphere annually, and the change in composition of the crust associated with this exchange. We estimate the flux to the hydrosphere to be $F_{hs} = 5.5 (\pm 3.7) \times 10^8$ (g ^{18}O/ a). This flux is based on a starting composition for basalts of 5.2 $\pm$ 0.3‰. If on the other hand the mantle source for Iceland is the same as MORB with

respect to $\delta^{18}O$ then the net flux of F_{hs} increases by about 30%. In either case, there is a considerable flux of ^{18}O to the hydrosphere from the rift-zones in Iceland (see below).

Our results suggest that the $\delta^{18}O$ of the crust is lowered by only 1 to 3 ‰ on average. This is somewhat surprising in light of the ≈15‰ difference between the $\delta^{18}O$ of the mantle and local precipitation. We note here that these results are based on near "zero" age material. It is possible that the lower crust in particular may be depleted further as it drifts away from the ridge axis, analogous to layer 3 gabbros (e.g. Gregory and Taylor, 1981). The role of these second order processes depend on how far down are surface derived fluids recharged, and for how long after the formation of crust such recharge continues.

4.6 Comparison to Oceanic Rifts

The estimated flux of ^{18}O through the rift is readily compared to ^{18}O-fluxes associated with hydrothermal alteration of gabbros at mid-ocean ridges. It is well known from studies of rocks drilled and dredged from the seafloor, and from studies on ophiolites, that seawater-rock interaction at mid-ocean ridges leaves a characteristic oxygen isotopic imprint on the oceanic crust. In brief, the upper part of the crust (roughly equivalent to seismic layer 2) is enriched in $\delta^{18}O$ and the lower (≈ seismic layer 3) is depleted in $\delta^{18}O$. High temperature (≈350°C) seawater rock interaction leads to a depleted crust and associated with it is a flux of ^{18}O to the oceans. In contrast, low temperature (<150°C) weathering of the upper oceanic crust results in a flux of ^{18}O from the ocean to the crust. The ocean also loses ^{18}O through weathering of continental crust. As a consequence of the opposing fluxes the $\delta^{18}O$ of sea water is maintained at a steady state value of ≈ 0 ± 2‰ (Muehlenbachs and Clayton, 1976; Gregory and Taylor, 1981; see also Muehlenbachs, this issue).

For comparison, we calculate the ^{18}O-flux out of layer 3 gabbros of mid-ocean ridges. For the calculation it is assumed that the gabbros had an average $\delta^{18}O$ composition of +5.7 ± 0.3‰ prior to alteration and an $\delta^{18}O$ of +4.5 ± 0.5‰ subsequent to the hydrothermal interaction. Scaling to the same length and spreading rate as for the Icelandic rift-zone the resultant flux is F_{mor} = 1.1 (±0.4) 10^8 (g ^{18}O/a) assuming 5 km thickness for the gabbroic section. This demonstrates that the rift-zones in Iceland are efficient in releasing ^{18}O into the hydrosphere. Annually they release up to 5 times the

amount of ^{18}O as does an equivalent length of mid-ocean ridge. This is a result of the much larger mass being cooled and exposed to the hydrosphere and the low $\delta^{18}O$ meteoric waters involved in the crust/hydrosphere reactions.

4.7 Discussion.

4.7.1 *^{18}O of Seawater*

The comparison between the ^{18}O-flux from the rift-zones in Iceland and mid-ocean ridges is of interest in that it allows us to address models that deal with the variation of the oxygen isotopic composition of seawater through time.

Lohman and Walker (1989) interpreted the $\delta^{18}O$ of abiotic marine calcite from Devonian age formations to reflect the isotopic composition of Devonian seawater. The data suggests that Devonian seawater was approximately -6 ±1 ‰ relative to present day seawater. This observation led Walker and Lohman (1989) to examine tectonic scenarios that would allow isotopically depleted seawater to persist. Specifically they suggested that such a low-^{18}O ocean could be maintained if sea level was much lower so that the mid ocean rift system would be largely or completely above sea level. Walker and Lohman (1989) proposed that such a tectonic configuration results in the termination of the ^{18}O-flux from the mantle to the ocean, since high-temperature, seawater-rock interaction at the mid-ocean ridges ceases.

We argue that the volcanic rift-zones in Iceland serve as a good model for mid-ocean ridges above sea level. To make a comparison independent of the thickness of the crust we normalize the flux F_{mor} and F_{hs} to the same volume of crust. We also have to examine whether the present day meteoric derived hydrothermal fluids are reasonable proxies for similar fluids derived from depleted seawater. Precipitation in coastal areas of Iceland ranges from -8 to -11 ‰ (Árnason, 1976). The isotopically light precipitation in Iceland plays a big role in the efficient, present day, transfer of ^{18}O to the hydrosphere. This may seem to render the comparison between the Icelandic rift-zones and past mid-ocean ridges meaningless. Given that the global average precipitation distilled from present day oceans (≈ 0 ‰) is ≈ -4 ‰ (e.g. Gat, 1996) we submit that the precipitation on Iceland is a good model analog for precipitation distilled from a -6 ±1 ‰ Devonian sea. A comparison between Iceland and mid-ocean ridges, purportedly surrounded by a depleted ocean, is therefore straightforward.

Normalizing the fluxes to equivalent volumes of altered crust we find F'_{mor} to be = 33 (± 12) 10^8 (g $^{18}O/km^3$) compared to 44 (±33) 10^8 (g $^{18}O/km^3$) for F'_{hs}. So on a

crustal volume equivalent basis, the flux of ^{18}O from the rift-zones in Iceland is comparable to that of present day mid-ocean ridges. We argue that Iceland is a good model analog for mid-ocean ridge system emerged from an ocean. If this tectonic configuration was ever prevalent, our results demonstrate that a substantial flux of ^{18}O from the mantle to the hydrosphere would still have occurred.

4.7.2 Low ^{18}O Magmas

Our summary warrants a comment on the mechanism of producing the enigmatic low $\delta^{18}O$ magmas in Iceland. This problem has often been debated (e.g. Muehlenbachs et al., 1974; Condomines, 1983; Taylor, 1986; Sheppard, 1986). Four contrasting origins have been proposed for the low $\delta^{18}O$ magmas in Iceland. 1) The anomaly is of primary origin i.e. reflects an anomalous mantle under Iceland; 2) Assimilation by magmas of hydrothermally altered and depleted wall rock; 3) Oxygen isotope exchange between magma and the depleted crust, i.e. the magma essentially equilibrates with the crust through isotopic exchange; 4) Surface derived fluids interact directly with the magma at depth.

Above we have attributed the anomaly in part to the mantle source. However most of the depletion must be related to processes in the crust. The second and third scenarios mentioned above are often postulated. In particular, some workers have proposed Assimilation-Fractional Crystallization (AFC) type models (e.g. Nicholson et al., 1991; Sigmarsson et al., 1991a). To satisfy the data, the oxygen isotopic composition of the assimilant is proposed to be very low in $\delta^{18}O$ ($\approx$ -8 to -10 ‰). Certainly hydrothermally altered basalts with $\delta^{18}O$ as low as -10‰ (SMOW) have been recovered from drill holes (Hattori and Muehlenbachs, 1982) from high temperature geothermal systems. These results seemingly provide support for the AFC type models. But such a low $\delta^{18}O$ crust is not ubiquitous. The rhyolites and dacites in the rift-zones are not nearly as depleted as the proposed assimilant, and if they are produced by 10 to 20 % melting of hydrothermally altered basalt, they provide the best estimate of the average depletion of the hydrothermally altered package. In light of our assessment of the oxygen isotopic composition of the Icelandic crust, the AFC type models are difficult to accept. The assumption of a -10 ‰ assimilant in these calculations is not realistic. It should be made clear, however, that we do not rule out assimilation of crustal material as an important process in the magmatic evolution of rift-zone volcanics. Rather we maintain that the $\delta^{18}O$ of the volcanic rocks unveil a process, more complicated than a simple AFC scenario. In particular the potential

role of direct interaction of deep seated surface derived fluids and magma should be investigated.

4.8 Conclusions

Analyses of the $\delta^{18}O$ data from Iceland leads us to conclude that interactions with the hydrosphere have lowered the $\delta^{18}O$ of the rift-zone crust by about 1 to 3‰ relative to the initial mantle value of $\delta^{18}O \approx 5.2 \pm 0.3$‰. In spite of the relatively small ^{18}O-depletion in the crustal rocks, the resulting ^{18}O-flux from the lithosphere to the hydrosphere is substantial.

The Icelandic rift-zones are efficient at transferring ^{18}O to the hydrosphere. We estimate that on a volume equivalent basis the rift-zones release comparable amounts of ^{18}O as do layer 3 mid-ocean ridge gabbros. It is therefore impossible to maintain low $\delta^{18}O$ ocean by simply raising the mid-ocean ridge systems above sea level. This only changes the source of the hydrothermal fluids but does not prevent a significant flux of ^{18}O to the hydrosphere. Other tectonic configurations, however, such as inland or epeiric seas (e.g. Holmden et al., 1997), which are in limited chemical communication with the ocean at large, could possibly maintain localized low $\delta^{18}O$ water masses for significant periods of time.

4.9 References

Árnason, B., 1976. Groundwater systems in Iceland traced by Deuterium. Societas Scientarium Islandica, 236 pp.

Baertschi, P., 1976. Absolute ^{18}O content of Standard Mean Ocean Water. Earth Planet. Sci. Lett. 31, 341-344.

Bjarnason, I.Th., Menke, W., Flóvenz, Ó.G. and Caress, D., 1993. Tomographic image of the Mid-Atlantic boundary in southwestern Iceland. J. Geophys. Res. 98, 6607-6622.

Brandsdóttir, B., Menke, W., Einarsson, P., White, R.S., Staples, R.K., 1997. Færoe-Iceland ridge experiment. 2. Crustal structure of the Krafla central volcano. J. Geophys Res. 102, 7867-7886.

Carmichael, I.S.E., 1964. The petrology of Thingmuli, a Tertiary volcano in eastern Iceland. J. Petrol. 5, 435-460.

Chiba, H., Chacko, T., Clayton, R.N., Goldsmith, J.R., 1989. Oxygen isotope fractionations involving diopside, forsterite, magnetite, and calcite. Geochim. Cosmochim. Acta 53, 2985-2995.

Clayton, R.N., Goldsmith, J.R., Mayeda, T.K., 1989. Oxygen isotope fractionations in quartz, albite, anorthite and calcite. Geochim. Cosmochim. Acta 53, 725-733.

Clayton, R.N., Onuma, N., Mayeda, T.K., 1971. Oxygen isotope fractionation in Apollo 12 rocks and soils. Geochim. Cosmochim. Acta Suppl. 2, 2, 1417-1420.

Condomines, M., Grönvold, K., Hooker, P.J., Muehlenbachs, K., O'Nions, R.K., Óskarsson, N. and Oxburgh, E. R., 1983. Helium, oxygen, strontium and neodymium isotopic relationships in Icelandic volcanics. Earth Planet. Sci. Lett. 66, 125-136.

Eiler, J.M., Farley, K.A., Valley, J.W., Hofman, A.W., Stolper, E.M., 1996. Oxygen isotope constraints on the sources of Hawaiian volcanism. Earth Planet. Sci. Lett. 144, 453-468.

Elderfield, H., Schultz, A., 1996. Mid-ocean ridge hydrothermal fluxes and the chemical composition of the ocean. Annu. Rev. Earth Planet. Sci. 24, 191-224.

Gat, J.R., 1996. Oxygen and hydrogen isotopes in the hydrologic cycle. Annu. Rev. Earth Planet. Sci. 24, 225-262.

Garcia, M.O., Muenow, D.W., Aggrey, K.E., O'Neil, J.R., 1989. Major element, volatile, and stable isotope geochemistry of Hawaiian submarine tholeiitic glasses. J. Geophys. Res. 94, 10525-10538.

Gautason, B., Muehlenbachs, K., Heinesen, M., Waagstein, R., 1995. δ ^{18}O of the Iceland Mantle plume: Evidence for recycling of oceanic crust? International Union of Geodesy and Geophysics, XXI General Assembly, Boulder Colorado, Abstracts Week B, p. B418

Gregory, R. T., Taylor, H. P., 1981. An oxygen isotope profile in a section of Cretaceous oceanic crust, Samail ophiolite, Oman: Evidence for δ ^{18}O buffering of the oceans by deep (> 5 km) seawater hydrothermal circulation at mid-ocean ridges. J. Geophys. Res. 86, 2737-2755.

Harmon, R. S., Hoefs, J., 1995. Oxygen isotope heterogeneity of the mantle deduced from global ^{18}O systematics of basalts from different geotectonic settings. Contrib. Mineral. Petrol. 120, 95-114.

Hattori, K., Muehlenbachs, K.(1982. Oxygen isotope ratios of the Icelandic crust. J. Geophys. Res. 87, 6559-6565.

Hémond, C., Condomines, M., Fourcade, S., Allégre, C., Óskarsson, N., Javoy, M., 1988. Thorium, strontium and oxygen isotopic geochemistry in recent tholeiites from Iceland: crustal influence on mantle-derived magmas. Earth Planet. Sci. Lett. 87, 273-285.

Hémond, C., Arndt, N.T., Lichtenstein, U., Hofmann, A.W., Óskarsson, N., Steinthórsson, S., 1993. The heterogeneous Iceland plume: Nd-Sr-O Isotopes and trace element constraints. J. Geophys. Res. 98, 15833-15850.

Holmden, C., Creaser, R.A., Muehlenbachs, K., Leslie, K., Bergstrom, S.M., 1997. Isotopic evidence for geochemical decoupling between ancient epeiric seas and bordering oceans: Implications for secular curves. Annual meeting of the Geological and Mineralogical Associations of Canada, Abstracts, 22, p. A-69.

Høj, J.W., 1993. Gabbro-anorthosite nodules from the Krisuvik fissure system and active zone of rifting, Reykjanes peninsula, SW Iceland. Neues Jb. Miner. Abh. 165, 168-169.

Ito, E., White, W.M., Göpel, C., 1987. The O, Sr, Nd and Pb isotope geochemistry of MORB. Chem. Geol. 62, 157-176.

Jakobsson, S.P., 1972. Chemistry and distribution patterns of Recent basaltic rocks in Iceland. Lithos 5, 365-386.

Jakobsson, S.P., 1979. Outline of the petrology of Iceland. Jökull 29, 57-73.

Jakobsson, S.P., Jónsson, J., Shido, F., 1978. Petrology of the western Reykjanes peninsula, Iceland. J. Petrol. 19, 669-705.

Jónasson, K., 1994. Rhyolite volcanism in the Krafla central volcano, north-east Iceland. Bull. Volcanol. 56, 516-528.

Kyser, T.K. O'Neil J.R., Carmichael, I.S.E., 1982. Genetic relations among basic lavas and ultramafic nodules: Evidence from oxygen isotope compositions. Contrib. Mineral. Petrol. 81, 88-102.

Lohman, K.C., Walker, J.C.G., 1989. The $\delta\ ^{18}O$ record of phanerozoic abiotic marine calcite cements. Geophys. Res. Lett. 16, 319-322.

Macdonald, R., Sparks, R.S.J., Sigurdsson, H., Mattey, D.P., McGarvie, D.W., Smith, R.L., 1987. The 1875 eruption of Askja volcano, Iceland: combined fractional crystallization and selective contamination in the generation of rhyolitic magma. Mineral. Mag. 51, 183-202.

Muehlenbachs, K., 1973. The oxygen isotope geochemistry of siliceous volcanic rocks from Iceland. Carnegie Inst. Wash. Yearb. 72, 593-597.

Muehlenbachs, K., Clayton, R.N., 1972. Oxygen isotope studies of fresh and weathered submarine basalts. Can. J. Earth Sci. 9, 172-184.

Muehlenbachs, K., Clayton, R.N., 1976. Oxygen isotopic composition of the oceanic crust and its bearing on seawater. J. Geophys. Res. 81, 4365-4369.

Muehlenbachs, K., Jakobsson, S.P., 1979. The $\delta\ ^{18}O$ anomaly in Icelandic basalts related to their field occurrence and composition. EOS 60, p.408.

Muehlenbachs, K., Anderson, A.T., Sigvaldason, G.E., 1974. Low-O^{18} basalts from Iceland. Geochim. Cosmochim. Acta 38, 577-588.

Nicholson, H., Condomines, M., Fitton, J. G., Fallick, A.E., Grönvold, K., Rogers, G., 1991. Geochemical and isotopic evidence for crustal assimilation beneath Krafla, Iceland. J. Petrol. 32, 1005-1020.

Onuma, N., Clayton, R.N., Mayeda, T.K., 1970. Oxygen isotope fractionations between minerals, and an estimate of the temperature of formation. Geochim. Cosmochim. Acta Suppl. 1, 2, 1429-1434.

Onuma, N., Clayton, R.N., Mayeda, T.K., 1972. Oxygen isotope cosmothermometer. Geochim. Cosmochim. Acta 36, 169-188.

Óskarsson, N., Sigvaldason, G.E., Steinthórsson, S., 1982. A dynamic model for the rift-zone petrogenesis and the regional petrology of Iceland. J. Petrol. 23, 28-74.

Óskarsson, N., Sigvaldason, G.E., Steinthórsson, S., 1985. Iceland geochemical anomaly: origin volcanotectonics, chemical fractionation and isotope evolution of the crust. J. Geophys Res. 90, 10011-10025.

Palin, J.M., Epstein, S., Stolper, E.M., 1996. Oxygen isotope partitioning between rhyolite glass/melt and CO_2: An experimental study at 550-950°C and 1 bar. Geochim Cosmochim Acta 60, 1963-1973.

Pálmason, G., 1986).Model of crustal formation in Iceland and application to submarine mid-ocean ridges. In P.R. Vogt and B.E. Tucholke, (Eds.). "The geology of North America, Volume M, The western North Atlantic region." Geological Society of America, 87-97.

Pálmason, G., Saemundsson, K., 1979. Summary of conductive heat flow in Iceland. In V. Cermak, L. Rybach (Eds.)."Terrestrial heat flow in Europe", Springer Verlag, 137-139.

Pineau, F., Javoy, M., Hawkins, J.W., Craig, H., 1976. Oxygen isotope variations in marginal basin and ocean-ridge basalt. Earth Planet. Sci. Lett. 28, 299-307.

Risku-Norja, H., 1985. Gabbro nodules from a picritic pillow basalt, Midfell, SW Iceland. Nordic Volcanol. Inst. Prof. Paper 8501.

Saemundsson, K., 1978. Fissure swarms and central volcanoes of the nevolcanic zones of Iceland. Geol. J. Spec. Issue 10, 415-432.

Saemundsson, K., 1979. Outline of the geology of Iceland. Jökull 29, 7-28

Sheppard, S.M.F., 1986. Igneous Rocks III. Isotopic case studies of magmatism in Africa, Eurasia and Oceanic Islands. In J.W. Valley, H.P. Taylor, J.R. O'Neil, (Eds.). Stable isotopes in high temperature geological processes. Reviews in Mineralogy 16, Mineralogical Society of America, 319-371.

Sigmarsson, O., Condomines, M., Grönvold, K. and Thórdarsson, Th., 1991a. Extreme magma homogeneity in the 1783-1784 Lakagigar eruption: Origin of a large volume of evolved basalt in Iceland. Geophys. Res. Lett. 18, 2229-2232.

Sigmarsson, O., Hémond, C., Condomines, M., Fourcade, S., Óskarsson, N., 1991b. Origin of silicic magma in Iceland revealed by Th isotopes. Geology 19, 621-624.

Sigmarsson, O., Condomines, M., Fourcade, S., 1992. Mantle and crustal contribution in the genesis of Recent basalts from off rift zones in Iceland: Constraints from Th, Sr and O isotopes. Earth Planet. Sci. Lett. 110, 149-162.

Sigmundsson, F., Einarsson, P., Bilham, R., Sturkell, E., 1995. Rift-transform kinematics in south Iceland: Deformation from Global Positioning System measurements, 1986-1992. J. Geophys. Res. 100, 6235-6248.

Sigurdsson, I.A., 1989. Gabbrohnydlingar i Hraunsvik a Reykjanesskaga. B.Sc. hon. thesis. University of Iceland, pp. 67.

Sigurdsson, H., 1977. Generation of Icelandic rhyolite by melting of plagiogranites in the oceanic layer. Nature 269, 25-28.

Sigurdsson, H., Sparks, R.S.J., 1981. Petrology of rhyolitic and mixed magma ejecta from the 1875 eruption Askja, Iceland. J. Petrol. 22, 41-84.

Spulber, S.D., Rutherford, M.J., 1983. The origin of rhyolite and plagiogranite in oceanic crust: an experimental study. J. Petrol. 24, 1-25.

Steinthórsson, S., 1987. Hradi landmyndunar og landeydingar. Náttúrufraedingurinn 57, 81-95.

Steinthórsson, S., Óskarsson, N., Arnórsson, S., Gunnlaugsson, E., 1987. Metasomatism in Iceland: Hydrothermal alteration and remelting of oceanic crust. In H.C. Helgeson (Ed.). Chemical transport in metasomatic processes. D. Reidel, Dordrecht, pp. 355-387.

Taylor, H.P., 1986. Igneous rocks II. Isotopic case studies in circumpacific magmatism. In J. W. Valley, H.P. Taylor, J.R. O'Neil, (Eds.). Stable isotopes in high temperature geological processes. Reviews in Mineralogy 16, Mineralogical Society of America, 273-317.

Thirlwall, M.F., Jenkins, C., Vroon, P.Z., Mattey, D.P., 1997. Crustal interaction during construction of ocean islands: Pb-Sr-Nd-O isotope geochemistry of the shield basalts of Gran Canaria, Canary Islands. Chem. Geol. 135, 233-262

Thorarinsson S., Saemundsson K., 1979. Volcanic activity in historical times. Jökull 29, 29-32.

Thy, P., Beard, J.S., Lofgren, G.E., 1990. Experimental constraints on the origin of Icelandic rhyolites. J. Geol. 98, 417-421.

Tryggvason E., 1974. Vertical crustal movement in Iceland. In L. Kristjánsson (Ed.) Geodynamics of Iceland and the North Atlantic area, D. Reidel, Dordrecht, pp. 241-262.

Tryggvason, K., Huseby, E.S., Stefánsson, R., 1983. Seismic image of the hypothesized Icelandic hotspot. Tectonophysics 100, 97-118.

Walker, G.P.L., 1959. Geology of the Reydarfjordur area eastern Iceland. Quat. J. Geol. Soc. London 114, 367-393.

Walker, J.C.G., Lohman, K.C., 1989. Why the oxygen isotopic composition of seawater changes with time. Geophys. Res. Lett. 16, 323-326.

Wolfe, C.J., Bjarnason, I.Th., VanDecar, J.C., Solomon, S.C., 1997. Seismic structure of the Iceland mantle plume. Nature 385, 245-247.

Table 4-1 Summary of flux calculations for the rift zones in Iceland and a comparison to similar fluxes associated with hydrothermal metamorphism at Mid-Ocean Ridges

Crustal domain	Mode of exchange	Final $\delta^{18}O$ ‰ (SMOW)	Flux per 300 km rift segment $x10^{-8}$ (g ^{18}O/a)	Flux per km^3 rock exchanged $x10^{-8}$ (g $^{18}O/km^3$)
Upper Crust	Subsolidus	+2.0 (±1.0)		
(≈ 10 km thick)	Supersolidus	+4.4 (±0.5)	F_{hs} = 5.5 (±3.7)	F'_{hs} = 44 (±33)
Lower Crust	Supersolidus	+4.4 (±0.5)		
(≈ 10 km thick)				
MORB gabbros	Subsolidus	+4.5 (±0.5)	F_{mor} = 1.1 (±0.4)	F'_{mor} = 33 (±12)
(≈ 5 km thick)				

Calculations assume 48% (wt.) oxygen and a density of 2.9 g/cm^3 for the crust

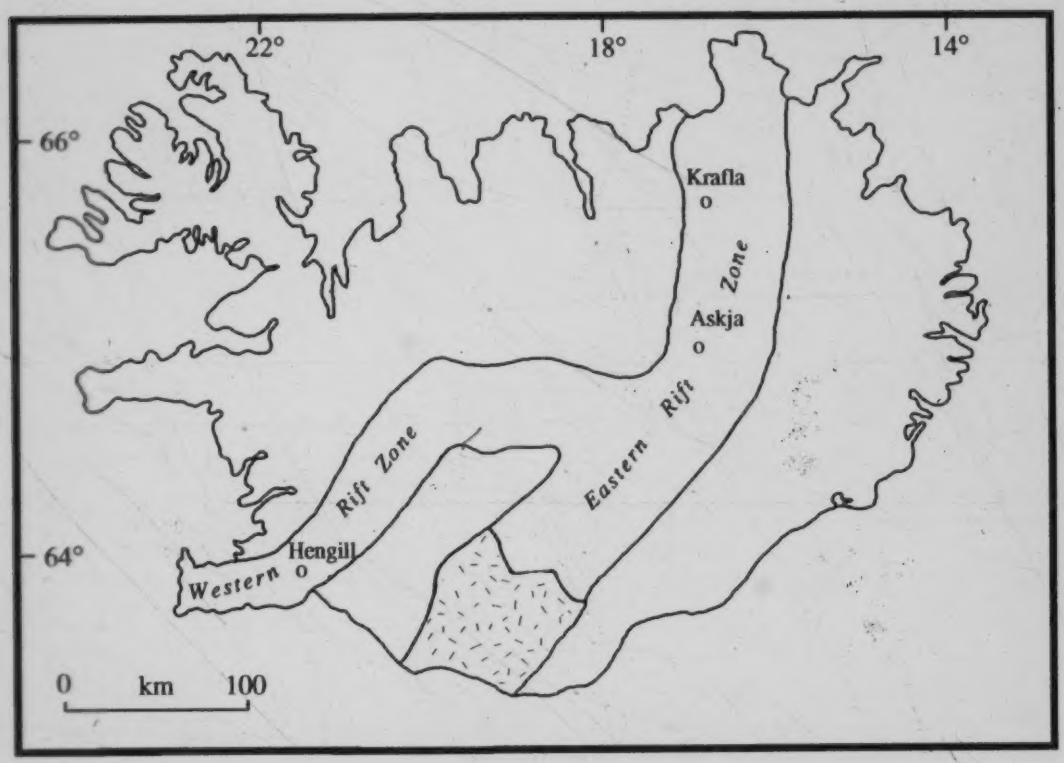

Figure 4-1 Simple map of iceland showing the outlines of the rift zones. Location of volcanic systems discussed in the text is also indicated. Stippled area shows the "propagating rift" dominated by transitional and alkalic volcanics.

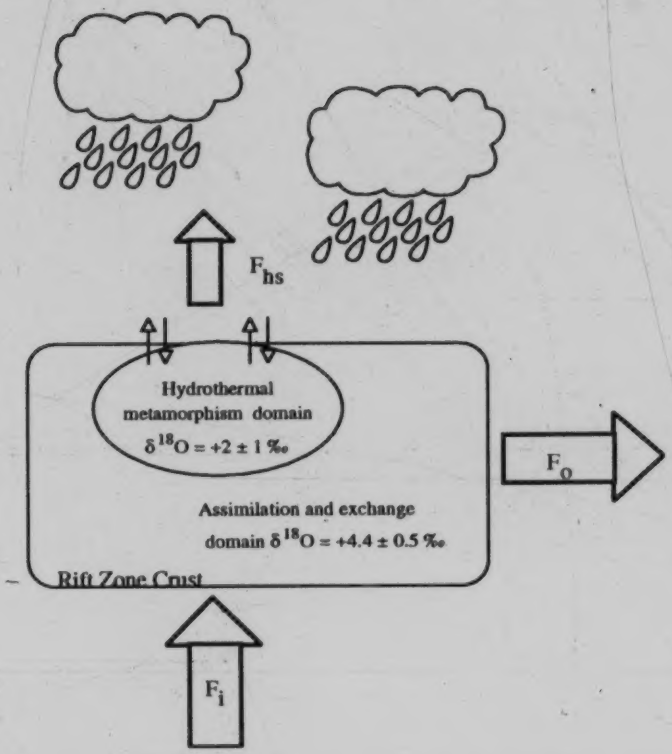

Figure 4-2. Cartoon illustrating the model used for calculating ^{18}O-fluxes associated with high-temperature processes in the rift zones. Fhs is the net ^{18}O-flux to the hydrosphere resulting from isotopic exchange between the crustand hydrosphere. The small arrows illustrate that this is an exchange process, i.e. water is not added to or lost from the hydrosphere. Fi and Fo are fluxes associated with mass transport. Fi denotes the ^{18}O-flux from the mantle to the crust. Fo is the flux out of the rift zone reservoir by erosion and seafloor spreading.

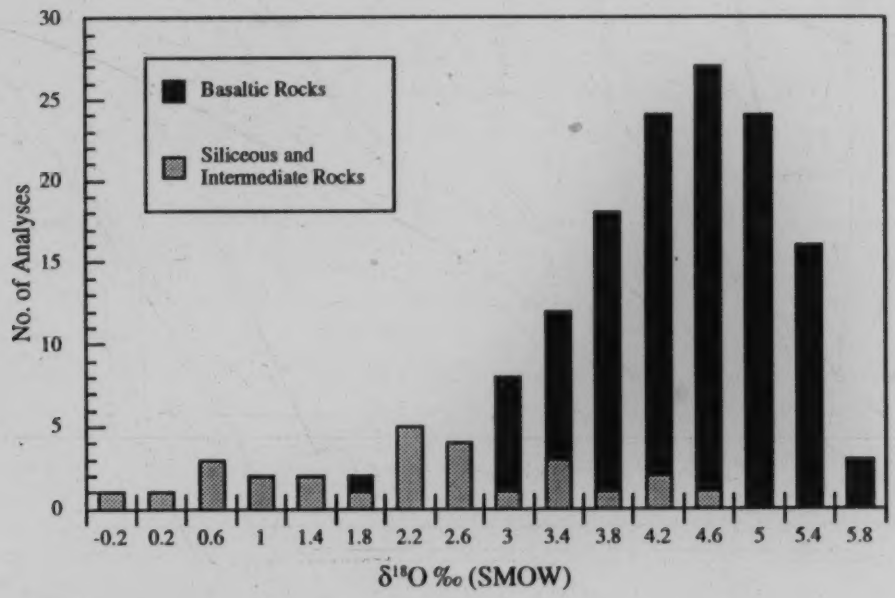

Figure 4-3 Histogram of $\delta^{18}O$ of fresh tholeitic volcanics (glasses and whole rocks) from the rift zones in Iceland. Data from: Muehlenbachs, 1973; Muehlenbachs et al., 1973; Condomines et al., 1983; Macdonald et al., 1987; Hémond et al., 1988; 1993; Nicholson et al., 1991; Sigmarsson et al., 1991b; 1992.

Chapter 5

MELT-MANTLE REACTIONS AS A POSSIBLE LINK BETWEEN ENRICHED AND DEPLETED MAFIC MELTS: EVIDENCE FROM REACTION TEXTURES AND TRACE-ELEMENT CONCENTRATIONS IN CLINOPYROXENE BEARING NODULES AND MEGACRYSTS IN THE DAGMÁLAFELL PICRITE, SW ICELAND.

5.1 Introduction

Early work on basalts from continents and the ocean basins established that the mantle is heterogeneous with respect to its trace-element and isotopic composition (Gast et al., 1964; Tatsumoto et al., 1965; Gast, 1968). In subsequent studies researchers attempted to resolve questions regarding the origin, dimensions and distribution of the various end-members (components) in the mantle (e.g. Zindler and Hart 1986; Allégre, 1987; Hofmann, 1997). Mapping of these heterogeneities in space and time will provide important insights into convection in the mantle through time. However, at this time a clear picture has not emerged.

With the ever increasing capacity to analyze small samples, it is becoming abundantly clear that the mantle is heterogeneous on a variety of length scales. One example of small scale heterogeneity is revealed in studies on abyssal peridotites. In these mantle samples REE (Rare Earth Element) abundances and abundance ratios in diopside vary greatly between samples of similar composition and mode, dredged or drilled in the same section (e.g. Johnson et al., 1990). Another example of small-scale heterogeneity is the extreme variation in trace-element abundance ratios and isotope ratios observed in olivine-hosted melt inclusions in mafic basalt from the ocean floor (Sobolev and Shimizu 1993; Saal et al., 1998).

---

1) A version of this chapter will be submitted to a peer reviewed journal for consideration, with Dr. K. Muehlenbachs as second author.

In the case of Iceland and its associated mantle plume, a simple mixing model was proposed in the early 70's, which suggested mixing of plume and MORB (mid-ocean ridge basalt) sources for lavas erupting along the rift traversing the island (Schilling 1973; Hart et al., 1973). Subsequently, workers have attempted to evaluate the length scale of mantle heterogeneities in the mantle beneath Iceland (Zindler et al., 1979; Furman et al., 1995) and/or the contributions of inferred mantle and crustal components to the magma budget in the various volcanic regions (Sigmarsson et al., 1992; Hémond et al., 1993). Again, a general consensus has not emerged. Of note in this context, however, is a recent contribution that confirmed early indications that compositional extremes (e.g. in incompatible element abundance ratios) are confined to relatively small volume lavas in the rift zones (Hardarson and Fitton 1997).

Among the mafic lavas erupted in the rift zones, the picrites are the most depleted in incompatible trace-elements. They also have the highest $^{143}Nd/^{144}Nd$ ratios and relatively low $^{206}Pb/^{204}Pb$ ratios (Zindler et al., 1979; Elliott et al., 1991; Hémond et al., 1993). As such, they form an end-member among Recent Icelandic basalts in terms of their trace-element and radiogenic isotopic composition. They are considered by some authors to be derived from a depleted (MORB-like) mantle component. The spectrum of mafic magmas from enriched (OIB-like) to depleted compositions, reflects mixing of mantle components or melts derived from them (Zindler et al., 1979; Hémond et al., 1993; Gee et al., 1998a). Alternatively, dynamic melting models have been suggested, where variation in melt fraction and depth of melting contribute to the compositional spectrum. The picrites are then derived by large degrees of melting from the top of the melting column (Elliott et al., 1991; Gurenko and Chaussidon 1995).

In this paper we document small, and fine-grained nodules (micro-nodules) consisting of clinopyroxene and Cr-spinel with or without olivine. These occur in the Dagmálafell picrite, a subglacial hyaloclastite from the Hengill area in SW-Iceland. The micro-nodules are found at the interface of the picrite groundmass and anorthositic gabbro-nodules. They are interpreted to be the remnants of a reaction corona formed during reactions between mafic melt and solids. The solid reactants may have re-crystallized during the reaction. This picrite is also host to clinopyroxene megacrysts, with rare Cr-spinel inclusions, and gabbroic plagioclase + clinopyroxene ± olivine nodules.

This paper presents new trace and rare earth element (REE) data on clinopyroxene from the Dagmálfell picrite. Large variation in trace and REE abundances among the three basic types of clinopyroxene (megacrysts, micro-nodules and gabbro-nodules) is demonstrated for the first time. In contrast, major-element variation among the three different types of clinopyroxene is small, and thus decoupled from the trace-element

abundances. On the basis of these findings and textural evidence, a melt-mantle reaction model is developed to account for the observations.

Complimentary evidence for melt-mantle reactions come from trace-element data from glass inclusions. Gurenko and Chaussidon (1995) demonstrated that olivine-hosted melt inclusions in the Dagmálafell picrite range from highly ("ultra-") depleted to highly enriched (E-MORB like) in incompatible trace-element abundances. It is argued that the melt-rock reaction model also provides insights into the relationships between volume of erupted magma, spatio-temporal factors and geochemical signatures. Finally, a compilation of isotopic and major-element data is presented to show that they vary in a fashion compatible with the model.

5.2 Occurrence, Texture and Mineralogy of the Micro-Nodules, Megacrysts and Gabbro-Nodules.

The Dagmálafell picrite contains phenocrysts of olivine and Cr-spinel and megacrystic plagioclase and clinopyroxene. Olivine phenocrysts are typically 3 to 10 mm in maximum diameter. The clinopyroxene megacrysts are similar in size to the olivine, however the plagioclase megacrysts are often up to 20 mm in maximum diameter. The outlines of the plagioclase megacrysts and intersecting sets of albite twins indicate that the megacrysts represent several individual crystals that have been fused together. The Dagmálafell picrite also hosts coarse-grained gabbro-nodules, mostly of a simple bi-mineralic plagioclase + clinopyroxene or plagioclase + olivine type, with rare plagioclase + clinopyroxene + olivine mineral assemblages. These coarse-grained gabbro-nodules are typically 3 to 10 cm in maximum diameter. Risku-Norja (1985) studied the petrology of the coarse-grained gabbro-nodules in this subglacial hyaloclastite. The micro-nodules are described here for the first time.

To date, five micro-nodules have been found. They are all located on the margins of two large (3 to 5 cm) anorthositic plagioclase-olivine gabbro-nodules. Three nodules contain only clinopyroxene and Cr-spinel, two also contain olivine. All the nodules are small, approximately 0.5 to 4 mm in diameter, and fine-grained. Clinopyroxene in three of the five clinopyroxene + Cr-spinel nodules is typically less than 0.5 mm with a few crystals between 0.5 and 1.0 mm. The other two clinopyroxene + Cr-spinel bearing nodules appear to contain a single clinopyroxene crystal with maximum diameter between 1 and 2 mm. The Cr-spinels vary in size in all nodules with individual grains having maximum diameters from 20 to 200 μm. Olivine in the olivine-bearing nodules have a maximum observable diameter in thin section of approximately 1.5 mm. In all the nodules Cr-spinel is concentrated at, but not restricted to, the contact between clinopyroxene and plagioclase

of the "host" anorthosite. A sixth sample possibly also a nodule, consists of a single grain of clinopyroxene without any Cr-spinel.

The grain size of the micro-nodules contrasts sharply with the larger grain size of the common, coarse-grained plagioclase-clinopyroxene and plagioclase-olivine gabbro-nodules in the picrite. In the coarse gabbro-nodules, clinopyroxene typically occurs as oikocrysts that are optically continuous over 20 to 30 mm. The oikocrysts enclose large plagioclase crystals that are from 4 and up to 10 millimeters in maximum diameter. The coarse-grained gabbro-nodules appear to be breaking up as groundmass, interpreted to rrepresnt quenched liquid, is often infiltrating along grain boundaries. In contrast the micro-nodules do not show evidence of disaggregation.

The plagioclase of the host nodule typically contains numerous inclusions of diopside and plagioclase (with rare spinel). Diopside is the dominant phase in most of the inclusions. Almost all of the inclusions contain a number of pits or holes. Some of these pits have negative crystal outlines (sharp boundaries and corners). In a few cases the composition of diopside changes towards these pits as indicated by back-scattered electron imaging. Hence, it seems likely, that at least some of the pits were occupied by a spinel phase that was plucked out during polishing. Where plagioclase and diopside coexist in inclusions plagioclase typically forms long slender needle-like crystals. The textures in these inclusions are akin to the textures in the rapidly cooled groundmass and consistent with their formation by rapid cooling or quenching of included liquid. Subhedral grains of olivine occurs in the host nodules in groups or forming elongate trains of crystals that are relatively uniform in size and composition.

It is important to understand the relationship between the anorthositic "host" and the micro-nodules. The host nodules may simply be a passive carrier unrelated to the fine-grained Cr-spinel clinopyroxene micro-nodules. Alternatively, the host nodule may be intimately linked with the origin of the micro-nodules. Given the concentration of Cr-spinel along the contact between plagioclase of the "host" and clinopyroxene of the micro-nodules (Fig. 5-1) the latter seems more probable. It is suggested here that the micro-nodules form as a result of reactions between a basaltic melt and the host nodule or a precursor of the host nodule. The micro-nodules then are remnants of a reaction corona. The quenched melt inclusions in the host are not consistent with long term annealing at subsolidus conditions, but imply recent crystallization or re-crystallization.

Based on textural evidence the clinopyroxene in the micro-nodules and clinopyroxene megacrysts are reacting with the host melt (Fig. 5-1). The groundmass adjacent to the micro-nodules is extremely rich in diopside and poor in plagioclase relative to the groundmass farther away from the nodule. It appears that droplets of diopside-rich

liquid were forming by dissolution. In one case, it seems that this diopside rich liquid was in the process of migrating away from the nodule and being replaced by invading liquid of the average groundmass composition (Fig. 5-1).

5.3 Major- and Trace-element Chemistry

5.3.1 Clinopyroxene

Clinopyroxene occurs as megacrysts and in both the micro-nodules and the coarse-grained gabbro-nodules. In spite of the considerable variation in the appearance and association they are similar in major-element composition (Table 5-1). The diopside megacrysts are often heavily resorbed. This texture was emphasized by Trønnes (1991) who suggested an important role for dissolution of diopside in the evolution of picrites in the Hengill region. Previous workers have concluded that most of the large clinopyroxene megacrysts originate from disintegrating gabbro-nodules (Risku Norja, 1985; Hansteen, 1991).

To explore further the major-element variation in diopside the analyses (Table 5-1) have been recalculated into cation proportions based on 6 oxygen atoms per formula unit (apfu) (Table 5-2). The cation proportions in all analyses show little variation except for the calculated Fe^{+3}. Diopside in the micro-nodules have Fe^{+3} from 0.01 to 0.03 (apfu), in contrast diopside in the gabbro-nodules have Fe^{+3} from 0.06 to 0.12 (apfu). Half the megacrysts appear to have little or no Fe^{+3} (<0.01 apfu), however the other megacrysts overlap with diopside from the gabbros and micro-nodules in terms of Fe^{+3}.

A subset of clinopyroxene grains from the micro-nodules, gabbro-nodules and megacrysts were analyzed for REE with the ion-microprobe (see Table 5-3). The REE patterns show three distinct compositional groups with only minor overlap (Fig. 5-2). Clinopyroxene from the coarse-grained gabbro-nodules are the most depleted in the light REE (LREE). In contrast, most of the clinopyroxene megacrysts are enriched in LREE relative to clinopyroxene in the gabbro-nodules and micro-nodules. Lanthanum abundances are five and up to ten times higher in the clinopyroxene megacrysts compared to clinopyroxene in the gabbro-nodules. Clinopyroxene in the micro-nodules is intermediate in LREE abundances. From the middle to the heavy REE (HREE) the patterns are fairly flat. Normalized abundances of the HREE vary by a factor of two to four, with the megacrysts consistently having the highest abundances and the clinopyroxene from gabbro-nodules the lowest abundances.

The grouping of clinopyroxene compositions is well illustrated in a plot of the normalized La/Sm ratio (denoted $(La/Sm)_N$) against the normalized La concentration (La_N) (Fig. 5-3). Of the seven megacrysts analyzed five have $(La/Sm)_N$ ratios above 0.2. The

two other megacrysts and clinopyroxene from the micro-nodules have $(La/Sm)_N$ ratios between 0.1 and 0.2. The three clinopyroxene grains from gabbro-nodules all have $(La/Sm)_N$ below 0.1. In Fig. 5-3, a change in slope occurs at $(La/Sm)_N \approx 0.2$. Below $(La/Sm)_N = 0.2$ changes in La abundances are accompanied by relatively small changes in Sm abundance compared to above $(La/Sm)_N = 0.2$ where Sm abundances vary more sympathetically with La abundances. This indicates a change in coupling between the light and heavy REE.

The trace-elements vary in a similar way to the REE (Table 5-4). V, Sr, Y and Zr are always enriched in the megacrysts compared to the micro-nodules and gabbro-nodules. Ti varies in a similar fashion, however Cr concentration is negatively correlated with Ti. Cr content is high in the clinopyroxene from the gabbronodules (Cr > 8000 ppm), but lower and somewhat variable in the megacrysts (3600 < Cr < 7700 ppm).

The variation in Ti and Zr is examined in Fig. 5-4. Most of the megacrysts plot on or around a straight line with slope ≈360. Clinopyroxene from gabbro and micro-nodules and the depleted megacrysts all plot close to a line with slope ≈580. In both the enriched megacrysts and micro-nodules diopside Ti and Zr co-vary. The limited data available on the gabbro-nodule clinopyroxene does not show simple covariation between Ti and Zr.

5.3.2 Cr-Spinel

In the Dagmálafell picrite Cr-spinel occurs in the micro-nodules, as inclusions in olivine phenocrysts, and as phenocrysts. It has not been observed in the common coarse-grained plagioclase-clinopyroxene-olivine nodules but does occur occasionally as inclusions in clinopyroxene megacrysts. The Cr-spinel in the micro-nodules and megacrysts have higher TiO_2 than the Cr-spinels associated with olivines or those occurring as phenocrysts. At a given Cr# (Cr#=100*Cr/(Cr+Al)) they may contain roughly twice the amount of TiO_2 as do the Cr-spinel phenocrysts and Cr-spinels included in olivine (Fig. 5-5). On a TiO_2 vs. Cr# plot, the enriched Cr-spinels define a trend of decreasing TiO_2 at nearly constant Cr# which is perpendicular to the trend of variable Cr# at almost constant TiO_2 content defined by the Cr-spinel phenocrysts and Cr-spinels included in olivine. Two separate vertical trends are apparent in Fig. 5-5, the reasons for this are not well understood at this time. It should be noted that analyses from the micro-nodules contribute to both "legs" although they fall dominantly in the lower Cr# group. Similarly, analyses of Cr-spinel included in clinopyroxene phenocrysts contribute to both trends but the bulk of points fall in the higher Cr# group.

The Cr-spinel occurring as phenocrysts and associated with or included in olivine show large compositional variation (Fig. 5-5). Some crystals display considerable compositional variation whereas other are homogeneous with only minor zoning towards the rim. Where zoning is present, Al increases and Cr decreases (lower Cr#) towards the rim, at nearly constant TiO_2 and MgO content. For example a relatively homogeneous crystal may have a core composition with Cr# 45.3 (average of 5 analysis) and rim with Cr# 43.2 whereas the TiO2 content is between 0.23 and 0.26 (wt %) (all six analysis). Extreme compositional variation is occasionally seen, for example a single grain with Cr# 47 near center falling to Cr# 27 near the rim. Concomitant TiO_2 variation is very small or from 0.22 (wt %) at the core to 0.16 near the rim. In spite of the large variation in Cr# in the whole population, MgO and TiO_2 content do not vary greatly. It is difficult to explain this variation in terms of crystal fractionation of olivine and Cr-spinel. Fractionation of these phases should lead to an increase in TiO_2 and a decrease in MgO in the liquid, which should be reflected in a corresponding increase in TiO_2 and decrease in MgO content of the spinel.

5.3.3 Plagioclase and Olivine

Plagioclase in the two anorthositic nodules that "host" the micro-nodules has a composition of An_{87}. As mentioned above, it contains a number of inclusions that all appear to be diopside and plagioclase (quenched) with minor spinel. There is gradation in size with many of the large inclusions having maximum diameters of 50 to 100 μm with a few extending to 200 or 300 μm. A myriad of smaller (<10μm) inclusion often concentrated along cleavage planes. At this time there is no evidence to indicate that the smaller inclusions differ in composition from the larger ones.

Plagioclase in the common gabbro-nodules typically has a composition of An_{86} to An_{88}. The megacrysts of plagioclase are similar in composition (An 88). Occasionally rounded olivine grains occur as inclusions in these megacrysts. Risku-Norja (1985) analyzed a number of plagioclase cores and rims from the gabbro-nodule and found a large compositional range from An_{83} to An_{93} with the bulk of the analyzed grains falling between An_{86} and An_{90}. In the same study the An content of the plagioclase megacrysts was found to range from An_{86} to An_{91} overlapping with the plagioclase in the gabbronodules (Risku-Norja 1985). A slight reverse zoning (usually 1 to 4 mol% An) was observed by Risku-Norja (1985) in several plagioclase grains from both the gabbro-nodules and megacrysts.

Olivine occurs in both types of nodules and as phenocrysts in the groundmass. The composition of olivine in the olivine-bearing micro-nodules is Fo_{87}, similar to olivine in the host anorthositic nodules (Fo_{87}-Fo_{88}). The composition of olivine phenocrysts varies from Fo_{84} to Fo_{91} with analyses of phenocrysts rims as low as Fo_{81}. There is no systematic variation in CaO or NiO with Fo content. Olivine in the coarse-grained gabbro-nodules shows a slightly narrower compositional range from Fo_{85} to Fo_{90}. A similar variation in olivine chemistry was observed by Risku-Norja (1985). Risku-Norja (1985) also found evidence of reverse zoning in some olivine phenocrysts from Dagmálafell. Examples of reverse zoning in olivine have also been recorded in the Maelifell picrite, also from the Hengill region (Hardardóttir, 1983; Hansteen, 1991).

5.4 Melt-Rock Reaction and the Origin of the Dagmálafell Picrite

In this section a general framework for a model of melt-rock reaction is developed. The models for this process currently discussed in the literature envision rising melts dissolving phases that are under saturated in the melt, and precipitating phases that are saturated in the melt. It is generally accepted that basaltic magmas rising through the mantle are under saturated with respect to clinopyroxene and orthopyroxene (e.g., Stolper 1980; Kelemen 1990; Hess 1992 and others). As temperature contrasts between melt and surrounding mantle are small dissolution is not limited by latent heat of crystallization, and the liquids are bound to react to some extent with surrounding pyroxene-bearing lithologies (e.g. Kelemen, 1990). The postulated reactions involve dissolution of pyroxenes and precipitation of olivine. Evidence for the operation of this type of process has come from studies on abyssal peridotites and mantle sections in ophiolites. Dunites and dunite dikes in these mantle samples are thought to form as a result of melt percolation through a residual mantle. Reactions between the melt and mantle result in replacement of pyroxene by olivine and the formation of dunite (e.g. Takazawa et al., 1992; Kelemen et al., 1992; 1995)

5.4.1 Textural Evidence for Melt-Rock Reaction

Based on the textural evidence discussed in the previous section it is suggested that the micro-nodules are remnants of a reaction selvage, or corona, surrounding the host nodule. It is also proposed here that the host nodules re-crystallized during the melt-rock reaction, that led to the formation of the micro-nodules. In this model the clinopyroxene and Cr-spinel in the micro-nodules would effectively be in major- and trace-element equilibrium with the melt being drawn off the solid reactant. Therefore the micro-nodules can be used to constrain the composition of the melt that forms during the reaction.

A second stage of melt-rock interaction is inferred from textural evidence consistent with reactions between micro-nodules and megacrysts on the one hand and the host liquid on the other hand. This second stage of melt-rock reaction may be associated with plagioclase replacing clinopyroxene as a near liquidus phase. That this stage has been reached, is evident from the ophitic textures of the plagioclase + clinopyroxene (± olivine) gabbro-nodules. In these nodules crystallization of plagioclase is followed by crystallization of clinopyroxene. These gabbro-nodules are considered to form last or at the lowest pressures.

5.4.2 Trace-elements in Clinopyroxene: Implications for Magma Composition

The large variation we observe in REE abundance in clinopyroxene cannot be explained by any simple closed system fractionation process. The relatively enriched (or least depleted) clinopyroxene megacrysts ($(La/Sm)_N > 0.2$) have trace-element abundances consistent with equilibration with an E-MORB like magma. The REE patterns of two model liquids estimated to be in equilibrium with the megacrysts are plotted in Fig. 5-6 (thin lines). The concentrations of REE element in the magma were estimated using partition coefficients from Kelemen et al. (1993). The model liquids are compared to an analysis of a pillow rim from Stapafell (thick line). The Stapafell subglacial hyaloclastite from the Reykjanes peninsula, is an example of an E-MORB like magma erupted in the region (Table 5-5). Recently Gee et al. (1998a), in their work on petrochemistry of Reykjanes lavas, attributed the geochemical variation among basalts to mixing between enriched and depleted magmas and used the Stapafell magma as an enriched end-member. In the same figure REE abundance in the Dagmálafell host (pillow rim) is compared to model liquids calculated from REE concentration in clinopyroxene from the plagioclase + clinopyroxene ± olivine gabbro-nodules. Given the uncertainty in Nernst partition coefficients ($D = C_{cpx}/C_{liq}$), and the abundance data (±10%), the match is considered close.

These results show that most of the megacrysts come from sources other than disintegrating gabbro-nodules. These results also indicate that enriched and depleted magmas are intimately associated at some point in their evolution. A claim that is further supported by the trace-element data on olivine-hosted glass inclusions from the work of Gurenko and Chaussidon (1995). Mixing of magmas that derive from enriched and depleted mantle lithologies is a possible explanation for these observations (e.g. Gee et al., 1998a). Dynamic melting models where depth and degree of melting are the key variables may also have some validity (e.g. Gurenko and Chaussidon, 1995). It is proposed here however, that a melt-rock reaction provides a better model, for explaining the data at hand.

5.4.3 Major-element Variation in Cr-spinel

The major-element chemistry of the Cr-spinels appear to be somewhat intermediate between Cr-spinels associated with enriched lavas and those commonly found in depleted picrites. In Fig. 5-7 the TiO_2 content is again plotted against Cr#. For comparison analysis of Cr-spinel from Eldborgarhraun lava (RE 286) from Sigurdsson (1994) are also plotted. This is a lava flow from the Reykjanes peninsula that is in many respects similar to the Stapafell magma with an E-MORB like REE pattern (Sigurdsson, 1994) . The Cr-spinels from RE286 contain more TiO_2 than their counterparts in the micro-nodules. Most of them also have lower Cr# but two analyses from Eldborgarhraun extend towards the composition of micro-nodule Cr-spinel. Several rim analyses in the Eldborgarhraun data set from Sigurdsson (1994) extend to higher TiO_2 values. These may represent in-situ fractionation and are not shown.

One problem in interpreting the chemical variation in the Cr-spinel is that we have no constraints on the spatial distribution of lithologies during the proposed melt-rock reaction. Furthermore any time component has to be inferred or assumed. However, the Cr-spinels composition does provide support for the general model proposed here. The chemical variation is consistent with Cr-spinel forming in a zone where a "parental" (enriched) magma is reacting with a depleted lithology. It is also suggested that the Cr-spinel phenocrysts and Cr-spinel inclusions in olivine formed near the end of the melt rock reaction and possibly during the formation of the gabbro-nodules when plagioclase crystallizes before clinopyroxene. That is, during and subsequent to the second stage of melt-rock reaction. The large variation in Cr# in this group seems to contradict the high Cr-content of the host liquid and picritic whole rocks in general. However, this variation may be the result of "in situ" fractionation. Growing olivine crystals capture and isolate Cr-spinel from the residual liquid leaving the liquid progressively depleted in Cr.

It is logical to compare the chemistry of Cr-spinels in the micro-nodules and megacrysts from Dagmálafell, to Cr-spinels that occur in oceanic mantle samples. For example, Cr-spinels in gabbroic selvages associated with dunite dikes from the Hess Deep (Dick and Natland, 1996; Kelemen et al., 1997) display a similar trend in composition. There, TiO_2 increases from ≈0.1 to 2.8 wt. % (only three analysis extend the trend beyond 1.8 wt. % TiO_2) and correlates positively with a small increase in Cr/(Cr+Al) values from 0.45 to 0.60 (Dick and Natland, 1996). These Cr-spinels overlap compositionally with Cr-spinels from MORB and this overlap is consistent with the Cr-spinels equilibrating with MORB like magmas (Kelemen et al., 1997). Therefore the chemistry of the Cr-spinel supports the contention that the dunite dikes may represent conduits of MORB magmas model (Dick and Natland, 1996; Kelemen et al., 1997). In Fig. 5-7 a subset of the Cr-

spinels from gabbroic selvages in the Hess Deep samples (Dick and Natland, 1996) are plotted along with the data from Dagmálafell and Eldborgarhraun. Note how they overlap in small part with the higher Cr# leg of the micro-nodule Cr-spinel.

It may appear paradoxical that Cr-spinel with relatively high TiO_2 is associated both with megacrysts (often very high TiO_2 and high LREE contents) and micro-nodules (low TiO_2 and low LREE contents)). However, from the megacrysts that have been analyzed the ones that have high LREE content do not contain Cr-spinel and the ones that contain Cr-spinel are fairly depleted in the LREE. More data is needed to establish this as a rule, however, at the present, there is no paradox. It appears that clinopyroxene megacrysts population contains both megacrysts that precipitated from the enriched parental magma and others that crystallized later during the melt rock-reaction (depleted in REE).

5.4.4 Melts: Bulk Samples and Glass Inclusions Revisited.

Melting experiments on simplified and natural fertile ultramafic compositions show that at pressures between 1 and 2 GPa, clinopyroxene is the dominant contributor to the melt (Walter et al., 1995; Kinzler and Grove, 1992). These melting reactions are derived from melting experiments on fertile ultramafic compositions, and it is not clear how they are affected by decreasing the fertility (≈ decreasing modal clinopyroxene). Because the exact nature of the solid reactant has not been established, it is not clear that the melting reactions derived from experiments on model and natural lherzolites are applicable. However, whether the lithology is a depleted lherzolite/harzburgite, garnet pyroxenite or wherlite, clinopyroxene will be the main host of the REE, and therefore the main control on their behavior. It is therefore assumed, as a first approximation, that the melt-rock reaction may be modeled as melt-clinopyroxene reaction from the perspective of trace-element evolution.

The variation in trace-element and REE abundance ratios produced by melting, are displayed well on a diagram of Ti/Zr versus $(La/Sm)_N$ (e.g. Shimizu, 1998). This plot is used to examine the relationships between "bulk" samples (i.e. pillow rims and whole rocks), melt inclusions and the clinopyroxene megacrysts and micro-nodules. In Fig. 5-8A the variations in these abundance ratios are displayed for all the melt inclusions and bulk samples. Also shown is a mixing trajectory of the least and most depleted melt inclusions. Simple binary mixing of the most enriched and depleted inclusions does not produce the array of melt inclusions. Other processes, besides simple magma mixing, must be at work. The bulk samples are displaced to higher $(La/Sm)_N$ at a given Ti/Zr ratio relative to the melt inclusions. The bulk samples appear to form an array sub-parallel to that of the depleted melt inclusions.

In Fig. 5-8B two compositions of clinopyroxene from a micro-nodule and from a megacryst, are plotted. Also displayed are the bulk samples as above and the most depleted melt inclusions ($(La/Sm)_N<1$). Two melt trajectories produced by fractional melting are also plotted. One showing instantaneous melts, the other accumulated melts. The trajectories are calculated assuming that a "pyroxenite" of the same composition as the megacryst is melting. The accumulated melt composition approaches that of the "pyroxenite" with increasing melting. The displacement of the bulk samples relative to that of the melt inclusions is similar to that of the instantaneous melts relative to that of the accumulated melts. Consequently, the melt inclusions may represent instantaneous fractional melts from a lithology that has a higher $(La/Sm)_N$ ratio than the megacryst. Similarly the bulk samples may represent accumulated melts derived by fractional melting from that same lithology. The bulk samples are then trending towards the composition of the parental lithology. The enriched melt inclusions cannot however be explained by fractional melting of the same lithology.

Alternatively, the melt inclusions may represent aggregated fractional melts produced from lithologies containing clinopyroxene with similar trace-element characteristics to those of the micro-nodules. In that case the bulk samples would represent samples of mixtures, between a series of aggregated melts and an enriched infiltrating magma. This however implies that the amount of melting is inversely proportional to the amount of infiltrated magma. Conceptual models may be constructed where such an effect is anticipated. As an example such an effect might be achieved where the proportion of infiltrated melt decreases upwards through a mantle column, and the amount of melt produced in the column in response to this infiltration increases upwards. However, at the present resolution the data does not require such a complicated model.

5.4.5 Modeling Melt-Rock Reactions

Two contrasting approaches have been used in the literature in an effort to quantify the effect of melt-rock reaction on trace-element concentrations in magmas. Several workers have applied DePaolo's (1981) Assimilation-Fractional-Crystallization formalism (Kelemen et al., 1997; Shimizu, 1998; Wagner et al., 1998). In essence the AFC formalism is not entirely satisfactory for the purpose of modeling melt-rock reactions, given that the lithology the magma is digesting imposes no compositional constraints (i.e. D) on the liquid. The second approach involves applying equations, initially derived to model water-rock interactions, to melt-mantle reactions. Several such studies have investigated melt-mantle reaction from a theoretical standpoint (e.g. Navon and Stolper 1987; Hauri 1997; Vernières 1997; Reiners, 1988). These equations probably provide a better description of

the melt-rock reaction process. However, their application to the present case requires assumptions to be made regarding poorly constrained variables (e.g. grain size, porosity etc.). In lieu of applying the more appropriate melt-percolation models, some specific results from a recent study (Verniéres, et al., 1997) modeling melt-mantle reactions are cited. Finally the composition of a magma that equilibrates with a residual mantle is evaluated.

Using DePaolo's (1981) equations the effect of an AFC process was calculated assuming: 1) an initial magma with REE concentrations of the Stapafell glass; 2) this initial magma assimilates clinopyroxene with the same REE concentrations as the micro-nodules; and 3) the magma crystallizes olivine which is removed from the system. Distribution coefficients used for olivine/liquid are as listed by Kelemen et al. (1993). The results of two calculations are compared to the Dagmálafell pattern in Fig. 5-9A. The result indicate that the appropriate direction and magnitude of depletion may be achieved. However, the shape of the calculated patterns deviate from the Dagmálafell magma in that LREE are enriched in the model magmas. The purpose of the calculation is not to argue for any particular set of values for the variables such as: mass of assimilate; mass of initial liquid; mass of final liquid; rate of crystallization relative to rate of assimilation etc. The intent is only to show that, within the boundary conditions of the AFC model, a depleted magma may be derived from an enriched magma through combined assimilation of clinopyroxene and fractionation of olivine.

Verniéres et al. (1997) specifically look at a problem similar to the present one. They modeled the effects of an LREE enriched melt infiltrating a depleted mantle column and inducing melting. Their results indicate that after extensive reaction, melts extracted from various parts of the model column, range in composition from E type to N type MORB. These results show that under favorable conditions a depleted (i.e. N-MORB) magmas can form when enriched melts react with the surrounding mantle and provide tentative support for the model presented here.

From the theoretical models describing melt-rock reactions (e.g., Reiners, 1988) certain generalizations can be made regarding the REE concentrations of the final magma. In the present scenario the concentration of any rare earth element *i* in the initial magma C_{im} is higher than of a melt in equilibrium with the clinopyroxene-bearing lithology the initial melt reacts with. That is $C_{im}>C_{is}/D$ where D is the distribution coefficient of element *i* between solid and melt and C_{is} is the concentration of element *i* in the solid. At constant melt mass, the melt will become progressively more depleted approaching the ratio C_{is}/D. The magma will approach equilibrium with the solid ($C_{im}=C_{is}/D$). If melt mass is increasing, as in the present case, the depletion of the melt is not limited by C_{is}/D (Reiners,

1988) and the magma may become more depleted. It is therefore instructive to explore the shape of REE profile for liquids in equilibrium with clinopyroxene (i.e. $C_{im}=C_{is}/D$) from depleted mantle peridotites. The Dagmálafell REE pattern is compared in Fig. 5-9B to two REE patterns calculated to be in equilibrium with clinopyroxene from depleted peridotites in the Vulcan Fracture zone (data from Johnson et al., 1990). Distribution coefficients used for clinopyroxene/liquid listed by Kelemen et al. (1993) were applied. The pattern derived from the least depleted clinopyroxene from the Vulcan fracture zone peridotites is similar to the Dagmálafell REE pattern, and clearly much more depleted liquids can form by interaction of melt and depleted mantle.

5.4.6 Melt Mantle Reaction; What is Known, What is Not

In the previous sections the following points have been raised: 1) There is extensive textural evidence to suggest that melt-rock reactions played a role in the evolution of the Dagmálafell picrite; 2) The composition of clinopyroxene from these selvages indicates that the melt thus formed was depleted in rare-earth and other trace-elements; 3) Some clinopyroxene megacrysts are in (or nearly in) rare-earth element exchange equilibrium with E-MORB like magmas; 4) Clinopyroxene from gabbro-nodules are in (or nearly in) Rare-Earth element exchange equilibrium with the host melt; 6) Enriched and depleted magmas are intimately associated at some point during their evolution; 7) The displacement, in $(La/Sm)_N$ vs Ti/Zr space, of olivine-hosted glass inclusions relative to bulk melt samples is similar to the displacement of instantaneous melts relative to accumulated melts calculated using simple fractional melting models. Based on these observations it is proposed that: 1) Enriched (E-MORB-like) and depleted mafic magmas (picrites) are related; and more specifically 2) depleted melts may be derived through reactions between an enriched infiltrating magma and a clinopyroxene-bearing lithology.

There are, however, some remaining issues that cannot be adequately dealt with at this time. For example, the composition and mode of the solid reactant is not known. It is assumed that clinopyroxene is key host of trace-elements in this lithology and therefore controls the trace-element chemistry of the magmas forming in the reaction. It has also been argued that the enriched infiltrating magma is saturated in clinopyroxene (the enriched megacrysts). This, however, requires that the infiltrating magma reacts with a phase that apparently is saturated in the magma. Can this happen? In this regard recent studies on mantle melting are of interest. Experiments on fertile peridotite indicate that the composition of clinopyroxene in equilibrium with melts at the solidus contain significant amounts of the Ca-Tschermaks molecule and that the composition of clinopyroxene changes significantly as temperature and melt fraction increases (Baker et al., 1991; Blundy

et al., 1998). Although the conditions in these experiments do not directly correspond to the present scenario, they are an indication that clinopyroxene-melt equilibria is sensitive to pressure, temperature and minor (Na, Al, Ti, Cr) and trace-element (REE) content in clinopyroxene. Hence a silicate liquid may react with clinopyroxene of one composition (in terms of minor and trace-elements) while precipitating clinopyroxene of a different composition.

The driving force for the reaction was discussed in the general framework of present melt-mantle reaction models. Given the relatively low melt productivity values sited in the literature (Kelemen et al., 1997) this mechanism may not provide an adequate increase in melt mass to obtain the desired depletion It is suggested here that the texture of the host nodules is of significance in this respect. If the interpretation set forth in this paper is correct, one must ask why the nodules re-crystallize. Two possibilities come to mind: 1) melting and re-crystallization due to heating; and 2) melting and re-crystallization due to decompression. Ignoring the inclusions in the host for the moment, the olivine + plagioclase assemblage is a higher temperature assemblage than the bordering clinopyroxene + Cr-spinel assemblage. This observation seems to preclude melting and re-crystallization in response to infiltration of a hot (relative to the solid) magma. Another more plausible scenario involves melting and re-crystallization in response to decompression. It may be achieved if the melt and solids rise together or alternatively if the solid reactant is emplaced at shallow levels in a meta-stable state prior to magma infiltration. For instance as the (residual) mantle rises due to convection, sections or slabs of spinel-lherzolite may be emplaced at low pressures (<1GPa) without re-crystallizing to plagioclase-lherzolite. Infiltration of enriched magma may then cause melting concomitant with re-crystallization of this (residual) mantle lithology to produce a depleted magma such as the Dagmálafell picrite.

It is evident that a volumetrically large outburst of magmatism followed the end Quaternary deglaciation in Iceland (Sigvaldason et al., 1992). The increased magmatism may be the result of an excess of magma, trapped in the upper mantle/lower crust, finding its way to the surface. Alternatively it may be the result of increased melting in response to isostatic uplift and associated mantle decompression (Jull and McKenzie, 1996). Decompression of mantle material in excess of what occurs in steady state upwelling has also been suggested as a mechanism for the generation of depleted melts (Hardarson and Fitton 1991; Gee et al., 1998b). Notably, Gee et al. (1998b) have demonstrated that on the Reykjanes Peninsula eruptions of highly depleted liquids (picrites) are concentrated in time, immediately following deglaciation events. Isostatic rebound may result in rapid emplacement of mantle material at shallow levels where it is relatively hot and reactive.

Melting of these lithologies in response to magma infiltration can then produce the depleted picrites.

5.5 High-MgO Basalts From the Rift Zones

In the previous section the possible role of melt-rock reaction in the formation of the Dagmálafell picrite was discussed. Below, this model is extended to high-MgO basalts in the rift zones in general. The reaction proposed to account for the relationship between enriched and depleted melts in this study may be represented schematically as:

$$\text{Melt E} + \text{Clinopyroxene (+Opx? +Sp? +Gnt?)} \Rightarrow \text{Melt D} + \text{Olivine} + \text{Cr-Spinel} \qquad (5 - 1)$$

Where Melt E is the infiltrating (enriched) melt and Melt D is the melt associated with depleted picrite depleted picrite.

First, the relationships between volume of erupted magma, incompatible element variation in magma and spatio-temporal factors is considered. The model presented in this paper, provides a logical framework for understanding the apparent relationships between these parameters. Then literature data is used to test the model. Isotopic and major-element data on the depleted end-member (picrites) was collected from Elliott et al., (1991), Hémond et al., (1993), Gurenko and Chaussidon (1995). The petrographic and chemical criteria for picrite from Jakobsson et al.(1978) and Meyer et al. (1985) were used. There is some overlap among the picrites in the data-sets from Elliott et al. (1991) and Hémond et al. (1993). This overlap allows us to examine the effect of modal variation of olivine and Cr-spinel on the chemistry of the lavas. The enriched end-member is represented by samples from Stapafell (pillow rim this work, whole rock from Gee et al., 1998a), Eldborgarhraun from Sigurdsson (1994) and sample IT4 from Elliott et al. (1991).

5.5.1 Relationship Between Magma Volume, Incompatible Element Variation and Spatio-Temporal Factors.

Sigvaldason (1974) noted a nearly ten-fold variation in K_2O concentration among volumetrically small lavas in the Eastern Rift Zone, but did not discuss the geographic distribution of vents. However, Condomines et al. (1983) noted that some of the picritic basalts used in their study were erupted "through old crust" consistent with their location peripheral to the main spreading centers. In their study of the Reykjanes peninsula basalts (on the Western Rift Zone), Jakobsson et al. (1978) mapped out the temporal and spatial relationships of the recent lava flows. In general the picrites form small lava shields that are situated at the perimeter of each volcanic system. Volumetrically they are insignificant

compared to the more evolved basalts. A progression in time from small picrite shields to larger olivine tholeiite shields and finally large tholeiite fissure eruptions was inferred. They suggested that volcanic activity was cyclic and that each cycle started with the eruption of picrites. The picrites therefore appear to form in domains that are temporally and/or spatially peripheral to the main magma plumbing systems. In a more recent contribution Hardarson and Fitton (1997) demonstrated that large variations in Zr/Nb ratios are confined to volumetrically small lavas in the rift zone. The relationship holds for glacial and interglacial lavas as well (Hardarson and Fitton, 1997). Hence, there is a definite relationship between volume and variability in trace-element ratios and possibly between volume and location of eruption vent.

The Zr/Nb ratio is commonly used in exploring trace-element variation in magma systems. In oceanic basalt systems Nb is more incompatible in partial melting and fractional crystallization processes is Zr. Nb is slightly more incompatible than La while Zr is similar in incompatibility to Sm (Sun and McDonough, 1989) and plot beside these REE in extended trace-element diagrams (spidergraphs). A large Zr/Nb ratio indicates that the melt is depleted in incompatible elements whereas a small ratio suggests a magma enriched in highly incompatible elements.

The data of Hardarson and Fitton is replotted in Fig. 5-10 with lava volume ($\log_{10}$) on the abscissa and Zr/Nb ratio on the ordinate. We have arbitrarily divided the volume data into groups at 10, 1.0 and 0.1 km^3 and so forth. The range of Zr/Nb ratios in each volume group is indicated by columns. If we define geochemical variance as the difference in the Zr/Nb ratio between the most depleted and most enriched sample in each volume group, it is clear that there is an inverse relationship between geochemical variance and volume. This increase in variability (in Zr/Nb) with decreasing volume is difficult to reconcile with magma mixing. The variation requires mixing of enriched and depleted magmas in specific (non-random) proportions to produce the "decay" in variance with increasing volume.

However, this variation can be understood in terms of melt-rock reactions. A useful and familiar analogy comes from water-rock interaction studies and concept of water/rock ratio. During hydrothermal interaction at high water/rock ratios the isotopic (e.g. H and O) composition of the altered rock may change drastically towards that of the fluid, in contrast at low water/rock ratios the rock "buffers" the composition of the fluid. We suggest that depleted magma may form as a result of interaction of small volumes of enriched magmas with a depleted (residual mantle ?) clinopyroxene-bearing lithology. If the initial mass of magma is small compared to the mass of the depleted lithology (i.e. low magma/rock ratio) the magma mass may increase by an order of magnitude during reaction

and, the resulting melt will have the characteristics of melt derived from a depleted lithology. As the ratio of initial melt to rock increases the effect of the depleted lithology decreases. This effect is likely to be more visible at the periphery of a magma plumbing systems, where smaller volumes are processed through the upper mantle. Closer to the center of the plumbing system larger volumes of magma are processed, possibly exhausting depleted lithologies at least locally. The mode of percolation may also contribute. For instance if infiltration is channelized, i.e. through dunite filled (long lived?) "dikes" (Kelemen et al., 1997) , the magma is presumably more isolated from, and less affected by, the surrounding mantle than if infiltration is pervasive.

The idea that the "effective" solid/liquid ratio plays an important role, is supported further by incorporating yet another group of small volume samples. The glass inclusions in olivine phenocrysts from the Dagmàlafell picrite represent one such group. In Fig. 5-10 we plot the data for glass inclusions from Gurenko and Chaussidon (1995) with the "lava" data of Hardarson and Fitton (1997). Again, the columns represents the variation in Zr/Nb ratio in each volume group. In the context of the present model the extreme depletion in the glass inclusions reflects very local (millimeter to centimeter scale) dissolution of clinopyroxene-bearing lithology in the immediate vicinity of crystallizing olivine grains. The most enriched inclusions on the other hand may represent the infiltrating magma immediately before the onset of melt-rock reaction. As melting of the depleted clinopyroxene-bearing lithology starts, one can expect that enriched and depleted melt droplets will be mingling and mixing over a some distance. It is therefore possible that olivine growing in response to the melt-rock reaction could incorporate either enriched or depleted melt droplets or both.

5.5.2 Melt Rock Reaction and Nd Isotope Ratios

The high-MgO basalts show a large variation in the isotope ratios of neodymium and lead. For example, in the data sets of Elliott et al. (1991) and Hémond et al.(1993) the $^{143}Nd/^{144}Nd$ varies from 0.51300 to 0.51316 (ε_{Nd} = +7 to + 10). The model proposed here assumes that an enriched parental liquid (relatively low ε_{Nd}) reacts with a clinopyroxene-bearing lithology (relatively high ε_{Nd}) to produce the micro-nodules. If the variation in Nd isotope ratios (Fig. 5-11) is a result of melt-rock reaction, this lithology must have been depleted in the geological past, and subsequently had time to mature high $^{143}Nd/^{144}Nd$ ratios. The variation (Fig. 5-11) is broadly consistent with reaction between an enriched magma and a isotopically depleted lithology. A two-stage model may be suggested. Initial reaction between melt and depleted mantle produces variation in both Nd

isotope ratios and La abundance. It is followed by a second stage of melt-rock reaction (e.g., dissolution textures associated with clinopyroxene in micro-nodules and megacrysts) that results in the depletion of La abundance with little or no change to Nd isotope ratio. Incorporation of "excess" modal olivine into the whole rock may also contribute to the decrease in La concentration.

5.5.3 Effect on Mineral-Liquid Equilibria

To evaluate the effect of clinopyroxene dissolution on olivine- and spinel-liquid equilibria it is useful to write out some simple chemical reactions.

$$(Mg_2SiO_4)_l + (Fe_2SiO_4)_s = (Mg_2SiO_4)_s + (Fe_2SiO_4)_l \qquad (5 - 2)$$

$$(2\text{-}X)(MgO)_l + X(FeO)_l + (SiO_2)_l = ((Mg,Fe)_2SiO_4)_s \qquad (5 - 3)$$

Equations 2 and 3 are written as exchange equilibria involving the end-members forsterite and fayalite, in the olivine solid solution series, and stoichiometric formation reaction of olivine respectively. Analogous reactions may be written for Cr-spinel involving for example the spinel ($MgAl_2O_4$), magnesiochromite ($MgCr_2O_4$), hercynite ($FeAl_2O_4$) and chromite ($FeCr_2O_4$) end-members. Increasing the MgO content of the liquid and the MgO/FeO ratio would favor formation of more Fo-rich olivine and, given enough time, existing olivine crystals would equilibrate with the new liquid (5 - 2). New crystals precipitating from the liquid would be more Fo rich than pre-existing ones (5 - 3). Similarly for spinel, the increasing concentration of the magnesiochromite component in the liquid results in an adjustment of the spinel composition (e.g. the hercynite component is exchanged for the magnesiochromite component) and/or the nucleation and growth of more MgO and Cr_2O_3 rich spinels. Therefore liquidus phases such as olivine and Cr-spinel, are capable of modifying the composition of the liquid and concealing to some extent the chemical signature of clinopyroxene dissolution. Given that re-equilibration between solids and magma would ultimately be controlled by diffusion of cations in the crystals it seems likely that formation of new crystals will be more important than diffusive equilibration in the drive towards a new equilibrium state.

It is proposed that the addition of diopside-rich melt is compensated for by crystallization of olivine and Cr-spinel. If the rate of dissolution is rapid the rate of crystallization may also be. One may therefore expect to find chemical and textural evidence consistent with an increase in for instance the Fo content of the liquid and relatively rapid growth rates. For example, the phenocryst populations expected to form in

response to diopside dissolution could display disequilibrium features such as "reverse" or irregular chemical zoning. As mentioned above reverse zoning has been recorded in olivine and plagioclase from both the Dagmálafell and Maelifell picrites in the Hengill area (Risku-Norja, 1985; Hardardóttir, 1983; Hansteen, 1991). Rapid growth rates may also favor the incorporation of melt droplets in growing olivines and could contribute to the high concentration of glass inclusions in olivine seen in some Icelandic picrites (Hardardóttir, 1983).

The above discussion, although qualitative, suggests that the effect of diopside addition on the chemistry of basaltic liquids would be greatly modified by the presence and continued crystallization of olivine and Cr-spinel. All major and moderately compatible elements in diopside, except CaO, would be modified to some extent by the olivine + Cr-spinel assemblage. CaO is expected to increase rapidly in the proposed scenario. That and the high CaO/Al_2O_3 ratio may stabilize plagioclase on the liquidus. Certainly many of the picritic lavas contain plagioclase phenocrysts that are highly anorthitic (An_{87}- An_{93}) (Hardardóttir, 1983; Risku-Norja, 1985; Gurenko et al., 1989; Hansteen, 1991). Their presence may be another manifestation of melt-rock reaction. A similar origin (i.e. melt-mantle reaction) for highly An rich plagioclase (i.e. An>90) in the oceanic environment has been forwarded by several investigators (e.g. Sinton et al., 1993; Dick and Natland, 1996; Ranipone et al., 1998)

5.5.4 High MgO Basalts: Major-element Variations

In this final section it is demonstrated that key aspect of major-element variation among the high-MgO lavas are consistent with addition of diopside and olivine crystallization as a major control on major-element composition.

The high-MgO lavas from the rift zones have a large variation in TiO_2 at MgO contents of about 8 to 10% wt (Fig. 5-12A). At higher MgO contents, TiO_2 decreases smoothly with increasing MgO content. This variation can be explained by diopside dissolution combined with precipitation of olivine and Cr-spinel. The arrow in Fig. 5-12A. indicates the effect of dissolving 40% of diopside into a high TiO_2 liquid. Tie-lines connect two analysis of the same lava showing the effect of variable modal contents of olivine and Cr-spinel.

The FeO content is plotted against MgO content of the lavas in Fig. 5-12B. An overall triangular pattern, similar to the pattern in Fig. 5-12A is apparent. Again the arrow in the Fig. 5-12B indicates the effect of diopside dissolution and tie-lines suggest the effect of modal olivine addition or removal.

The variation in CaO/Al_2O_3 with MgO is shown in Fig. 5-12C. It shows considerable scatter in the data, however. We suggest that the present model allows the following interpretation. The data may be divided into two elongated groups. Both start at relatively low CaO/Al_2O_3 ratios (≈0.8) and MgO content of 8 to 10 wt.%. One extends to higher CaO/Al_2O_3 ratios with increasing MgO the other is nearly vertical and CaO/Al_2O_3 increases at constant MgO. The former data are nearly parallel to the clinopyroxene addition vector (shown in Fig. 5-12C), consistent with the effect of adding diopside to an enriched liquid. The second group of data are dominated by (un-equilibrated) glass inclusions. They represent melts that have, subsequent to diopside addition, undergone olivine crystallization. Data points to the left of the two groups demonstrate the effect of including modal olivine and Cr-spinel phenocrysts in the whole rock analysis. The tie lines in Fig. 5-12C are consistent with control by olivine addition (horizontal) or olivine + Cr-spinel addition (sub-horizontal). To summarize, the major-element data (12A, B and C) are consistent with diopside addition as a major control and scatter being induced by modal variation of olivine and spinel.

In the preceding figures (Figs. 12A, B and C) the direction and magnitude of the effect of dilution was indicated by arrows. In the case of CaO/Al_2O_3 ratio only ≈20% addition was needed to produce the vertical component in Fig.12C. However 40% diopside dissolution only accounted for about 1/2 of the TiO_2 variation in the lavas (Fig. 5-12A). As indicated by the tie-lines in Fig. 5-12A some additional depletion in TiO_2 can be the result of addition of modal olivine. However, an additional phase may be involved in balancing the major-elements. Thus, if the solid reactant is for instance a depleted lherzolite orthopyroxene and/or an aluminous spinel probably contribute to the melt.

It was suggested above that the anorthite-rich plagioclase found in many of these lavas may form in response to dissolution of clinopyroxene. Preferential incorporation of plagioclase ($CaO/Al_2O_3 \approx 0.5$) into the whole rock does have a modifying effect on the CaO/Al_2O_3 ratio. Although assimilation of plagioclase may be feasible from the standpoint of major-element chemistry it should be noted that textural evidence for that such a process is lacking. Simple crystallization calculations using the (1 bar) computer algorithm of Nielsen (1988) also indicate that dissolution of clinopyroxene leads to early (higher temperature) saturation of plagioclase. Therefore crystallization rather than dissolution of plagioclase is expected in this scenario.

5.6 Summary

The Dagmálafell picrite from SW-Iceland is host to gabbroic nodules of various mineral assemblages (gabbroic, troctolitic, anorthositic) in addition to megacrysts of clinopyroxene and plagioclase and phenocrysts of olivine and Cr-spinel. Small fine-grained nodules (micro-nodules) of clinopyroxene + Cr-spinel ± olivine occur along the margins of anorthositic gabbro-nodules. Based on textural evidence it is suggested that they are the remnants of a reaction corona or selvage that formed as a result of reactions between melt and the "host" anorthosite. The host nodule may have re-crystallized at the same time.

The host picrite is depleted in REE and trace-element abundances. Concentrations of REE and trace-elements in clinopyroxene from the different "lithologies" vary considerably. Clinopyroxene from coarse-grained gabbro-nodules appear to be in or close to trace-element equilibrium with the host melt. Some clinopyroxene megacrysts are enriched in LREE by a factor of five to ten relative to their counterparts in the coarse-grained gabbro-nodules. Clinopyroxene from fine-grained gabbro-nodules (micro-nodules) are intermediate between the two other groups.

The large variation in REE abundance in clinopyroxene and the large variation in trace-element abundance previously recorded in olivine-hosted glass inclusions form the same picrite (Gurenko and Chaussidon, 1995), demand that mafic enriched magmas (E-MORB like) and depleted magmas are closely associated at some point in their evolution.

A melt-rock reaction model is proposed to account for these observations. In this model a magma enriched in REE is exposed to and reacts with clinopyroxene-bearing lithology. This lithology must have suffered depletion in the geological past and had time to mature high $^{143}Nd/^{144}Nd$ isotope ratios. This model accounts for the heterogeneity in REE and trace-element abundances and abundance ratios in the various clinopyroxene-bearing lithologies. It also predicts close association of enriched and depleted melts immediately after the onset of melt rock reaction thus offering to account for the variability in trace-element content of olivine-hosted glass inclusions. The model also provides a framework for understanding the relationship between lava volume and variation in incompatible element abundance ratios.

5.7 References

Allégre, C.J., 1987. Isotope geodynamics. Earth Planet. Sci. Lett. 86, 175-203.

Anders, E. Grevesse, N., 1989. Abundances of the elements: Meteoritic and solar. Geochim. Cosmochim. Acta 53, 197-214.

Baker, M.B., Hirschmann, M.M., Ghiorso, M.S., Stolper, E.M., 1995. Compositions of near-solidus peridotite melts from experiments and thermodynamic calculations. Natue 375, 308-311.

Blundy, J.D., Robinson, J.A.C., Wood, B.J., 1998. Heavy REE compatibility in clinopyroxene on the spinel lherzolite solidus. Earth Planet. Sci. Lett. 160, 493-504.

Condomines, M., Grönvold, K., Hooker, P.J., Muehlenbachs, K., O'Nions, R.K., Óskarsson, N., Oxburgh, E. R., 1983. Helium, oxygen, strontium and neodymium isotopic relationships in Icelandic volcanics. Earth Planet. Sci. Lett. 66, 125-136.

DePaolo, D.J., 1981. Trace element and isotopic effect of combined wallrock assimilation and fractional crystallization. Earth Planet. Sci. Lett. 53, 189-202.

Dick, H.J.B., Natland, J.H., 1996. Late-stage melt evolution and transport in the shallow mantle beneath th East Pacific rise. In: Mével, C., Gillis, K. M. and Meyer P. S. (Eds.), Proceedings of the Ocean Drilling Program, Scientific Results, 147. Ocean Drilling Program, College Station, TX, pp. 103-134.

Droop, G.T.R., 1987. A general equation for estimating Fe^{+3} concentrations in ferromagnesian silicates and oxides from microprobe analyses, using stoichiometric criteria. Mineral. Mag. 51, 431-435.

Elliott, T.R., Hawkesworth, C.J. and Grönvold K., 1991. Dynamic melting of the Iceland plume. Nature 351, 201-206.

Furman, T. Frey, F., Park, K-H., 1995. The scale of heterogeneity beneath the Eastern neovolcanic zone, Iceland. J. Geol. Soc., London, 152, 997-1002.

Gast, P.W., 1968. Trace lement fractionation and the origin of tholeiitic and alkaline magma types. Geochim. Cosmochim. Acta 32, 1057-1086.

Gast, P.W., Tilton, G.R., Hedge, C., 1964. Isotopic composition of lead and strontium from Ascension and Gough Islands. Science 145, 1181-1185.

Gee, M.A.M., Thirlwall, M.F., Taylor, R.N., Lowry, D., Murton, B.J., 1998a. Crustal Processes: Major controls on Reykjanes peninsula lava chemistry, SW Iceland. J. Petrol. 39, 819-839.

Gee, M.A.M., Taylor, R.N., Thirlwall, M.F., Murton, B.J. 1998b. Glacioisostacy controls chemical and isotopic characteristics of tholeiites from the Reykjanes Peninsula, SW Iceland. Earth Planet. Sci. Lett. 164, 1-5.

Gurenko A.A., Chaussidon, M., 1995. Enriched and depleted primitive melts included in olivine from Icelandic Tholeiites: Origin by continous melting of a single mantle column. Geochim. Cosmochim. Acta 59, 2905-2917.

Gurenko, A.A., Sobolev, A.V., Kononkova, N.N., 1991. Petrology of the primary magma of the Reykjanes Peninsula rift tholeiites. Geochem Intl. 28, 58-71.

Gurenko, A.A., Sobolev, A.V., Polyakov, A.I., Kononkova, N.N., 1989. Primary rift tholeiites of Iceland: composition and condition of crystallization. Doklady Akademi Nauk SSSR 301, 179-184.

Hansteen, T.H., 1991. Multi stage evolution of the picritic Maelifell rocks, SW Iceland: Constraints from mineralogy and inclusions of glass and fluid in olivine. Contrib. Mineral. Petrol. 109, 225-339.

Hardardottir, V., 1983. The petrology of the Hengill volcanic system, southern Iceland. M.Sc. Thesis, McGill Univ., Montreal, pp. 260.

Hardarson, B.S., Fitton, J.G., 1991. Increased mantle melting beneath Snaefellsjökull volcano during Late Pleistocene deglaciation. Nature 353, 62-64.

Hardarson, B.S., Fitton, J.G., 1997. Mechanism of crustal accretion in Iceland. Geology 25, 1043-1046.

Hart, S.R., Schilling, J.-G. and Powell, J.L., 1973. Basalts from Iceland and along the Reykjanes Ridge: Sr isotope geochemistry. Nature 246, 104-107.

Hauri, E. H., 1997. Melt migration and mantle chromatography, 1: simlified theory and conditions for chemical and isotopic decoupling. Earth Planet. Sci. Lett. 153, 1-19.

Hess, P.C., 1992. Phase equilibria constraints on the origin of ocean floor basalts. In: Phipps Morgan J. Blackman D.K. and Sinton, J.M. (Eds.) Mantle flow and melt generation at Mid-Ocean Ridges. Geophysical Monographs 71, American Geophysical Union, Washington DC. pp.67-102.

Hémond, C., Arndt, N.T., Lichtenstein, U., Hofmann, A.W., Óskarsson, N., Steinthórsson, S., 1993. The heterogeneous Iceland plume: Nd-Sr-O Isotopes and trace element constraints. J. Geophys. Res. 98, 15833-15850.

Hofmann, A.W., 1997. Mantle geochemistry: the message from oceanic volcanism. Nature 385, 219-229.

Jakobsson, S.P., Jónsson, J., Shido, F., 1978. Petrology of western Reykjanes peninsula, Iceland. J. Petrol. 19, 669-705.

Johnson, K.T.M., Dick, H.J.B., Shimizu, N., 1990. Melting in the oceanic upper mantle: An ion-microprobe study of diopsides in abyssal peridotites. J. Geophys. Res. 95, 2661-2678.

Jull, M., McKenzie, D., 1996. The effect of deglaciation on mantle melting beneath Iceland. J. Geophys. Res. 101, 21815-21828.

Kamenetsky, V.S., Eggins, S.M., Crawford, A.J., Green, D.H., Gasparon, M. Falloon, T.J., 1998. Calcic melt inclusions in priomitive olivine at 43°N MAR: evidence for melt rock reaction/melting involving clinopyroxene-rich lithologies during MORB generation. Earth Planet. Sci. Lett. 160, 115-132.

Kelemen, P.B., 1990. Reaction between ultramafic rock and fractionating basaltic magma I. Phase rtelations, the origin of calc-alkaline magma series, and the formation of discordant dunite. J. Petrol 31, 51-98.

Kelemen, P.B., Dick, H.J.B., Quick, J.E., 1992. Formation of harzburgite by pervasive melt/rock reaction in the upper mantle. Nature 358, 635-641.

Kelemen, P.B., Shimizu, N., Dunn, T., 1993. Relative depletion of niobium in some arc magmas and the continental crust: partitioning of K, Nb, La and Ce during melt/rock rteactionin the upper mantle. Earth Planet. Sci. Lett. 120, 111-134.

Kelemen, P.B. Shimizu, N. Salters, V.J.M., 1995. Extraction of mid-ocean-ridge basalt from the upwelling mantle by focused flow of melt in dunite channels. Nature 375, 747-753.

Kelemen, P.B., Hirth G., Shimizu, N., Spiegelman, M. and Dick, H.J.B., 1997. A review of melt migration processes in the adiabatically upwelling mantle beneath oceanic spreading ridges. Phil. Trans. Roy. Soc. Lond. A 355, 283-318.

Kinzler, R.J. and Grove, T.L., 1992. Primary magmas of mid-ocean ridge basalts: I. Experiments and methods. J. Geophys. Res. 97, 6885-69006.

Klein, E.M., Langmuir, C.H., 1987. Global correlations of ocean ridge basalt chemistry with axial depth and crustal thickness. J. Geophys. Res. 92, 8089-8115.

Meyer, P.S., Sigurdsson, H.S., Schilling, J.-G., 1985. Petrological and geochemical variations along Iceland's neovolcanic zones. J. Geophys. Res. 90, 10043-10072.

Navon, O., Stolper, E., 1987. Geochemical consequences of melt percolation: The upper mantle as a chromatographic column. J. Geol. 95, 285-307.

Nielsen, R.L., 1988. TRACE.FOR: A program for the calculation of combined major and trace-element liquid lines of descent for natural magmatic systems. Comp. Geosci. 14, 15-35.

Rampone, E. Piccardo, G.B., Vanucci, R., Bottazzi, P., 1998. Chemistry and origin of trapped melts in ophiolitic peridotites. Geochim. Cosmochim. Acta 61,4557-4569.

Reiners, P.W., 1998. Reactive melt transport in the mantle and geochemical signatures of mantle-derived magmas. J. Petrol. 39, 1039-1061.

Risku-Norja, H., 1985. Gabbro nodules from a picritic pillow basalt, Midfell, SW Iceland, Nordic Volcanol. Inst. Prof. Paper 8501, pp. 71.

Roden, M.F. and Shimizu, N., 2000. Trace element abundances in mantle derived minerals which bear on compositional complexities in the lithosphere of the Colorado Plateu. Chem. Geol. 165, 283-305.

Saal, A.E., Hart, S.R., Shimizu, N., Hauri, E.H., Layne, G.D., 1998. Pb isotopic variability in melt inclusions from oceanic island basalts, Polynesia. Science 282, 1481-1484.

Schilling, J.-G., 1973. Iceland mantle plume: Geochemical study of Reykjanes Ridge. Nature 242, 566-571.

Shimizu, N., 1998. The geochemistry of olivine-hosted melt inclusions in a FAMOUS basalt ALV 519-4-1. Phys Earth Planet. Int. 107, 183-201.

Shimizu, N., Hart S.R., 1982. Applications of the ion microprobe to geochemistry and cosmochemistry. Annu. Rev. Earth Planet. Sci. 10, 483-526.

Sigmarsson, O., Condomines, M., Fourcade, S., 1992. mantle and crustal contributions to Recent basalts from the off-rift zones in Iceland: Constraints from Th, Sr and O isotopes. Earth planet. Sci. Lett. 110, 149-162.

Sigurdsson, I.A., 1994. Primitive magmas in convergent margins and at oceanic spreading ridges: Evidence from early formed phenocryst phases and their melt inclusions. Ph.D. Thesis, University of Tasmania, Hobart, pp. 243.

Sigvaldason, G.E., 1974. Basalts from from the centre of the assumed Icelandic mantle plume. J. Petrol. 15, 497-524.

Sigvaldason, G.E., Annertz, K., Nilsson, M., 1992. Effect of glacier loading/deloading on volcanism: Postglacial volcanic production rate of the Dyngjufjöll area, central Iceland. Bull. Volcanol. 54, 385-392.

Sinton, C.W., Christie, D.M., Coombs, V.L. Nielsen, R.L. and Fisk, M.R., 1993. Near primary melt inclusions in anorthite phenocrysts from the Galapagos Platform. Earth Planet. Sci. Lett. 119, 527-537.

Sobolev, A.V. Shimizu, N., 1993. Ultra-depleted primary melt included in an olivine from the Mid-Atlantic Ridge. Nature 363, 151-154.

Stolper, E. 1980. A phase diagram for mid-ocean ridge basalts: preliminary results and implications for petrogenesis. Contrib Mineral. Petrol. 74, 13-27

Sun S.-S. and McDonough, W.F., 1989. Chemical and isotopic systematics of oceanic basalts: Implications for mantle composition and processes, in : Magmatism in the

ocean basins. In: Saunders, A.D.and Norry, M.J. (Eds.), Geol. Soc. London Spec. Publ. 42, 313-345.

Takazawa, E., Frey, F.A., Shimizu, N., Obata, M. and Bodinier, J.L., 1992. Geochemical evidence for melt migration and reaction in the upper mantle. Nature 359, 55-58.

Tatsumoto, M., Hedge, C.E., Engel, A.E.J., 1965. Potassium, rubidium, strontium, thorium, uranium, and the ratio of Sr-87 to Sr 86 in oceanic tholeiitic basalt. Science 150, 886-888.

Thirlwall, M.F., 1991. Long term reproducibility of multicollector Sr and Nd isotope ratio analysis. Chem. Geol. 94, 85-104.

Trønnes, R.G., 1991. Basaltic melt evolution of the Hengill volcanic system, SW Iceland, and evidence for clinopyroxene assimilation in primitive tholeiitic magmas. J. Geophys. Res. 95, 15893-15910.

Vernières, J., Godard, J., Bodinier, J.-L., 1997. A plate model for the simulation of trace element fractionation during partial melting and magma transport in the Earth's upper mantle. J. Geophys. Res. 102, 24771-24784.

Wagner, T.P., Grove, T.L., 1998. Melt/harzburgite reaction in the petrogenesis of tholeiitic magma from Kilauea volcano, Hawaii. Contrib. Mineral. Petrol. 131,1-12.

Walter, M.J., Sisson, T.W., Presnall, D.C., 1995. A mass proportion method for calculating melting reactions and application to melting of model upper mantle lherzolite. Earth Planet. Sci. Lett. 135, 77-90.

Zindler, A., Hart, S.R., Frey, F.A., Jakobsson, S.P., 1979. Nd and Sr isotope ratios and rare earth element abundances in Reykjanes peninsula basalts: Evidence for mantle heterogeneity beneath Iceland. Earth Planet. Sci. Lett. 45, 249-262.

Zindler, A. and Hart, S. R., 1986. Chemical Geodynamics. Ann. Rev. Earth Planet. Sci.14, 493-571.

Table 5-1 Major element composition (wt. %) of clinopyroxene megacrysts and of clinopyroxene in fine grained nodules (micro-nodules) and coarse grained gabbro nodules.

Sample Megacrysts	Points	SiO_2	TiO_2	Al_2O_3	Cr_2O_3	FeO	MnO	MgO	CaO	Na_2O	K_2O	Total
PM 12 Gr 2	3	51.3	0.32	4.67	1.07	4.55	0.10	17.2	20.7	0.22	0.02	100.2
	sd	0.3	0.13	0.09	0.02	0.01	0.01	0.2	0.2	0.01	0.02	
PM 12 Gr3	3	51.2	0.24	4.98	0.99	4.31	0.09	17.1	21.0	0.21	0.02	100.1
	sd	0.3	0.03	0.05	0.20	0.12	0.01	0.2	0.1	0.01	0.01	
PM 12 Gr 4	3	51.8	0.33	3.76	0.74	4.91	0.12	17.4	20.9	0.23	0.02	100.2
	sd	0.2	0.03	0.01	0.02	0.09	0.01	0.1	0.1	0.01	0.01	
PM13 Gr A	3	52.0	0.14	4.30	1.41	3.78	0.11	17.9	20.6	0.22	0.01	100.5
	sd	0.0	0.01	0.15	0.03	0.02	0.03	0.2	0.1	0.02	0.01	
PM13 Gr B-1	3	51.2	0.30	4.84	1.09	4.49	0.10	16.9	21.4	0.22	0.02	100.6
	sd	0.2	0.03	0.07	0.05	0.01	0.01	0.1	0.0	0.01	0.02	
PM13 Gr B-2	3	50.9	0.25	5.83	1.16	4.38	0.11	17.2	20.3	0.27	0.02	100.4
	sd	0.2	0.02	0.24	0.03	0.09	0.03	0.1	0.1	0.03	0.01	
PM13 Gr B-3	2	52.3	0.26	3.53	0.93	4.51	0.12	17.9	20.9	0.22	0.01	100.6
	sd	0.7	0.01	0.62	0.19	0.19	0.00	0.8	0.6	0.01	0.01	
PM13 Gr B-4	2	51.7	0.52	3.65	0.56	6.04	0.14	17.0	20.7	0.23	0.02	100.5
	sd	0.0	0.03	0.04	0.01	0.04	0.03	0.1	0.2	0.01	0.02	
Micro nodules												
PM 14 Gr A	9	51.6	0.26	3.98	0.97	4.45	0.09	17.3	21.3	0.23	0.02	100.3
w/Cr-sp	sd	0.4	0.03	0.34	0.20	0.08	0.02	0.3	0.1	0.02	0.01	
PM 14 Gr B	5	51.4	0.32	4.64	0.65	4.81	0.09	17.2	21.0	0.21	0.02	100.4
	sd	0.2	0.05	0.09	0.11	0.08	0.01	0.1	0.1	0.01	0.01	
PM 15 Gr A	3	51.1	0.30	4.80	1.29	4.50	0.09	16.8	21.4	0.21	0.02	100.5
	sd	0.1	0.04	0.16	0.03	0.07	0.00	0.1	0.1	0.01	0.00	
PM 15 Gr B	3	51.2	0.31	4.82	1.13	4.51	0.11	16.9	21.3	0.21	0.02	100.6
	sd	0.3	0.03	0.34	0.13	0.03	0.02	0.1	0.1	0.01	0.01	
Gabbro nodules												
PM 1 Gr 7	1	52.0	0.28	4.48	1.02	4.39	0.11	17.4	20.9	0.21	0.02	101.0
PM 1 Gr 11	1	51.7	0.26	4.66	1.04	4.26	0.08	17.5	20.9	0.14	0.02	100.6
PM 1 Gr 13	1	52.0	0.28	4.42	0.81	4.85	0.13	17.3	21.2	0.22	0.02	101.2

1) Minerals were analyzed for major elements on the JEOL JXA 8900 electron microprobe at the University of Alberta. Analysis were performed in WDS mode, with a 15kV acceleration potential and 20 nA sample current.

Table 5-2 Cation proportion in clinopyroxene from Dagmálafell based on 6 oxygens per formula unit (pfu)[1].

Sample											
Megacrysts	**Si^{+4}**	**Ti^{+4}**	**Al^{+3}**	**Cr^{+3}**	**Fe^{+3}**	**Fe^{+2}**	**Mn^{+2}**	**Mg^{+2}**	**Ca^{+2}**	**Na^{+}**	**K^{+}**
PM 12 Gr 2	1.865	0.009	0.200	0.031	0.000	0.138	0.003	0.931	0.806	0.016	0.001
PM 12 Gr3	1.859	0.007	0.213	0.028	0.001	0.130	0.003	0.925	0.818	0.015	0.001
PM 12 Gr 4	1.883	0.009	0.161	0.021	0.005	0.144	0.004	0.943	0.813	0.017	0.001
PM13 Gr A	1.876	0.004	0.183	0.040	0.081	0.033	0.003	0.965	0.798	0.016	0.001
PM13 Gr B-1	1.857	0.008	0.207	0.031	0.034	0.103	0.003	0.912	0.829	0.016	0.001
PM13 Gr B-2	1.841	0.007	0.249	0.033	0.048	0.085	0.003	0.927	0.788	0.019	0.001
PM13 Gr B-3	1.889	0.007	0.150	0.027	0.064	0.072	0.004	0.962	0.808	0.015	0.001
PM13 Gr B-4	1.881	0.014	0.156	0.016	0.000	0.184	0.004	0.922	0.805	0.016	0.001
Micro nodules											
PM 14 Gr A	1.874	0.007	0.170	0.028	0.014	0.121	0.003	0.938	0.828	0.016	0.001
PM 14 Gr B	1.866	0.009	0.198	0.019	0.025	0.121	0.003	0.930	0.815	0.015	0.001
PM 15 Gr A	1.853	0.008	0.205	0.037	0.023	0.113	0.003	0.910	0.831	0.015	0.001
PM 15 Gr B	1.856	0.008	0.206	0.032	0.034	0.103	0.003	0.915	0.828	0.015	0.001
Gabbro nodules											
PM 1 Gr 7	1.876	0.008	0.190	0.029	0.094	0.038	0.003	0.937	0.808	0.015	0.001
PM 1 Gr 11	1.869	0.007	0.199	0.030	0.060	0.069	0.002	0.945	0.808	0.010	0.001
PM 1 Gr 13	1.870	0.007	0.187	0.023	0.118	0.028	0.004	0.930	0.816	0.015	0.001

1) Cation proportions calculated assuming stoichiometry and charge balance (Droop, 1987). Proportion of Fe+3 is estimated from sum of cations (all Fe as Fe+2) in excess of the ideal 4 (pfu). The cations are subsequently normalized to a sum of 4. Prior to normalization, cation sums based on 6 oxygens from the microprobe analysis (Table 1) range from 3.995 to 4.040.

Table 5-3 Rare Earth element abundances (ppm) in clinopyroxene megacrysts and in clinopyroxene in fine grained nodules (micronodules) and coarse grained gabbro nodules. Data obtained with the Cameca IMS 3f Ion Microprobe (WHOI). Details of analytical procedures is given in Shimizu and Hart (1982), Johnson et al. (1990) and Shimizu (1998). Analytical precision based on multiple analysis in this and previous studies (e.g. Roden and Shimizu, 2000) employing the same machine and analytical procedure, is typically better than ±10% for trace elements other than the REE and ±10-20% for the REE. Precision may be significantly worse, ±30-50%, for REE present in low abundances (<0.1 (ppm)).

Sample									
Megacrysts	**Points**	**La**	**Ce**	**Nd**	**Sm**	**Eu**	**Dy**	**Er**	**Yb**
PM 12 Gr 2	2	0.29	1.31	1.58	0.78	0.32	1.34	0.80	0.66
	sd	0.04	0.21	0.33	0.15	0.04	0.30	0.09	0.07
PM 12 Gr 3	1	0.25	1.21	1.42	0.71	0.38	1.35	0.79	0.72
PM 12 Gr 4	1	0.26	1.09	1.43	0.75	0.34	1.17	0.69	0.74
PM 12 Gr 8	1	0.36	1.28	1.67	0.89	0.32	1.26	0.90	0.75
PM 13 Gr A	2	0.11	0.48	1.02	0.59	0.22	1.08	0.57	0.45
	sd	0.07	0.12	0.12	0.12	0.06	0.16	0.04	0.04
PM 13 B-4	1	0.11	0.55	0.93	0.62	0.26	1.18	0.73	0.54
PM 13 OB-4	1	0.49	1.78	2.23	1.12	0.41	1.68	1.08	0.85
Micro nodules									
PM 14 Gr A	2	0.09	0.41	0.88	0.55	0.18	1.02	0.57	0.55
	sd	0.03	0.07	0.11	0.10	0.03	0.09	0.04	0.04
PM 14 Gr B	1	0.12	0.48	1.06	0.55	0.34	1.13	0.94	0.66
PM 15 Gr A	2	0.14	0.51	0.78	0.58	0.20	1.01	0.59	0.53
	sd	0.02	0.09	0.25	0.00	0.01	0.04	0.06	0.13
Gabbro nodules									
PM 1 Gr 7	1	0.05	0.39	0.67	0.44	0.17	0.76	0.50	0.42
PM 1 Gr 11	2	0.04	0.32	0.62	0.41	0.19	0.72	0.47	0.35
	sd	0.02	0.02	0.10	0.06	0.01	0.06	0.05	0.07
PM 1 Gr 13	1	0.08	0.30	0.64	0.51	0.20	0.90	0.56	0.41

Table 5-4 Trace element abundances (ppm) in clinopyroxene megacrysts and in clinopyroxene in fine grained nodules (micronodules) and coarse-grained gabbro nodules (analytical details as given in Table 5-3).

Sample								
Megacrysts	**n**	**Ti**	**V**	**Cr**	**Sr**	**Y**	**Zr**	**Ti/Zr**
PM 12 Gr 2		2534	243	5692	15.9	7.4	7.3	345
PM 12 Gr 3		2114	237	5853	14.1	7.0	5.8	365
PM 12 Gr 4		2060	230	5068	13.5	7.1	5.6	369
PM 12 Gr 8		2020	229	4742	12.8	6.4	5.3	382
PM 13 Gr A	2	1581	212	7666	10.6	5.6	2.8	556
	sd	38	2	944	0.3	0.1	0.2	
PM 13 B-4		1594	219	4985	11.4	5.9	3.2	505
PM 13 OB-4	2	3037	272	3643	16.7	9.3	7.8	388
	sd	115	8	69	1.2	0.2	0.2	
Micro nodules								
PM 14 Gr A	2	1617	192	7148	10.7	5.6	2.8	580
	sd	19	2	146	0.2	0.5	0.0	
PM 14 Gr B		1870	235	5091	10.6	6.7	3.4	546
PM 15 Gr A	p1	1429	200	4326	13.1	5.1	2.3	627
PM 15 Gr A	p2	1816	200	8446	12.4	5.7	3.3	555
Gabbro nodules								
PM 1 Gr 7		1532	190	8475	10.5	5.1	3.2	484
PM 1 Gr 11		1668	191	8402	11.2	5.7	2.3	721
PM 1 Gr 13		1747	200	8830	10.1	5.7	2.2	780

Table 5-5 Major element composition (wt. %) and Rare Earth element abundances (ppm) in pillow rim glasses. Dmf is the host picrite and Stp is Stapafell an enriched mafic melt used for modelling (analytical details as in Table 5-1 and Table 5-3).

Major Elements (wt%)											
	n	**SiO_2**	**TiO_2**	**Al_2O_3**	**FeO**	**MnO**	**MgO**	**CaO**	**Na_2O**	**K_2O**	**P_2O_5**	**Sum**
Dmf	6	47.9	0.74	15.5	9.38	0.17	9.83	14.2	1.51	0.01	0.02	99.20
	sd	0.5	0.02	0.2	0.12	0.05	0.14	0.1	0.06	0.01	0.02	
Stp	2	48.6	1.66	15.0	10.7	0.13	8.07	12.2	2.00	0.22	0.20	98.73
	sd	0.6	0.01	0.2	0.1	0.03	0.03	0.1	0.04	0.02	0.02	

Rare Earth Elements (ppm)								
	n	**La**	**Ce**	**Nd**	**Sm**	**Dy**	**Er**	**Yb**
Dmf	3	1.33	3.10	2.75	1.20	1.94	1.27	1.20
	sd	0.13	0.11	0.23	0.13	0.07	0.09	0.01
Stp	3	11.24	25.17	12.66	3.37	3.66	1.95	1.99
	sd	0.18	0.02	0.59	0.11	0.19	0.20	0.05

Trace Elements (ppm)								
	n	**Ti**	**V**	**Cr**	**Sr**	**Y**	**Zr**	**Ti/Zr**
Dmf	3	4928	262	484	128	12.9	34.9	141
	sd	70	1	7	4	0.5	7.7	
Stp	3	10954	306	423	237	22.3	128	85
	sd	128	2	5	6	0.7	14	

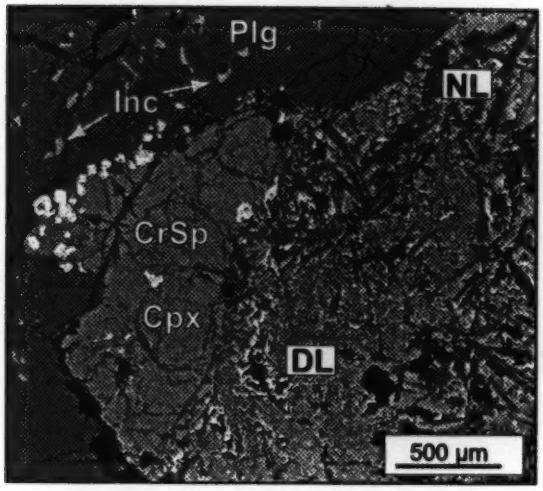

Figure 5-1 Micro nodule of Cr-Spinel and clinopyroxene located at the margin of a plagioclase + olivine gabbro nodule. Note the concentration of Cr-spinel (CrSp) at the contact between the host (Plg) and clinopyroxene (Cpx) in the micro nodule. Note also enrichment in diopside in the liquid adjacent to the micro nodule. In the "top" part, fresh undiluted liquid (NL = normal liquid) appears to be invading to replace the diopside-rich (DL = diopside-rich liquid) melt adjacent to the nodule. Broken line delineates the boundary between plagioclase-rich and plagioclase-poor liquid. White arrows in plagioclase point to inclusions (Inc) in the host, see text.

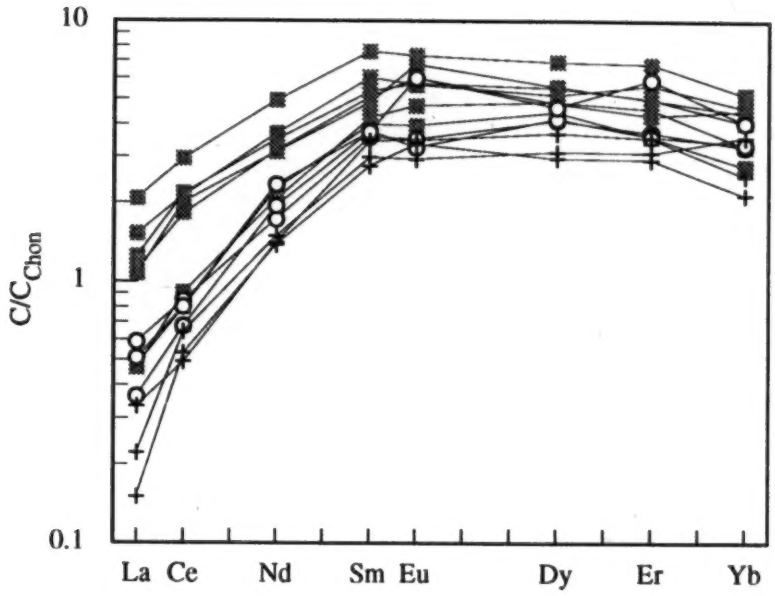

Figure 5-2 REE patterns for three types of clinopyroxene occurring in the Dagmálafell picrite: megacrysts = shaded squares; clinopyroxene in micro nodules = circles; clinopyroxene in gabbro nodules = crosses. Abundances normalized to chondritic abundances from Anders and Grevesse (1989).

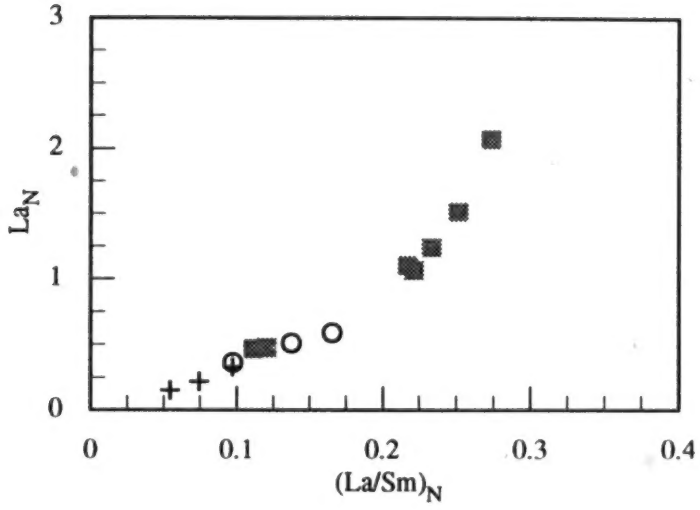

Figure 5-3 Variation in La/Sm normalized ratio ($(La/Sm)_N$) plotted against normalized La abundance (La_N). Note compositional grouping and change in slope. Symbols and normalization as in Figure 5-2.

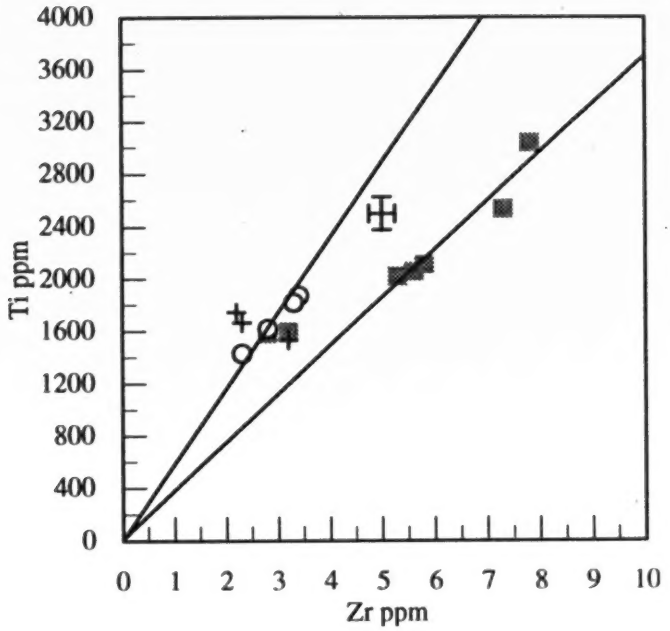

Figure 5-4 Variation in Ti and Zr in clinopyroxene from Dagmálafell. Symbols as in Figure 5-3. Note that Zr and Ti covary in the dataset as a whole and also among the megacrysts and apparently in the micronodules. Two lines of constant slope (Ti/Zr ratio) are shown (note also that the current data on megacrysts may be fitted to a "gentle" curve).

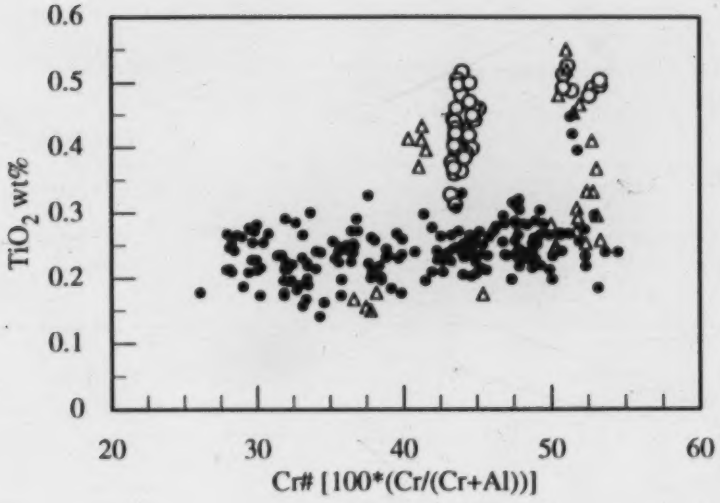

Figure 5-5 Variation of TiO_2 content with Cr# (Cr#=100Cr/(Cr+Al)) in Cr-spinels from Dagmálafell. Cr-spinel phenocrysts and inclusions in olivine = solid dots; Cr-spinel in micro nodules = circles; Cr-spinel included in clinopyroxene = triangles.

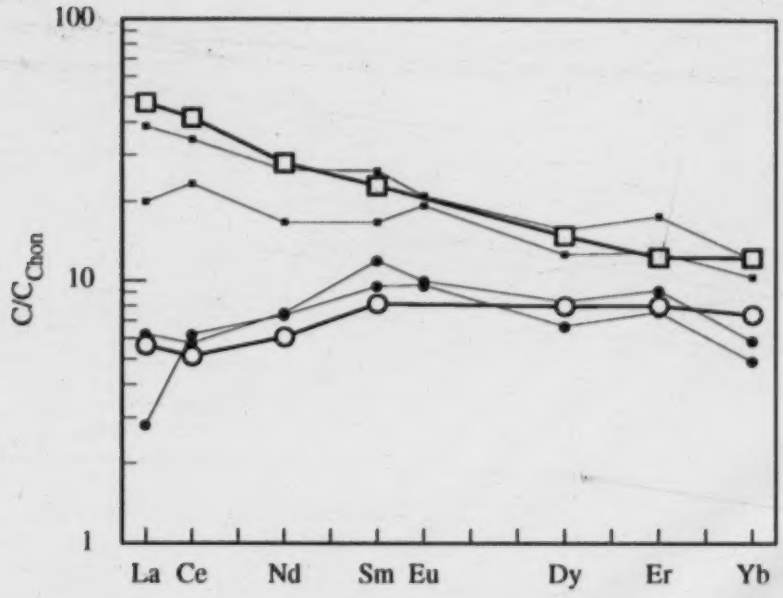

Figure 5-6 REE element profiles of liquids calculated to be in equilibrium with Megacrysts (solid squares) and clinopyroxene from coarse grained gabbro nodules (solid circles) compared to host liquid (open circles) (i.e. Dagmálafell) and Stapafell (open squares) an enriched basalt on Reykjanes peninsula (Table 5).

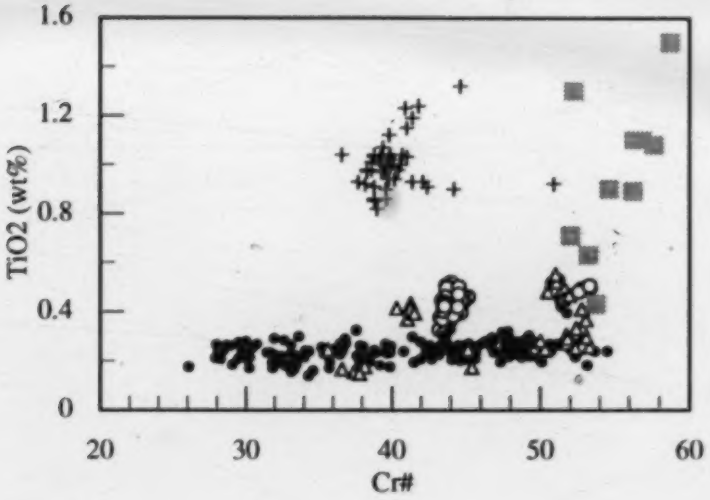

Figure 5-7 Variation of TiO_2 content with Cr# (Cr#=100Cr/(Cr+Al)) in Cr-spinels from Dagmálafell plotted again, symbols as in Fig. 4. Also shown for comparison are data for Cr-spinels from Re286 (Sigurdsson, 1994) representing the enriched endmember (crosses) and a subset of Cr-spinels (shaded boxes) from gabbroic selvages in harzburgites from the Hess Deep (Dick and Natland, 1996).

Figure 5-8 A and B (Following page).

A: Variation in Ti/Zr versus $(La/Sm)_N$ for enriched and depleted liquids. Open circle and filled square are Dagmalafell picrite and Stapafell respectively (this study). All other data from Gurenko and Chaussidon (1996). Open dot-centered circle = Dagmálafell pillow rim; open squares = Dagmálafell whole rock; triangles = Maelifell picrite (Hengill area); shaded diamonds = glass inclusions in olivine from picrites in SW-Iceland. Tie line shows effect of binary mixing. (numbers by boxes indicate percent enriched liquid in mixture).

B: Same plot showing "depleted end" only. Dot centered squares are "bulk" samples (pillow rim and whole rocks) from Dagmálafell only. Crosses are glass inclusions in olivine. Solid square and triangle are clinopyroxene megacryst and micro nodule. Shaded and open square represent accumulated and instantaneous melts respectively, calculated assuming fractional melting. The squares are labeled indicating the amount of melting in percent.

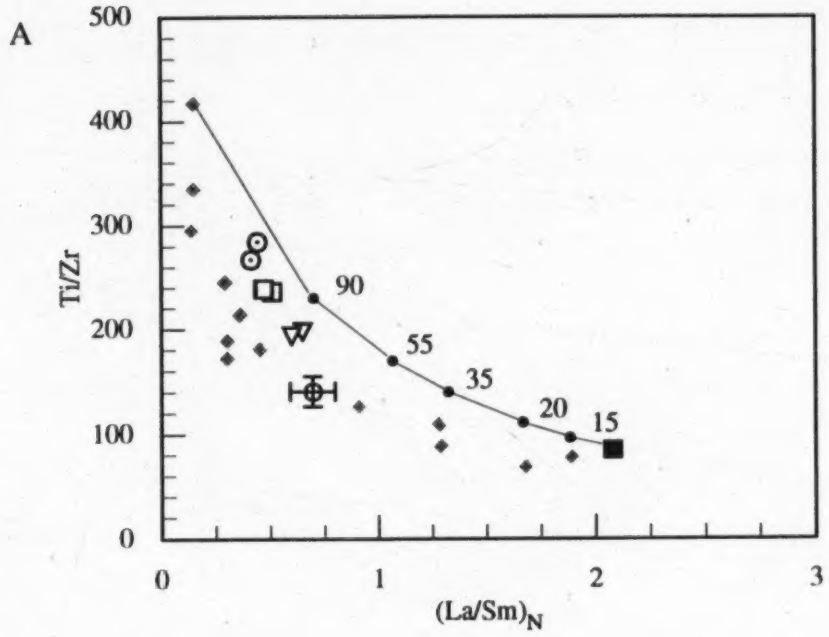
A
500
400
300
200
100
0
Ti/Zr
90
55
35
20
15
0
1
2
3
(La/Sm)N

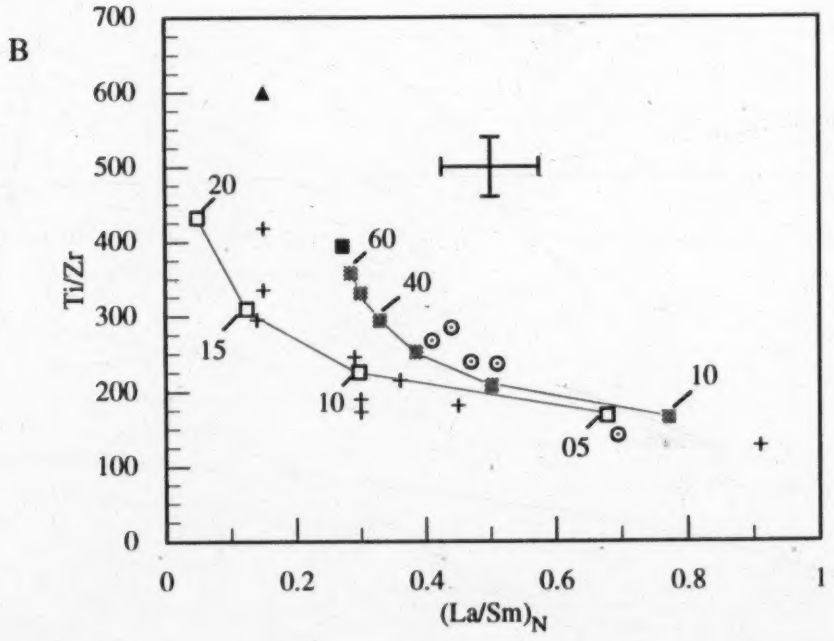
B
700
600
500
400
300
200
100
0
Ti/Zr
20
60
40
15
10
10
05
0
0.2
0.4
0.6
0.8
1
(La/Sm)N

Figure 5-9 A and B (Following page).

A: Two model liquids (thin lines) produced by "Assimilation-Fractional-Crystallization" using DePaolo's (1981) model (Equation 6a) compared to the Dagmálafell picrite (open circles). Initial liquid of (Stapafell) assimilates clinopyroxene and crystallizes olivine. Composition of initial liquid is given in Table 5-5. Clinopyroxene from Hess Deep harzburgite (895E 7R-4, 37-40) with La, Ce, Nd, Sm, Eu, Dy, Er and Yb concentrations of 0.013, 0.020, 0.038, 0.032, 0.017, 0.144, 0.169 and 0.231 ppm (Dick and Natland, 1996). Partition coefficients for olivine liquid as listed in Kelemen et al. (1993). More depleted liquid obtained by assuming r = (Rate of Assimilation/Rate of crystallization) = 5 and F = (Mass of magma/Initial massof magma) = 10. All parameters for calculating the less depleted liquid were the same except for F = 5.

B: Two model liquids (thin lines) estimated to be in equilibrium with clinopyroxene from residual peridotites compared to the Dagmálafell picrite (open cicles). Residual peridotite data from Vulcan Fracture Zone (Johnson et al., 1990) and Hess Deep (Dick and Natland, 1996). Samples from Vulcan fracture zone: 1 = Vulc5:41-15(8) and 2 = Vulc5:41-33(6) and Hess Deep: 3 = 895E 7R-4,37-40 (used in AFC calculation in Fig 5-9A) and 4 = 895D 3R-1,116-120.

A

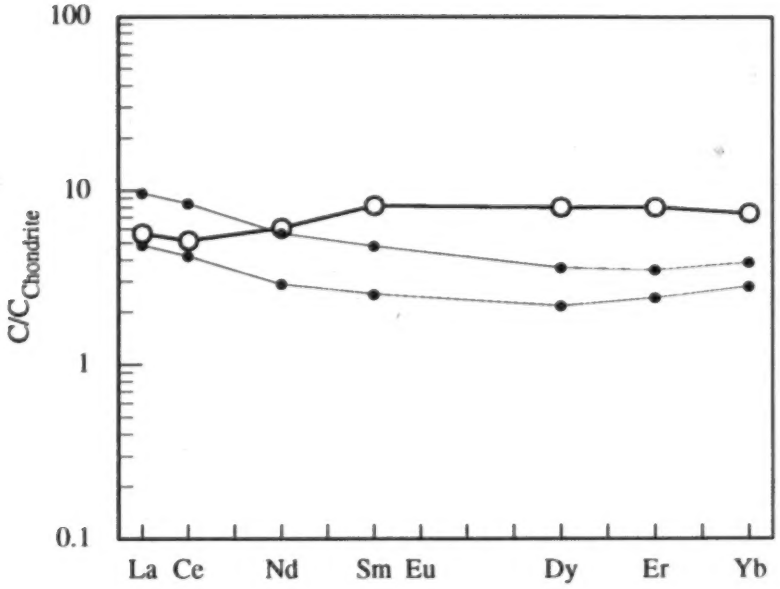
100
10
1
0.1
C/C Chondrite
La Ce Nd Sm Eu Dy Er Yb

B

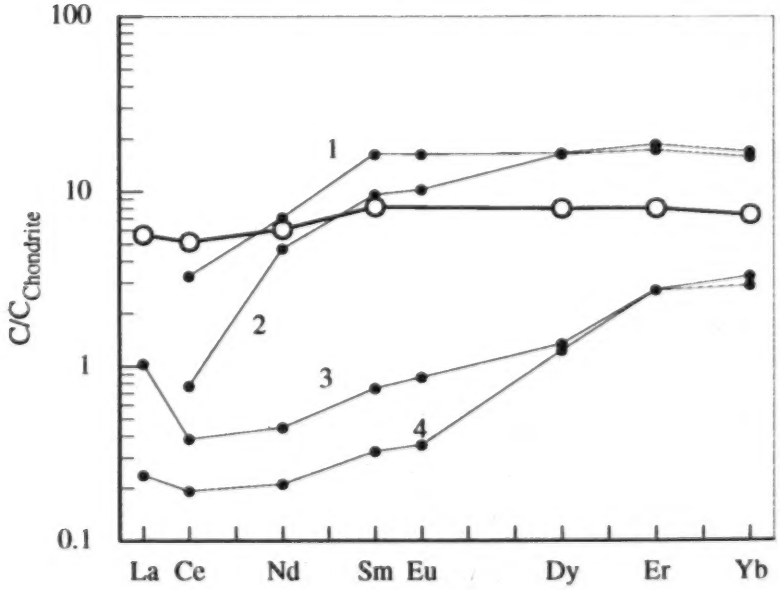
100
10
1
0.1
C/C Chondrite
1
2
3
4
La Ce Nd Sm Eu Dy Er Yb

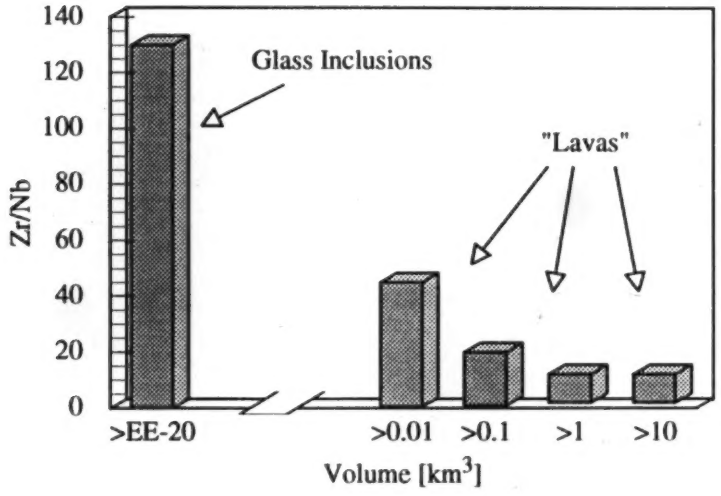

Figure 5-10 Relationship between volume and trace element abundance ratio for Icelandic lavas and subglacial formations (hyaloclastites) labeled collectively "lavas" (data from Hardarson and Fitton 1997) and glass inclusions (data from Gurenko and Chaussidon 1995). Each column represents the total variation in a particular volume "group."

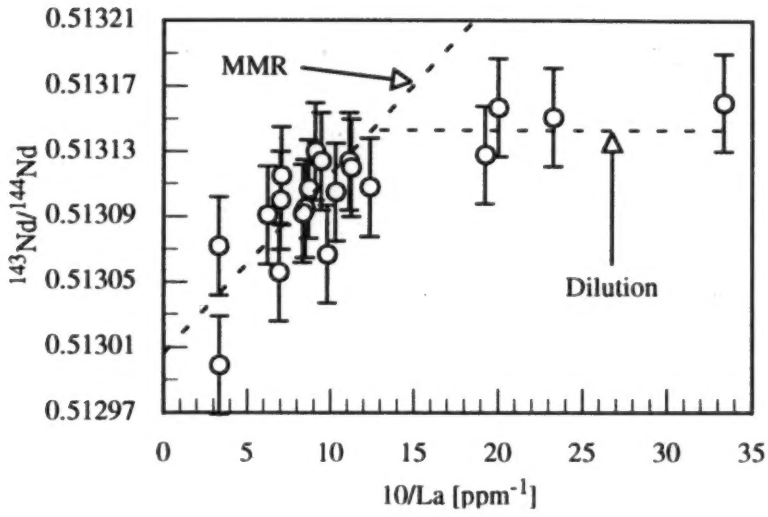

Figure 5-11 $^{143}Nd/^{144}Nd$ isotope ratios plotted against 10/La (ppm-1). Data from Elliott et al., (1991) and Hémond et al., (1993). The Nd isotope data were normalized to values of 0.512640 and 0.511850 for the BCR 1 and La Jolla standards respectively, consistent with a difference between the two standards of $7.87*10^{-4}$ ($\pm$ $3*10^{-6}$) obtained by Thirlwall (1991). Error bars of ±3x10-5 are shown. The data forms an array that may be interpreted in terms of melt-mantle reaction (MMR) i.e. an enriched melt (high La low $^{143}Nd/^{144}Nd$) reacting with a lithology that suffered depletion in the geological past (low La high $^{143}Nd/^{144}Nd$). Horizontal component may be due to modal olivine.

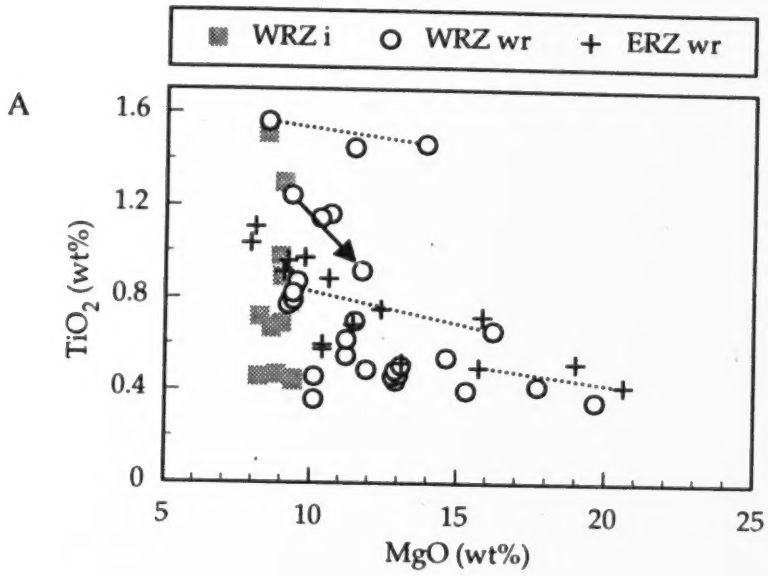

Figure 5-12 A, B and C.

A (Above): Variation in TiO_2 with MgO for high MgO lavas from the rift zones. Arrow indicated the effect 40% addition of diopside to an enriched liquid. Tielines (broken) connect two analyses from the same lava or formation with different modes, indicating the effect of adding or removing olivine and or Cr-spinel. The tieline at highest MgO links two whole rock analyses. The other two, link whole-rock and pillow rim (=liquid) analyses. Abbreviations: WRZ=West Rift Zone; ERZ=East Rift Zone; i = glass inclusion; wr=whole rock.

B (Following page): Variation in FeO with MgO. Arrow indicates the effect of adding 40% of diopside to an enriched lava. Tielines and symbols as in A.

C (Following page): Variation in CaO/Al_2O_3 ratio with MgO content. Arrow indicates effect of adding 20% of diopside to an enriched liquid. Tielines and symbols as in A.

Data from Elliott (1991); Hémond et al., (1993); Sigurdsson (1994); Gurenko and Chaussidon (1995); Gee et al., (1998a).

B

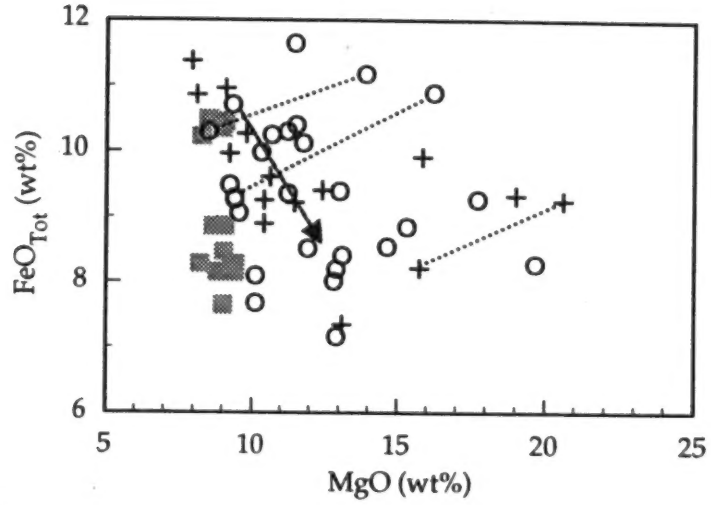
12
10
8
6
5
10
15
20
25
FeO$_{Tot}$ (wt%)
MgO (wt%)

C

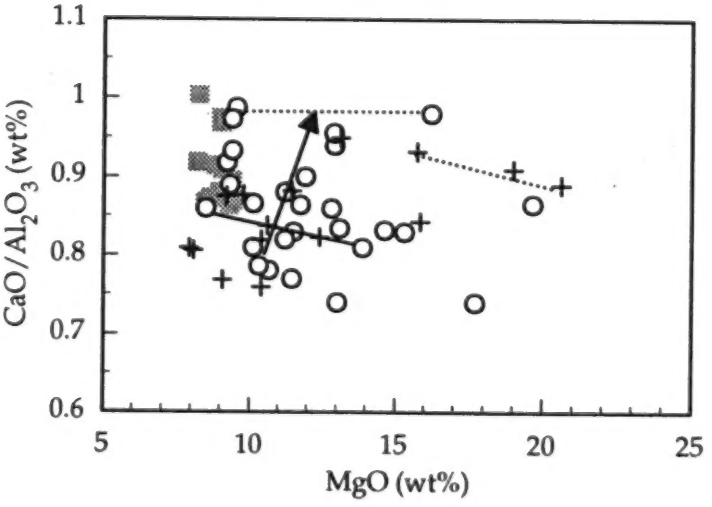
1.1
1
0.9
0.8
0.7
0.6
5
10
15
20
25
CaO/Al$_2$O$_3$ (wt%)
MgO (wt%)

Chapter 6

THESIS CONCLUSIONS

6.1 Summary

The oxygen isotopic composition of early and late Tertiary basalts associated with the Iceland mantle plume are depleted in ^{18}O relative to common mid-ocean ridge basalts. The isotope chemistry is consistent with the presence of a ^{18}O-depleted component in the mantle plume.

Based on oxygen isotope data from gabbro nodules and coeval lavas and hyaloclastites, a model for transferring ^{18}O from magmas residing in the crust to the hydrosphere is proposed. In this model isotopic exchange between magma and crust is achieved efficiently through a large surface area between crust and magma, in a magma-mush reservoir in the lower crust.

A summary of oxygen isotope data from the Icelandic rift zones allows constraints to be placed on the oxygen isotopic composition of the crust. In turn the total flux of ^{18}O from the mantle, through the crust, to the hydrosphere may be estimated from knowledge of the change in $\delta^{18}O$ of the crust due to high temperature processes. The flux of ^{18}O to the hydrosphere is at least comparable (on a mass equivalent basis) to the ^{18}O flux associated with high temperature hydrothermal metamorphism at mid-ocean ridges.

Melt-mantle reactions play an important role in the generation of picrites from the Icelandic rift-zones. A model is proposed where enriched mafic melts (E-MORB like) interact with a depleted clinopyroxene lithology to produce the picrites. The melt rock reactions are dominated by the dissolution of clinopyroxene and crystallization of olivine and Cr-spinel. This model also provides a framework for understanding the relationship between lava volume and variation in incompatible abundance ratios among rift zone magmas. It is suggested that olivine-hosted melt inclusions can be thought as small volume samples affected by the same melt-rock reaction process as the erupted lavas, but to a much greater extend because of their small volume (mass).

6.2 Future Research Projects

As a continuation of the work and results of this thesis (summarized above) I am interested in carrying out further research within the same general themes. Specific project include

determining the oxygen isotopic composition of basalts and picrites from East Greenland; Do they complement the lavas from the Faeroe Islands? I suggest in this thesis that an ^{18}O-depleted component is associated with the plume, if this is true the East Greenland picrites should also be ^{18}O-depleted by about 0.5 ‰ relative to common mid-ocean ridge basalts.

Another important question regards the depth of origin of the plume. Recent seismic studies suggest the Iceland mantle plume originates at the core mantle boundary (CMB) (Bijwaard and Spakman, 1999). From a geochemical point of view, Os isotope systematic were recently used to suggest a core-component in the Hawaiian plume, indicating a CMB origin for that plume as well (Brandon et al., 1998). Currently, I am involved in a project that seeks to establish whether the Icelandic picrites contain a "core signature."

The model presented in *Chapter 3* suggests that ^{18}O-zoning may be presented in minerals such as plagioclase in some gabbro nodules at a level (≈1 ‰) where it may be detectable by micro-analytical techniques (ion-probe). If this can be confirmed it will lend support to the model presented in this thesis.

Major element analysis of the quench phases observed in inclusions in plagioclase from the anorthositic nodules discussed in *Chapter 5* may shed some light on the history of the host nodule. With the same goal in mind I am interested in obtaining trace element analysis of the plagioclase host. Given that trace elements often lag behind major elements in solid-solid and melt-solid reactions, the trace element budget of the plagioclase may give information as to its precursor.

6.3 Final Speculative Remarks

It is tempting to propose that the pyroxene-bearing lithology which I suggest is involved in the formation of the picrites is also responsible for a small ^{18}O-depletion in magmas derived from the plume. This might be the case if the lithology is recycled oceanic crust (eclogite). The idea that plumes contain recycled oceanic crust is an old one (Hoffmann and White, 1982) and it is probably going to be a recurring theme in the geological literature for some time to come. It is of interest to further test this hypothesis in an attempt to validate or falsify it as the case may be, since knowledge of the fate of subducted material is key to understanding the overall convection pattern in the Earth's mantle.

I suggest in this thesis (*Chapter 5*) that the relationship between volume of erupted lava and variability in incompatible element abundance ratios may be understood in terms of a melt-rock reaction model, where the "effective" melt/rock ratio is an important factor.

I also allude to a possible link between volume and eruption site relative to the main spreading centers.

A recent detailed study (Perfit et al., 1994) of lava chemistry across the East Pacific Rise (EPR) at ≈ 9°N, found that lavas erupted outside the axial summit caldera (ASC), were much more variable in minor and trace element chemistry than the lavas from the within ASC. Is there a logical link between these observations at the EPR and the model presented here for the picrites? I suggest that there is.

In short, the increasing variance in incompatible element abundance ratios with decreasing volume in the Icelandic rift zones is mirrored by the increasing geochemical variance with increasing distance away from the ASC on the EPR. I therefore expect that the lavas erupted outside the ASC are small in volume compared to those erupted within the ASC.

How does this regular distribution come about? In *Chapter 5* it is suggested that the Icelandic picrites originate through melt-rock reactions in the uppermost mantle, and that these reactions are important in regions peripheral to the main plumbing system. In the main plumbing system lavas may volumetrically large and therefore able to "exhaust" lithologies such as those purported to play a crucial role in generating the picrites. Of course the mode of melt transport is also important. Thus, near the center of the main plumbing system long lived (dunite filled ?) dikes may exist that repeatedly act as conduits for magma transport. Such dikes will minimize the interaction between the rising melts and the surrounding uppermost mantle. This simple picture may also apply to the mid-ocean rift system. It does, however, not explain why the enriched lavas erupted off-axis at 9°N EPR, are more enriched than the lavas from the ASC. Although it may surprise the reader, I shall, at this time, refrain from speculating on this issue!

A final note regarding the march of ideas. It seems to me that the quest for mapping out the oceanic mantle in compositional space (major-elements, minor- and trace-elements, and isotope ratios) has been a trek towards increasing heterogeneity. Early studies indicated differences in isotopic composition of mantle domains on the scale of the ocean basins. More detailed work in any given region often indicated smaller scale subdivisions. Similarly major element variation in mid-ocean ridge basalts may be divided into "global" and "local" trends (Klein and Langmuir, 1987). In the "global trend" major elements vary systematically with bathymetry. Bathymetry reflects crustal thickness which relates to "melt thickness" and mean depth of melting, suggesting that the temperature of the upwelling mantle is a key control on the volume and chemistry of magma erupted at mid-ocean ridges (Klein and Langmuir, 1987). The "local" trend however was thought by Langmuir et al.(1992) to be dominated by local small scale heterogeneities in the mantle.

This may be understood given that initial sampling of ridges is dominated by dredges at the ridge axis. The samples so obtained are probably biased toward large volume lavas from near the main spreading axis. The chemistry of these lavas may be dominated by the temperature of the upwelling mantle. The isotopic differences among these samples may reflect real differences in isotopic composition of the deeper parts of the upwelling mantle. With increasing coverage on any given segment the smaller volume lavas erupted peripherally to the main spreading axis become more important in the samples representing the region. Thus the scatter in isotope ratios and incompatible element abundance ratios appear in the data-sets. In major element composition, these lavas contribute to the "local trend." The chemistry of these peripheral small volume lavas is dominated by the processed heterogeneous uppermost mantle.

An similar development of ideas and arguments may be inferred from the literature on the geochemistry of Icelandic lavas. Initial studies indicated mixing of relatively large mantle domains involving a plume and a MORB source (Schilling, 1973; Hart et al., 1973). Subsequent studies revealed simultaneous production of enriched (plume-like) and depleted lavas (MORB-like) lavas within specific volcanic systems (Sigvaldason et al., 1976) indicating small-scale mantle heterogeneities.

From what has been said above it should be clear that it is important to factor in parameters such as vent location and lava volume when comparisons are to be made between ocean basins, rift segments, spreading centers etc. This holds true for plume magmatism as well. In the case of Iceland an important question is the nature and history of the solid reactant that contributes to the formation of the picrites. Is it a residual lithology from previous melting episodes (in the Iceland mantle plume?) or is it a integral component of the plume (e.g. eclogite) that is added disproportionately to low volume magmas at relatively low pressures.

6.4 References

Bijwaard, H., Spakman, W. 1999. Tomographic evidence for a narrow whole mantle plume below Iceland. Earth Planet. Sci. Lett. 166, 121-126.

Brandon, A.D., Walker, R.J., Morgan, J.W., Norman, M.D., Prichard, H.M., 1998. Coupled ^{186}Os and ^{187}Os evidence for core-mantle interaction. Science 280, 1570-1573. Hoffmann, A., White W.M., 1982. Mantle plumes from ancient oceanic crust. Earth Planet. Sci. Lett. 57, 421-436.

Hart, S.R., Schilling, J.-G., Powell, J.L., 1973. Basalts from Iceland and along the Reykjanes Ridge: Sr isotope geochemistry. Nature 246, 104-107.

Klein, E.M., Langmuir, C.H., 1987. Global correlations of ocean ridge basalt chemistry with axial depth and crustal thickness. J. Geophys. Res. 92, 8089-8115.

Langmuir, C.H., Klein, E. M., Plank, T., 1992. Petrological systematics of Mid-Ocean Ridge basalts: Constraints on melt generation beneath ocean ridges. In: Phipps Morgan J., Blackman D.K. and Sinton, J.M. (Eds.) Mantle flow and melt generation at Mid-Ocean Ridges. Geophysical Monographs 71, American Geophysical Union, Washington DC. pp.183-280.

Perfit, M.R., Fornari, D.J., Smith, M.C., Bender, J.F., Langmuir, C.H. Haymon, R.M., 1994. Small-scale spatial and temporal variations in mid-ocean ridge crest magmatic processes. Geology 22, 375-379.

Schilling, J.-G., 1973. Iceland mantle plume: Geochemical study of Reykjanes Ridge. Nature 242, 566-571.

Sigvaldason, G.E., Steinthórsson, S., Óskarsson, N., Imsland. P., 1976. The simultaneous production of basalts, enriched and depleted in large lithophilic trace ions (LIL), within the same fissure swarms in Iceland. Bull. Soc. Geol. France 18, 863-867.

APPENDIX A

Table A-I: Composition of clinopyroxene from gabbronodules.

Formation	Comment	No	SiO_2	TiO_2	Al_2O_3	Cr_2O_3	FeO	MnO	MgO	CaO	Na_2O	Total	Mg#
Dagmálafell	X A	1	51.4	0.24	5.21	0.80	4.24	0.06	17.0	20.9	0.24	100.2	88
	X A	2	50.2	0.27	6.11	0.94	4.24	0.13	16.9	20.6	0.28	99.7	87
	X A	3	50.9	0.26	6.33	1.05	4.28	0.08	16.8	20.9	0.24	100.8	87
	X A	4	51.7	0.25	4.57	0.77	4.65	0.10	17.3	20.9	0.22	100.4	87
	X A	5	50.9	0.28	6.25	1.05	4.17	0.04	16.7	20.8	0.21	100.3	88
	X A	ave	51.0	0.26	5.69	0.92	4.32	0.08	16.9	20.8	0.24	100.3	87
		sd	0.6	0.02	0.77	0.13	0.19	0.03	0.2	0.1	0.03		
	X A2	1	51.6	0.39	4.34	1.19	4.88	0.14	16.8	21.1	0.30	100.6	86
	X A2	2	51.6	0.38	4.16	1.20	4.66	0.12	17.0	20.9	0.23	100.2	86
	X A2	3	50.9	0.25	6.00	1.29	4.24	0.07	16.2	21.0	0.20	100.2	87
	X A2	4	51.1	0.33	5.70	0.94	4.95	0.12	16.7	20.4	0.23	100.4	85
	X A2	5	51.2	0.28	4.72	1.14	4.58	0.06	16.9	20.9	0.25	100.1	87
	X A2	ave	51.3	0.33	4.98	1.15	4.66	0.10	16.7	20.9	0.24	100.3	86
		sd	0.3	0.06	0.82	0.13	0.28	0.03	0.3	0.3	0.04		
	XA3 edge	1	50.9	0.26	4.86	1.23	4.23	0.14	16.9	20.9	0.22	99.7	87
	XA3 edge	2	50.9	0.28	4.81	1.19	4.50	0.10	16.9	20.7	0.21	99.6	87
	XA3 edge	3	51.5	0.31	4.68	0.91	4.53	0.13	16.8	20.8	0.21	99.8	87
	XA3 edge	ave	51.1	0.28	4.78	1.11	4.42	0.12	16.9	20.8	0.21	99.7	87
		sd	0.3	0.03	0.09	0.17	0.17	0.02	0.0	0.1	0.01		
X2	p 1 gr 1-1	17	51.4	0.26	4.24	1.04	4.33	0.09	18.0	21.8	0.21	101.5	88
	p 1 gr 1-2	18	50.9	0.65	4.06	0.81	5.09	0.11	17.4	21.6	0.28	100.9	86
	p 1 gr 1-3	19	51.8	0.17	3.83	0.55	4.17	0.08	18.4	21.9	0.22	101.3	89
	p 1 gr 1-4	20	51.5	0.28	4.69	1.11	4.36	0.06	17.4	21.7	0.24	101.3	88
	p 1 gr 1-5	21	51.4	0.20	3.78	0.58	4.26	0.10	18.1	21.8	0.26	100.5	88
		ave	51.4	0.31	4.12	0.82	4.44	0.09	17.9	21.8	0.24	101.1	88
		sd	0.4	0.20	0.37	0.26	0.37	0.02	0.4	0.1	0.03		
X2	p 1 gr 2-1	22	52.3	0.21	3.83	0.46	4.11	0.12	18.2	20.8	0.14	100.3	88
	p 1 gr 2-2	23	51.4	0.28	4.15	0.76	4.28	0.11	18.0	21.0	0.17	100.2	88
	p 1 gr 2-3	24	52.0	0.20	4.32	0.65	3.99	0.09	18.2	21.0	0.22	100.7	89
	p 1 gr 2-4	25	51.8	0.30	4.25	0.70	4.43	0.12	18.1	20.7	0.17	100.6	88
	p 1 gr 2-5	26	51.6	0.26	4.14	0.67	4.33	0.09	17.9	20.8	0.22	100.1	88
		ave	51.8	0.25	4.14	0.65	4.23	0.11	18.1	20.9	0.18	100.3	88
		sd	0.3	0.04	0.19	0.12	0.18	0.02	0.1	0.1	0.04		

Tabel A-I (Continued).

Formation	Comment	No	SiO_2	TiO_2	Al_2O_3	Cr_2O_3	FeO	MnO	MgO	CaO	Na_2O	Total	Mg#
Dagmálafell	PM 1 gr 1	4	51.8	0.26	4.49	1.14	4.24	0.12	17.4	21.3	0.18	101.0	88
DMF 9302	PM 1 gr 2	5	53.1	0.22	3.51	0.89	3.48	0.10	18.8	21.3	0.12	101.5	90
G3- A	PM 1 gr 3	6	51.5	0.29	5.23	1.27	4.35	0.11	17.3	21.0	0.21	101.3	87
	PM 1 gr 4	7	52.0	0.26	4.60	1.01	4.41	0.09	17.3	21.1	0.18	101.0	87
	PM 1 gr 5	8	51.8	0.23	4.62	1.13	4.14	0.10	17.1	21.2	0.14	100.5	88
	PM 1 gr 6	9	51.6	0.21	5.23	1.27	4.10	0.09	17.2	21.1	0.17	101.0	88
	PM 1 gr 7	10	52.0	0.28	4.48	1.02	4.39	0.11	17.4	20.9	0.21	101.0	87
	PM 1 gr 8	11	51.5	0.25	4.77	1.26	4.63	0.13	17.0	21.4	0.20	101.1	86
	PM 1 gr 9	12	51.5	0.24	5.72	0.77	4.72	0.09	17.4	20.5	0.19	101.1	87
	PM 1 gr 10	13	51.8	0.30	4.53	1.17	4.29	0.09	17.4	21.4	0.23	101.2	88
	PM 1 gr 11	14	51.7	0.26	4.66	1.04	4.26	0.08	17.5	20.9	0.14	100.6	88
	PM 1 gr 12	15	51.9	0.31	4.57	0.92	4.67	0.11	17.2	21.1	0.25	101.0	87
	PM 1 gr 13	16	52.0	0.28	4.42	0.81	4.85	0.13	17.3	21.2	0.22	101.2	86
	PM 1 gr 14	17	52.5	0.30	4.26	0.68	4.62	0.09	17.4	21.1	0.23	101.2	87
	PM 1 gr 15	18	51.9	0.28	5.21	1.09	4.20	0.08	17.3	20.9	0.22	101.2	88
G3-B	PM 1 gr 16	19	52.5	0.29	4.18	0.67	4.64	0.13	17.7	21.0	0.19	101.5	87
	PM 1 gr 17	20	52.4	0.30	4.20	0.64	4.66	0.09	17.6	21.2	0.17	101.3	87
	PM 1 gr 18	21	52.1	0.29	4.54	1.35	4.11	0.10	17.6	21.3	0.23	101.5	88
	PM 1 gr 19	22	52.3	0.24	4.48	1.24	4.27	0.09	17.1	21.2	0.20	101.1	88
	PM 1 gr 20	23	51.7	0.30	6.16	0.71	4.73	0.09	17.0	20.5	0.24	101.4	86
	PM 1 gr 21	24	51.2	0.33	5.19	1.27	4.34	4.00	16.9	20.6	0.17	100.1	78
	PM 1 gr 22	25	50.8	0.36	5.16	1.20	4.40	0.09	16.4	20.6	0.24	99.3	87
	PM 1 gr 23	26	50.7	0.28	5.24	1.40	4.13	0.09	16.6	20.5	0.23	99.2	87
	PM 1 gr 24	27	51.6	0.23	4.71	1.13	4.19	0.10	17.0	21.1	0.19	100.3	88
	PM 1 gr 25	28	51.7	0.30	4.62	1.29	4.26	0.09	17.1	21.0	0.15	100.6	88
	PM 1 gr 26	29	51.2	0.30	5.45	1.65	4.32	0.08	16.7	20.9	0.23	101.0	87
	PM 1 gr 27	30	51.8	0.32	4.75	1.26	4.44	0.07	16.8	21.0	0.16	100.6	87
	PM 1 gr 28	31	52.7	0.31	4.20	0.62	4.72	0.07	17.7	21.1	0.23	101.7	87
	PM 1 gr 29	32	52.0	0.32	4.68	1.27	4.06	0.07	16.8	21.2	0.19	100.6	88
	PM 1 gr 30	33	52.0	0.32	4.77	1.16	4.19	0.06	17.1	21.0	0.20	100.9	88
	PM 1 gr 31	34	51.4	0.28	4.65	1.21	4.36	0.07	17.2	20.6	0.18	100.0	87
	PM 1 gr 32	35	51.8	0.35	4.76	1.12	4.57	0.08	17.1	20.9	0.19	101.0	87
	9302	1C	52.3	0.28	4.28	0.80	4.62	0.12	17.1	21.2	0.28	101.0	87
	9302	2R	52.0	0.27	4.59	0.88	4.33	0.07	17.3	21.1	0.21	100.8	87

Table A-I: Composition of clinopyroxene from gabbronodules (Continued).

Formation	Comment	No	SiO_2	TiO_2	Al_2O_3	Cr_2O_3	FeO	MnO	MgO	CaO	Na_2O	Total	Mg#
	9302	1C	52.1	0.25	4.13	0.73	4.49	0.12	17.3	21.0	0.32	100.5	87
	9302	2R	52.2	0.28	4.27	0.75	4.51	0.09	17.2	21.3	0.21	100.7	87
Dagmálafell	9302	1C	51.2	0.27	4.60	0.97	4.32	0.07	17.1	21.2	0.22	100.0	87
	9302	2R	51.7	0.29	4.36	0.83	4.47	0.13	17.0	21.2	0.22	100.2	87
Tjarnar-hnúkshraun	PM 2 gr 1	85	52.6	0.36	2.71	0.09	5.86	0.12	16.8	20.5	0.24	99.4	83
	PM 2 gr 2	86	52.5	0.34	3.23	0.26	5.30	0.11	16.9	20.7	0.24	99.6	85
	PM 2 gr 3	87	53.1	0.33	2.76	0.13	5.78	0.12	16.8	20.8	0.21	100.1	84
	PM 2 gr 4	88	52.9	0.33	3.24	0.25	5.62	0.12	17.0	20.8	0.23	100.5	84
	PM 2 gr 5	89	53.1	0.32	3.02	0.45	4.94	0.11	17.0	21.1	0.17	100.2	86
	PM 2 gr 6	90	52.7	0.35	3.11	0.40	5.10	0.11	17.1	21.0	0.23	100.1	85
	PM 2 gr 7	91	53.1	0.27	2.95	0.45	5.01	0.09	17.4	20.9	0.20	100.3	86
	PM 2 gr 8	92	53.2	0.30	3.09	0.49	4.90	0.11	17.2	21.1	0.18	100.6	86
	PM 2 gr 9	93	52.3	0.33	3.70	0.65	4.99	0.10	17.1	21.2	0.24	100.6	86
	PM 2 gr 10	94	53.5	0.31	2.83	0.22	5.21	0.11	17.6	20.8	0.22	100.8	86
	PM 2 gr 11	95	52.3	0.35	3.82	0.68	4.99	0.13	16.7	20.9	0.20	100.1	85
	PM 2 gr 12	96	53.1	0.32	3.20	0.42	4.89	0.10	17.4	21.2	0.22	100.8	86
	PM 2 gr 13	97	53.1	0.33	3.09	0.31	5.18	0.12	17.0	21.1	0.24	100.5	85
	PM 2 gr 14	98	52.7	0.31	3.28	0.43	5.05	0.11	17.0	20.9	0.23	100.1	85
	PM 2 gr 15	99	52.9	0.31	2.96	0.41	4.96	0.11	17.2	21.1	0.21	100.1	86
	PM 2 gr 16	100	52.7	0.32	3.37	0.53	5.01	0.10	16.8	21.1	0.22	100.1	85
	PM 2 gr 17	101	52.6	0.37	3.21	0.24	5.62	0.17	17.0	20.3	0.23	99.8	84
	PM 2 gr 18	102	53.2	0.28	2.77	0.49	4.85	0.11	16.9	21.0	0.23	99.9	86
	PM 2 gr 19	103	53.1	0.29	2.79	0.26	5.21	0.12	17.0	20.8	0.22	99.8	85
	PM 2 gr 20	104	52.6	0.37	3.33	0.36	5.32	0.11	17.5	20.4	0.24	100.3	85
	PM 2 gr 21	105	53.1	0.32	2.79	0.44	5.00	0.14	17.8	21.1	0.22	100.9	86
	PM 2 gr 22	106	52.8	0.37	3.56	0.66	5.08	0.11	17.3	20.9	0.21	101.0	86
	PM 2 gr 23	107	52.3	0.39	3.76	0.72	5.17	0.11	17.1	20.8	0.27	100.7	85
Hraunsvík	PM 5 gr 1	36	51.9	0.35	3.73	1.14	4.9	0.12	17.5	20.1	0.14	100.0	86
	PM 5 gr 2	37	53.2	0.32	1.99	0.63	5.6	0.11	17.8	19.8	0.17	99.7	85
	PM 5 gr 4	39	54.0	0.27	2.02	0.66	4.9	0.14	18.4	19.9	0.09	100.5	87

Table A-I: Composition of clinopyroxene from gabbronodules (Continued).

Formation	Comment	No	SiO_2	TiO_2	Al_2O_3	Cr_2O_3	FeO	MnO	MgO	CaO	Na_2O	Total	Mg#
	PM 5 gr 6	41	53.7	0.28	1.78	0.42	6.0	0.14	18.6	19.0	0.11	100.0	85
	PM 5 gr 7	42	53.0	0.32	2.42	0.39	5.5	0.11	17.8	20.1	0.13	99.9	85
	PM 5 gr 8	43	52.0	0.37	3.15	0.99	5.1	0.13	17.7	20.2	0.19	99.8	86
Hraunsvík	PM 5 gr 9	44	53.0	0.35	2.96	0.51	5.8	0.15	17.9	20.1	0.15	101.0	84
	PM 5 gr 10	45	52.5	0.29	3.42	1.01	4.9	0.07	17.6	20.4	0.18	100.5	86
	PM 5 gr 11	46	52.6	0.27	3.22	1.03	5.1	0.12	17.6	20.6	0.20	100.8	86
	PM 5 gr 12	47	52.6	0.28	3.49	1.24	5.0	0.16	18.1	19.8	0.14	100.9	86
	PM 5 gr 13	48	52.5	0.28	3.12	1.05	5.1	0.13	17.6	20.5	0.17	100.6	86
	PM 5 gr 14	49	53.2	0.25	2.45	0.74	5.1	0.11	18.0	20.4	0.16	100.5	86
	PM 4 gr 1	67	53.2	0.16	3.21	1.11	3.4	0.09	18.0	21.5	0.16	100.8	90
	PM 4 gr 2	68	52.8	0.15	2.77	0.79	3.5	0.07	18.2	21.1	0.14	99.6	90
	PM 4 gr 4	69	52.1	0.26	3.08	0.64	4.8	0.07	17.2	20.8	0.22	99.1	86
	PM 4 gr 5	70	52.5	0.27	3.42	0.77	4.7	0.13	17.9	20.0	0.17	99.9	87
	PM 4 gr 6	71	52.4	0.12	2.75	0.95	3.3	0.06	18.1	21.4	0.12	99.2	91
	PM 4 gr 7	72	52.1	0.22	3.70	0.81	4.9	0.11	17.2	20.6	0.19	99.7	86
	PM 4 gr 8	73	52.6	0.28	3.57	0.71	5.1	0.11	17.4	20.7	0.21	100.7	86
	PM 4 gr 9	74	52.1	0.25	3.60	0.78	5.1	0.11	16.7	20.6	0.26	99.6	85
	PM 4 gr 10	75	52.2	0.16	2.79	0.92	3.4	0.05	17.6	21.3	0.16	98.6	90
	PM 4 gr 11	76	52.1	0.26	3.75	0.82	5.0	0.10	17.1	20.6	0.25	100.1	86
	PM 4 gr 12	77	51.6	0.40	4.08	0.99	5.3	0.10	17.0	20.1	0.24	99.9	85
	PM 4 gr 13	78	52.5	0.19	3.00	1.05	3.4	0.08	17.9	21.5	0.14	99.8	90
	PM 4 gr 14	79	51.9	0.41	3.82	0.79	5.1	0.08	17.1	20.4	0.23	99.8	85
	PM 4 gr 15	80	53.3	0.17	2.71	0.74	3.4	0.06	18.1	21.0	0.16	99.7	90
	PM 4 gr 16	81	53.1	0.18	2.81	0.80	3.6	0.06	17.8	21.3	0.15	99.9	90
	7795	1	53.3	0.10	3.17	1.09	3.5	0.06	18.0	21.16	0.17	100.6	90
	7795	2	53.4	0.25	2.93	0.50	4.9	0.14	18.2	19.77	0.23	100.4	87
	7795	1	53.5	0.26	2.73	0.47	4.8	0.13	18.1	19.96	0.23	100.1	87
	7795	2	52.5	0.15	3.85	1.24	3.6	0.09	17.4	20.70	0.17	99.7	89
	7795	1	52.5	0.23	3.48	1.02	4.1	0.08	18.0	19.84	0.24	99.5	88
	7795	2	53.2	0.28	3.41	0.71	4.6	0.09	18.0	19.68	0.28	100.3	87
	7795	3	53.1	0.29	3.20	0.60	4.9	0.14	18.2	19.34	0.28	100.1	86
	7795	1	52.4	0.23	3.43	0.88	4.9	0.12	17.6	19.83	0.29	99.7	86
	7795	2	52.4	0.22	3.41	1.02	4.7	0.15	17.6	19.82	0.24	99.6	87

Table A-I: Composition of clinopyroxene from gabbronodules (Continued).

Formation	Comment	No	SiO_2	TiO_2	Al_2O_3	Cr_2O_3	FeO	MnO	MgO	CaO	Na_2O	Total	Mg#
	7795	1	52.5	0.32	3.12	0.86	5.0	0.10	18.0	19.34	0.28	99.5	86
	7795	2	52.1	0.38	3.10	0.50	5.3	0.16	17.6	19.64	0.20	99.0	85
	7795	3	52.3	0.37	3.15	0.91	5.1	0.10	18.0	19.60	0.25	99.7	86
Seydisholar	9377 Cpx 1	19	52.4	0.47	3.59	0.22	5.4	0.15	16.3	22.06	0.34	101.0	84
	9377 Cpx 2	20	52.5	0.49	3.58	0.19	6.0	0.17	17.4	20.37	0.32	101.1	83
	9377 Cpx 3	21	52.3	0.66	3.74	0.29	6.4	0.16	17.5	19.63	0.34	101.1	83
	9377 Cpx 4	22	51.5	0.61	4.41	0.26	5.8	0.14	15.7	21.36	0.40	100.3	83
	9377 Cpx 5	23	51.9	0.54	4.29	0.28	5.8	0.15	16.6	20.77	0.33	100.7	83
	9375 gr 1	1	51.1	0.72	4.25	0.11	8.8	0.22	16.7	17.73	0.49	100.1	77
	9375 ge 1	2	50.4	0.87	4.56	0.12	7.6	0.22	15.0	20.41	0.52	99.8	77
	9375 gr 1	3	50.9	0.98	4.22	0.09	7.6	0.20	15.2	20.47	0.53	100.2	78
	9375 gr 1	4	52.0	0.69	3.79	0.09	9.8	0.24	18.5	15.20	0.41	100.7	77
	9375 gr 1	ave	51.1	0.82	4.21	0.10	8.5	0.22	16.4	18.45	0.49	100.2	77
		sd	0.7	0.14	0.32	0.02	1.0	0.02	1.6	2.52	0.05		
	9375 gr 2	1	51.0	0.74	4.37	0.09	7.2	0.18	16.0	20.05	0.39	100.0	80
	9375 gr 2	2	51.0	0.75	4.39	0.08	8.0	0.20	16.0	19.23	0.47	100.0	78
	9375 gr 2	3	50.5	0.69	4.30	0.03	7.3	0.11	15.4	20.03	0.41	98.7	79
	9375 gr 2	4	50.9	0.67	4.21	0.13	8.3	0.23	16.3	18.57	0.42	99.7	77
	9375 gr 2	5	50.7	0.66	4.19	0.16	8.0	0.18	16.2	18.40	0.46	99.0	78
	9375 gr 2	ave	50.8	0.70	4.29	0.10	7.7	0.18	16.0	19.26	0.43	99.5	78
		sd	0.2	0.04	0.09	0.05	0.5	0.04	0.3	0.78	0.03		
	9375 gr 3	1	50.8	0.70	4.34	0.05	8.0	0.17	16.0	18.96	0.46	99.5	78
	9375 gr 3	2	50.7	0.93	4.11	0.07	8.3	0.21	16.4	18.49	0.47	99.6	77
	9375 gr 3	ave	50.8	0.82	4.23	0.06	8.1	0.19	16.2	18.73	0.47	99.6	78
		sd	0.1	0.16	0.16	0.01	0.2	0.03	0.2	0.33	0.01		
Graenavatn	SH-1 gr 1	1	51.2	0.60	2.35	0.02	12.2	0.34	15.1	16.88	0.24	98.86	68
	SH-1 gr 1	2	52.1	0.49	2.38	0.03	8.9	0.23	16.3	18.74	0.28	99.45	76
	SH-1 gr 2	1	51.3	0.58	2.28	0.00	11.4	0.35	14.8	17.75	0.29	98.76	69
	SH-1 gr 2	2	51.7	0.21	0.98	0.00	14.0	0.36	12.1	19.04	0.18	98.55	60
	SH-1 gr 3	1	52.4	0.49	1.48	0.02	18.7	0.44	19.3	6.88	0.12	99.87	64
	SH-1 gr 3	2	51.8	0.74	2.04	0.01	12.5	0.33	15.4	16.12	0.22	99.12	68
	SH-1 gr 4	1	51.1	0.75	2.12	0.00	12.2	0.39	14.5	18.06	0.21	99.33	67
	SH-1 gr 4	2	52.3	0.42	1.26	0.00	20.7	0.45	21.6	1.81	0.08	98.64	64

Table A-II: Composition of olivine from gabbronodules.

Formation	Comment	No.	SiO_2	TiO_2	Al_2O_3	Cr_2O_3	FeO	MnO	MgO	CaO	NiO	Total	Fo
Dagmálafell	101N-Average	A	40.1	0.02	0.12	0.04	11.5	0.19	46.8	0.34	0.19	99.3	88
	sd (n=5)		0.2	0.03	0.03	0.04	0.17	0.04	0.26	0.01	0.04		
Dagmálafell	PM-11 gr 1	13	40.6	0.01	0.07	0.02	12.5	0.16	47.1	0.34	0.20	100.9	87
	PM-11 gr 2	14	40.0	0.00	0.05	0.01	14.2	0.19	45.5	0.31	0.14	100.5	85
	PM-11 gr 3	15	40.0	0.05	0.04	0.01	14.6	0.19	45.0	0.31	0.11	100.2	85
	PM-11 gr 4	16	40.0	0.00	0.05	0.01	14.8	0.22	45.2	0.30	0.13	100.7	84
	PM-11 gr 5	17	39.8	0.02	0.07	0.04	12.9	0.20	45.9	0.32	0.22	99.5	86
Hraunsvík	PM-11 gr 6	18	39.9	0.02	0.03	0.03	15.2	0.19	44.6	0.28	0.15	100.3	84
	PM-11 gr 7	19	40.1	0.03	0.05	0.03	14.4	0.19	45.7	0.31	0.19	101.0	85
	PM-11 gr 8	20	40.4	0.02	0.01	0.04	12.4	0.16	46.6	0.26	0.16	100.1	87
	PM-11 gr 9	21	40.5	0.00	0.03	0.03	12.6	0.17	46.9	0.20	0.17	100.6	87
	PM-11 gr 10	22	40.0	0.01	0.02	0.03	14.2	0.20	45.4	0.29	0.16	100.4	85
	PM-11 gr 11	23	39.6	0.03	0.06	0.02	16.6	0.25	43.8	0.33	0.18	100.9	82
	PM-11 gr 12	24	39.7	0.00	0.03	0.05	16.4	0.24	43.8	0.31	0.17	100.7	83
Tjarnar-	PM-11 gr 13	25	39.3	0.03	0.04	0.00	19.2	0.32	41.9	0.32	0.09	101.2	80
hnúkshraun	PM-11 gr 14	26	39.0	0.00	0.02	0.03	18.8	0.27	41.7	0.31	0.15	100.3	80
	PM-11 gr 15	27	39.2	0.03	0.04	0.03	19.1	0.28	41.6	0.32	0.12	100.7	80
	PM-11 gr 16	28	38.9	0.01	0.04	0.01	19.4	0.25	41.4	0.29	0.14	100.4	79
	PM-11 gr 17	29	39.2	0.03	0.03	0.00	19.2	0.26	42.2	0.32	0.10	101.3	80
	PM-11 gr 18	30	39.4	0.04	0.04	0.00	18.8	0.28	42.1	0.29	0.12	101.1	80
	PM-11 gr 19	31	39.2	0.02	0.03	0.00	19.1	0.30	42.1	0.31	0.11	101.1	80
	PM-11 gr 20	32	39.6	0.01	0.04	0.01	19.2	0.27	42.0	0.30	0.10	101.5	80
	PM-11 gr 21	33	39.4	0.00	0.03	0.03	19.1	0.27	41.7	0.29	0.07	101.0	80

Table A-III: Composition of plagioclase in gabbro-nodules and plagioclase pheno/xenocrysts.

Formation	Comment	No	SiO_2	Al_2O_3	FeO	MnO	CaO	Na_2O	K_2O	Total	An
Dagmálafell	Ave A n=2	A	46.6	33.1	0.66	0.03	16.9	1.67	0.02	99.0	85
		sd	0.5	0.2	0.06	0.04	0.2	0.14	0.01		
	Ave B n=5	B	46.8	33.7	0.55	0.01	17.1	1.67	0.02	99.8	85
		sd	0.3	0.3	0.06	0.02	0.2	0.05	0.01		
	PM-8 gr 1	15	46.8	34.2	0.48	0.01	17.2	1.34	0.03	100.1	88
	PM-8 gr 2	16	46.5	34.6	0.47	0.02	17.3	1.34	0.03	100.3	88
	PM-8 gr 3	17	46.9	33.9	0.44	0.02	16.9	1.41	0.02	99.6	87
	PM-8 gr 4	18	47.4	33.9	0.47	0.02	16.8	1.55	0.03	100.1	86
	PM-8 gr 5	19	47.1	34.3	0.48	0.02	16.9	1.51	0.02	100.3	86
	PM-8 gr 6	20	46.7	34.4	0.44	0.01	17.2	1.29	0.03	100.1	88
	PM-8 gr 8	22	46.8	34.4	0.54	0.00	17.2	1.38	0.02	100.4	87
	PM-8 gr 9	23	46.3	34.4	0.43	0.00	17.3	1.27	0.03	99.7	88
	PM-8 gr 10	24	47.0	34.3	0.39	0.00	17.2	1.38	0.02	100.4	87
	PM-8 gr 11	25	47.8	33.4	0.49	0.01	16.8	1.66	0.03	100.2	85
	PM-8 gr 12	26	47.2	34.0	0.49	0.01	17.3	1.59	0.04	100.6	86
	PM-8 gr 13	27	46.0	35.1	0.43	0.00	18.1	1.06	0.04	100.8	90
	PM-8 gr 14	28	47.0	34.1	0.49	0.00	17.2	1.46	0.04	100.3	86
	PM-8 gr 15	29	46.9	34.2	0.46	0.00	17.3	1.43	0.04	100.3	87
	PM-8 gr 16	30	47.3	34.2	0.49	0.02	17.3	1.55	0.03	100.9	86
	PM-8 gr 17	31	47.1	34.3	0.52	0.00	17.4	1.47	0.03	100.9	87
	PM-8 gr 18	32	47.2	34.3	0.49	0.00	17.2	1.49	0.04	100.8	86
Hraunsvík	PM-8 gr 19	33	47.5	33.7	0.35	0.00	16.9	1.67	0.05	100.2	85
	PM-8 gr 20	34	48.1	33.4	0.34	0.01	16.7	1.88	0.04	100.4	83
	PM-8 gr 21	35	47.6	34.0	0.43	0.00	16.7	1.80	0.06	100.6	83
	PM-8 gr 22	36	48.0	33.8	0.39	0.00	16.5	1.95	0.05	100.7	82
	PM-8 gr 23	37	48.0	33.7	0.40	0.00	16.6	1.93	0.06	100.7	82
	PM-8 gr 24	38	48.3	33.9	0.43	0.00	16.5	2.06	0.05	101.3	81
	PM-8 gr 25	39	48.0	33.9	0.35	0.00	16.7	1.86	0.04	100.8	83
	PM-8 gr 26	40	48.1	34.0	0.41	0.00	16.6	1.90	0.05	101.1	83

Table A-III: (Continued).

Formation	Comment	No	SiO_2	Al_2O_3	FeO	MnO	CaO	Na_2O	K_2O	Total	An
Tjarnar-	PM-7 gr 1	41	45.9	34.1	0.56	0.00	17.0	1.21	0.04	98.9	88
hnúkshraun	PM-7 gr 2	42	46.7	34.5	0.55	0.00	17.7	1.47	0.03	101.0	87
	PM-7 gr 3	43	46.9	34.0	0.52	0.01	17.3	1.49	0.04	100.2	86
	PM-7 gr 4	44	46.3	34.9	0.52	0.00	17.7	1.33	0.03	100.8	88
	PM-7 gr 5	45	46.7	34.2	0.51	0.00	17.5	1.49	0.01	100.5	87
	PM-7 gr 6	46	46.3	34.7	0.48	0.00	17.8	1.26	0.01	100.6	89
	PM-7 gr 7	47	46.7	34.3	0.50	0.00	17.6	1.35	0.01	100.4	88
	PM-7 gr 8	48	46.4	34.3	0.54	0.00	17.3	1.27	0.02	99.8	88
	PM-7 gr 9	49	46.7	34.4	0.46	0.00	17.5	1.42	0.02	100.4	87
	PM-7 gr 10	50	46.3	34.8	0.47	0.00	17.6	1.27	0.02	100.5	88
	PM-7 gr 11	51	46.9	34.7	0.55	0.00	17.7	1.28	0.01	101.2	88
	PM-7 gr 12	52	46.7	34.3	0.52	0.00	17.4	1.32	0.01	100.3	88
	PM-7 gr 13	53	48.2	35.5	0.55	0.00	18.2	1.42	0.01	103.8	88
	PM-7 gr 14	54	46.4	34.5	0.51	0.00	17.6	1.24	0.02	100.3	89
	PM-7 gr 15	55	46.6	34.4	0.52	0.00	17.5	1.32	0.01	100.3	88
	PM-7 gr 16	56	47.4	34.5	0.57	0.01	17.3	1.51	0.01	101.3	86
	PM-7 gr 18	58	46.6	34.6	0.56	0.00	17.6	1.33	0.01	100.6	88
	PM-7 gr 19	59	47.0	34.6	0.54	0.00	17.3	1.49	0.02	101.0	86
Graenavatn	Grain A	ave	47.2	33.5	0.83	0.01	16.6	1.87	0.03	100.2	83
	n=4	sd	0.2	0.2	0.03	0.02	0.2	0.07	0.01		
	Grain B	ave	47.0	33.6	0.78	0.00	16.7	1.80	0.04	100.0	84
	n=4	sd	0.1	0.1	0.03	0.01	0.1	0.04	0.01		
	Grain C	ave	47.3	32.7	0.82	0.01	16.4	2.10	0.04	99.4	81
	n=2	sd	0.4	0.0	0.00	0.01	0.2	0.05	0.00		

Table A-III: (Continued).

Formation	Comment	No	SiO_2	Al_2O_3	FeO	MnO	CaO	Na_2O	K_2O	Total	An
Dagmálafell	PM-9 gr 1	60	46.7	34.7	0.58	0.00	17.4	1.44	0.03	100.9	87
	PM-9 gr 2	61	46.6	34.8	0.50	0.00	17.6	1.29	0.02	100.8	88
	PM-9 gr 3	62	47.1	34.4	0.52	0.00	17.5	1.53	0.04	101.1	86
	PM-9 gr 4	63	46.8	34.5	0.49	0.01	17.5	1.40	0.04	100.7	87
	PM-9 gr 5	64	46.7	34.3	0.52	0.00	17.2	1.41	0.03	100.2	87
	PM-9 gr 6	65	47.2	34.4	0.47	0.00	17.2	1.39	0.04	100.7	87
	PM-9 gr 7	66	47.3	34.3	0.47	0.01	17.0	1.57	0.04	100.6	85
	PM-9 gr 8	67	47.5	34.0	0.46	0.00	16.7	1.65	0.04	100.4	85
	PM-9 gr 9	68	47.5	34.2	0.49	0.00	16.9	1.65	0.03	100.8	85
	PM-9 gr 10	69	46.9	34.7	0.44	0.00	17.1	1.42	0.03	100.5	87
	PM-9 gr 12	71	46.6	34.9	0.40	0.00	17.3	1.35	0.03	100.6	87
	PM-9 gr 13	72	46.8	34.6	0.44	0.00	17.4	1.36	0.03	100.6	87
Hraunsvík	89 Left	5	52.2	30.5	0.64	0.00	12.8	3.67	0.11	99.9	65
	89 Leftcentre	6	52.1	30.6	0.67	0.00	12.9	3.63	0.10	100.0	66
	89 Centre	7	52.2	30.6	0.68	0.00	12.8	3.64	0.13	100.1	66
	89 Centright	8	52.3	30.7	0.52	0.00	12.5	3.58	0.10	99.7	65
	89 Right	9	51.7	30.5	0.64	0.00	12.7	3.50	0.10	99.2	66
	987 Left	10	48.5	33.5	0.46	0.01	16.2	1.94	0.03	100.6	82
	87 Leftcentre	11	52.7	30.4	0.43	0.00	13.2	3.50	0.06	100.3	67
	87 Centre	12	52.9	30.4	0.44	0.00	13.2	3.54	0.07	100.5	67
	87 Centright	13	52.5	30.5	0.39	0.00	13.2	3.52	0.06	100.2	67
	87 Right	14	52.6	30.5	0.58	0.00	13.0	3.66	0.09	100.4	66

Table A-IV Composition of Cr-spinel from Dagmálafell.

Comment	No.	SiO_2	TiO_2	Al_2O_3	Cr_2O_3	FeO	MnO	MgO	NiO	Total	Cr#	Mg#
X1 gr 1 p 6 rim	7	0.09	0.23	29.4	33.4	17.4	0.21	15.6	0.17	96.6	43.2	70.4
X1 gr 1 p 1-5	av 2-6	0.09	0.25	28.6	35.4	18.2	0.21	15.6	0.20	98.5	45.3	69.3
	std	0.01	0.01	0.4	0.2	0.1	0.01	0.2	0.01			
X1 gr 2 p 6 rim	13	0.12	0.28	29.5	34.7	17.8	0.24	16.0	0.19	98.9	44.1	70.3
X1 gr 2 p 7 rim	14	0.14	0.21	30.4	33.9	17.6	0.19	15.9	0.20	98.6	42.8	70.0
X1 gr 2 p 1-5	av 8-12	0.10	0.26	28.0	36.2	18.2	0.20	15.5	0.18	98.7	46.4	69.0
	std	0.01	0.01	0.3	0.3	0.2	0.02	0.1	0.02			
X1 gr 3 p 6 rim	20	0.11	0.28	28.4	36.1	17.9	0.23	15.5	0.16	98.7	46.0	68.8
X1 gr 3 p 7 rim	21	0.12	0.25	28.0	36.6	18.0	0.24	15.4	0.17	98.7	46.7	68.6
X1 gr 3 p 1-5	av 15-19	0.12	0.28	27.4	36.9	18.2	0.22	15.4	0.20	98.7	47.5	68.7
	std	0.01	0.01	0.8	0.8	0.1	0.02	0.1	0.03			
X1 gr 4 p 6 rim	27	0.11	0.30	31.0	33.1	17.7	0.25	16.2	0.19	98.8	41.7	70.7
X1 gr 4 p 7 rim	28	0.10	0.33	30.8	32.9	17.6	0.21	16.3	0.17	98.4	41.7	71.5
X1 gr 4 p 1-5	av 22-26	0.11	0.32	30.4	33.6	17.6	0.22	16.2	0.19	98.5	42.6	71.0
	std	0.01	0.03	0.2	0.3	0.1	0.02	0.1	0.01			
X1 gr 5 p 6 rim	34	0.14	0.31	30.4	33.2	17.7	0.19	16.1	0.22	98.3	42.2	70.7
X1 gr 5 p 7 rim	35	0.11	0.35	30.6	33.8	18.1	0.21	16.2	0.24	99.6	42.6	70.7
X1 gr 5 p 1-5	av 29-33	0.10	0.32	29.8	34.3	17.7	0.21	16.0	0.20	98.7	43.6	70.5
	std	0.00	0.03	0.1	0.3	0.1	0.02	0.1	0.02			
X1 gr 6 p 6 rim	41	0.11	0.25	28.9	35.7	17.4	0.21	15.9	0.17	98.7	45.4	70.5
X1 gr 6 p 7 rim	42	0.10	0.27	28.5	35.9	17.4	0.23	16.0	0.17	98.6	45.7	70.9
X1 gr 6 p 1-5	av 36-40	0.10	0.24	26.3	38.8	17.4	0.21	15.6	0.19	98.8	49.7	69.9
	std	0.01	0.02	0.6	0.8	0.1	0.03	0.2	0.01			
X1 gr 7 p 6 rim	48	0.11	0.26	31.1	33.1	18.1	0.23	16.1	0.19	99.2	41.7	70.1
X1 gr 7 p 7 rim	49	0.09	0.30	31.3	32.2	17.9	0.22	16.2	0.16	98.4	40.8	71.0
X1 gr 7 p 1-5	av 43-47	0.09	0.25	29.1	34.8	18.0	0.23	15.7	0.18	98.3	44.5	69.5
	std	0.01	0.03	0.7	1.0	0.2	0.01	0.1	0.02			
X1 gr 8 p 6 rim	55	0.08	0.22	31.1	33.2	17.7	0.20	15.8	0.18	98.6	41.8	69.6
X1 gr 8 p 7 rim	56	0.08	0.27	31.0	33.0	17.6	0.20	15.7	0.15	98.0	41.7	69.5
X1 gr 8 p 1-5	av 50-54	0.09	0.24	27.9	37.0	17.9	0.23	15.4	0.16	98.9	47.1	68.6
	std	0.01	0.01	1.2	1.2	0.1	0.02	0.2	0.02			
X1 gr 9 p 6 rim	62	0.11	0.24	29.1	35.0	17.9	0.22	15.6	0.16	98.3	44.7	69.1
X1 gr 9 p 7 rim	63	0.06	0.25	31.5	32.1	17.8	0.20	16.2	0.17	98.3	40.6	71.0

Table A-IV Composition of Cr-spinel from Dagmálafell (Continued).

Comment	No.	SiO_2	TiO_2	Al_2O_3	Cr_2O_3	FeO	MnO	MgO	NiO	Total	Cr#	Mg#
X1 gr 9 p 1-5	av 57-61	0.08	0.23	26.3	38.8	18.0	0.23	15.2	0.19	99.0	49.8	68.1
	std	0.01	0.01	0.3	0.4	0.1	0.02	0.1	0.03			
X1 gr 10 p 6 rim	69	0.09	0.21	32.6	31.2	17.5	0.18	16.2	0.14	98.1	39.1	70.8
X1 gr 10 p 1-5	av 64-68	0.08	0.27	31.3	32.8	17.6	0.20	16.0	0.16	98.3	41.3	70.2
	std	0.01	0.02	0.4	0.2	0.1	0.02	0.2	0.02			
X1 gr 11 p 6 rim	75	0.08	0.27	36.4	27.0	17.8	0.20	16.8	0.25	98.9	33.2	71.9
X1 gr 11 p 7 rim	76	0.09	0.26	35.2	28.3	17.6	0.19	16.5	0.18	98.3	35.0	71.2
X1 gr 11 p 1-5	av 70-74	0.09	0.27	32.3	31.5	17.8	0.20	16.1	0.18	98.4	39.5	70.1
	std	0.01	0.03	1.1	1.3	0.2	0.02	0.2	0.03			
X1 gr 12 p 6 rim	82	0.11	0.23	38.3	24.5	17.8	0.15	17.2	0.17	98.4	30.1	72.7
X1 gr 12 p 7 rim	83	0.11	0.35	38.7	23.4	18.1	0.18	17.0	0.23	98.1	28.8	72.2
X1 gr 12 p 1-5	av 77-81	0.13	0.20	36.5	26.8	17.6	0.17	16.8	0.20	98.4	33.0	72.0
	std	0.08	0.03	1.0	1.2	0.1	0.02	0.3	0.02			
X2 gr 1 p 6 rim	89	0.11	0.22	25.9	40.2	17.2	0.25	15.8	0.16	99.8	51.1	70.0
X2 gr 1 p 7 rim	90	0.12	0.24	24.8	40.9	17.1	0.26	15.4	0.15	98.9	52.6	69.3
X2 gr 1 p 1-5	av 84-88	0.11	0.26	25.0	40.8	17.2	0.26	15.5	0.15	99.2	52.3	69.4
	std	0.00	0.01	0.2	0.3	0.1	0.02	0.1	0.01			
X2 gr 2 p 7 rim	97	0.08	0.25	27.4	37.8	17.2	0.22	15.8	0.20	99.0	48.1	70.4
X2 gr 2 p 2-5	av 92-95	0.10	0.23	27.6	36.9	18.2	0.24	15.3	0.17	98.8	47.3	68.5
	std	0.02	0.02	0.3	0.4	0.0	0.03	0.1	0.03			
X2 gr 3 p 6 rim	103	0.12	0.22	25.8	38.1	17.0	0.20	15.1	0.22	96.7	49.8	69.1
X2 gr 3 p 7 rim	104	0.19	0.50	35.4	25.4	21.5	0.21	15.3	0.22	98.7	32.5	65.8
X2 gr 3 p 1-5	av 98-102	0.09	0.23	24.2	42.0	17.9	0.25	14.9	0.19	99.8	53.8	67.1
	std	0.01	0.02	0.5	0.6	0.3	0.01	0.1	0.03			
X2 gr 4 p 1	105	0.13	0.21	27.7	37.1	17.8	0.21	16.1	0.26	99.5	47.3	71.1
X2 gr 4 p 2	106	0.12	0.19	28.2	36.8	17.6	0.23	16.1	0.24	99.6	46.7	71.1
X2 gr 4 p 3 med ph	107	0.15	0.23	32.8	31.8	17.3	0.19	16.8	0.24	99.5	39.4	72.3
X2 gr 4 p 4 med ph	108	0.13	0.20	33.4	30.5	17.4	0.20	16.8	0.27	98.8	37.9	72.5
X2 gr 4 p 5 drk ph	109	0.08	0.16	37.6	26.3	17.1	0.14	17.5	0.23	99.1	32.0	73.9
X2 gr 4 p 6 drk ph	110	0.11	0.17	37.6	26.6	17.1	0.20	17.5	0.24	99.5	32.2	73.8
X2 gr 4 p 7 rim +drk	111	0.09	0.17	40.4	22.8	16.9	0.17	18.1	0.26	98.9	27.4	75.7
X2 gr 5 p 1	112	0.13	0.21	28.3	35.5	17.8	0.22	15.2	0.20	97.5	45.7	68.5
X2 gr 5 p 2	113	0.14	0.19	27.9	35.7	17.8	0.21	15.2	0.26	97.4	46.2	68.6
X2 gr 5 p 3	114	0.13	0.21	32.3	31.4	17.6	0.20	15.9	0.23	97.8	39.5	69.9

Table A-IV Composition of Cr-spinel from Dagmálafell (Continued).

Comment	No.	SiO_2	TiO_2	Al_2O_3	Cr_2O_3	FeO	MnO	MgO	NiO	Total	Cr#	Mg#
X2 gr 5 p 4	115	0.12	0.22	32.4	31.4	17.6	0.17	16.0	0.22	98.0	39.4	70.2
X2 gr 5 p 5 med ph	116	0.12	0.20	35.7	27.1	17.3	0.17	16.5	0.17	97.2	33.8	71.6
X2 gr 5 p 6 med ph	117	0.10	0.18	36.0	26.9	17.4	0.17	16.5	0.21	97.6	33.4	71.6
X2 gr 5 p 7 rim	118	0.13	0.25	36.8	25.2	18.2	0.17	16.7	0.17	97.6	31.5	71.6
X2 gr 6 p 1	119	0.14	0.23	27.7	36.9	17.5	0.24	15.6	0.20	98.4	47.2	69.6
X2 gr 6 p 2	120	0.13	0.20	28.9	35.7	17.3	0.23	16.0	0.23	98.7	45.3	70.7
X2 gr 6 p 3	121	0.14	0.21	27.6	37.5	17.4	0.21	15.8	0.25	99.0	47.7	70.2
X2 gr 6 p 4	122	0.13	0.25	26.8	37.7	17.5	0.24	15.5	0.20	98.3	48.5	69.5
X2 gr 6 p 5 med ph	123	0.11	0.21	36.1	26.7	17.3	0.15	16.7	0.18	97.4	33.1	72.1
X2 gr 6 p 6 med ph	124	0.10	0.20	35.7	27.2	17.0	0.19	16.8	0.19	97.4	33.8	72.8
X2 gr 7 p 6 rim	131	0.14	0.26	31.1	30.4	19.2	0.21	15.3	0.18	96.8	39.6	68.1
X2 gr 7 p 1-5	av 126-130	0.13	0.25	25.2	39.0	18.3	0.25	14.7	0.20	98.0	51.0	67.0
	std	0.01	0.02	0.2	0.5	0.2	0.02	0.1	0.02			
X2 gr 8 p 6 rim	138	0.12	0.28	28.5	35.3	18.5	0.21	15.5	0.20	98.5	45.4	68.7
X2 gr 8 p 7 rim	139	0.23	0.30	31.9	29.9	19.2	0.20	15.3	0.20	97.2	38.7	67.5
X2 gr 8 p 1-5	av 133-137	0.11	0.26	28.7	35.3	18.2	0.20	15.5	0.20	98.5	45.2	68.9
	std	0.01	0.02	0.4	0.5	0.2	0.01	0.1	0.01			
X2 gr 9 p 6 rim	145	0.13	0.26	29.0	34.5	18.2	0.23	15.6	0.18	98.0	44.4	69.4
X2 gr 9 p 7 rim	146	0.11	0.24	28.1	35.1	18.3	0.26	15.5	0.17	97.8	45.6	69.4
X2 gr 9 p 1-5	av 140-144	0.10	0.27	28.6	35.2	17.9	0.22	15.6	0.19	98.1	45.2	69.6
	std	0.01	0.04	0.1	0.2	0.2	0.02	0.1	0.03			
X2 gr 10 p 6 rim	153	0.12	0.23	32.8	29.2	17.9	0.22	16.1	0.17	96.8	37.4	71.1
X2 gr 10 p 1-5	av 147-152	0.12	0.29	27.8	36.3	18.1	0.24	15.3	0.20	98.3	46.7	68.4
	std	0.01	0.02	0.5	0.5	0.2	0.02	0.2	0.01			
X-2 gr 1a p 2-5	av 261-264	0.09	0.21	38.0	24.3	17.0	0.18	17.5	0.21	97.5	30.0	74.9
	std	0.00	0.04	1.1	1.0	0.2	0.01	0.2	0.02			
X-2 gr 1b-5	269	0.15	0.24	28.4	35.6	18.0	0.25	15.7	0.23	98.5	45.7	69.7
X-2 gr 1b-6 corner	270	0.10	0.24	36.8	25.5	17.2	0.19	17.2	0.19	97.5	31.7	74.0
X-2 gr 1b p 1-4	av 265-268	0.12	0.27	25.3	39.4	17.9	0.25	15.2	0.21	98.7	51.1	68.6
	std	0.01	0.03	1.0	1.6	0.1	0.02	0.2	0.03			
X-2 gr 2-4	274	0.12	0.21	30.6	33.0	17.3	0.16	15.9	0.15	97.5	42.0	70.6
X-2 gr 2-5	275	0.09	0.22	36.2	27.2	17.4	0.18	16.8	0.14	98.1	33.5	72.2
X-2 gr 2 p 1-3	av 271-273	0.11	0.24	27.1	37.3	17.5	0.21	15.4	0.19	98.0	48.0	69.1
	std	0.02	0.00	0.7	0.6	0.2	0.01	0.3	0.03			

Table A-IV Composition of Cr-spinel from Dagmálafell (Continued).

Comment	No.	SiO_2	TiO_2	Al_2O_3	Cr_2O_3	FeO	MnO	MgO	NiO	Total	Cr#	Mg#
X-2 gr 3-4	279	0.09	0.22	26.2	38.0	17.5	0.20	15.1	0.17	97.6	49.3	68.5
X-2 gr 3-5	280	0.09	0.26	28.7	34.6	17.4	0.21	15.6	0.14	97.0	44.7	70.0
X-2 gr 3 p 1-3	av 276-278	0.10	0.22	24.0	41.5	17.2	0.25	14.7	0.16	98.0	53.8	67.2
	std	0.01	0.03	0.3	0.5	0.1	0.02	0.0	0.01			
X-2 gr 4-1	281	0.08	0.24	28.5	34.8	17.6	0.20	15.6	0.13	97.1	45.1	70.1
X-2 gr 4-2	282	0.09	0.21	29.1	35.4	18.0	0.23	15.7	0.19	98.9	45.0	69.4
X-2 gr 4-3	283	0.08	0.17	37.4	26.1	17.1	0.15	17.0	0.17	98.2	31.9	72.7
X-2 gr 4-4	284	0.11	0.23	37.1	26.0	17.1	0.16	17.3	0.18	98.1	32.0	73.8
X-2 gr 4-5	285	0.08	0.26	37.6	24.5	17.6	0.16	17.2	0.21	97.6	30.4	73.8
X-2 gr 5-4	289	0.10	0.24	25.8	39.6	16.8	0.25	15.5	0.22	98.5	50.7	70.0
X-2 gr 5-5	290	0.10	0.24	32.1	31.8	16.9	0.22	16.7	0.21	98.4	39.9	73.0
X-2 gr 5 p 1-3	av 286-288	0.10	0.24	24.8	40.4	16.8	0.22	15.4	0.17	98.1	52.2	69.8
	std	0.02	0.02	0.2	0.3	0.2	0.01	0.1	0.02			
X-2 gr 6-1	291	0.09	0.28	26.9	37.7	18.0	0.26	15.4	0.20	98.8	48.4	68.8
X-2 gr 6-2	292	0.10	0.27	27.5	37.5	17.9	0.24	15.6	0.16	99.3	47.8	69.3
X-2 gr 6-3	293	0.08	0.28	27.9	36.7	18.0	0.26	15.8	0.16	99.2	46.9	70.0
X-2 gr 6-4	294	0.10	0.26	28.6	36.1	18.1	0.21	15.9	0.15	99.3	45.8	70.0
X-2 gr 6-5	295	0.09	0.21	37.0	25.8	17.4	0.15	17.3	0.20	98.1	31.9	73.7
X-2 gr 7-2	296	0.10	0.24	27.4	37.6	17.4	0.22	15.6	0.19	98.8	47.9	69.5
X-2 gr 7-3	297	0.10	0.26	27.9	36.5	17.3	0.20	15.5	0.16	97.9	46.7	69.4
X-2 gr 7-4	298	0.09	0.23	29.5	34.8	17.2	0.19	16.2	0.20	98.4	44.2	71.7
X-2 gr 8-1	299	0.10	0.23	29.6	35.8	17.4	0.22	16.0	0.18	99.6	44.9	70.1
X-2 gr 8-2	300	0.12	0.23	29.5	34.7	17.4	0.21	15.9	0.17	98.1	44.1	70.4
X-2 gr 8-3	301	0.10	0.27	30.2	34.3	17.4	0.21	15.7	0.16	98.3	43.3	69.5
X-2 gr 8-4	302	0.13	0.20	33.3	30.1	17.3	0.19	16.6	0.15	98.0	37.8	72.1
X-2 gr 8-5	303	0.11	0.20	36.9	26.3	16.7	0.19	17.3	0.18	97.8	32.3	74.0
X-2 gr 9-4	307	0.13	0.21	30.1	33.5	16.5	0.22	16.3	0.23	97.2	42.7	72.4
	av 304-306	0.13	0.23	27.5	37.2	16.7	0.20	16.0	0.21	98.2	47.5	71.6
	std	0.01	0.01	0.4	0.2	0.1	0.02	0.1	0.02			
X-2 gr 10-1 up lft	308	0.12	0.18	32.2	31.8	16.7	0.17	16.1	0.17	97.4	39.9	71.0
X-2 gr 10-2	309	0.13	0.20	27.6	37.0	17.8	0.25	15.9	0.19	99.0	47.3	70.6
X-2 gr 10-3	310	0.15	0.20	32.9	30.7	17.1	0.17	16.6	0.23	97.9	38.5	72.3
X-2 gr 10-4	311	0.13	0.16	35.4	27.9	16.9	0.17	17.1	0.21	97.9	34.6	73.6
X-2 gr 10-6	312	0.09	0.18	37.5	26.1	16.8	0.18	17.4	0.21	98.5	31.9	73.9
X-2 gr 10-9 lo rgt	314	0.09	0.29	36.2	25.3	18.7	0.23	16.5	0.18	97.4	31.9	71.3

Table A-IV Composition of Cr-spinel from Dagmálafell (Continued).

Comment	No.	SiO_2	TiO_2	Al_2O_3	Cr_2O_3	FeO	MnO	MgO	NiO	Total	Cr#	Mg#
X-2 gr 11-1	315	0.09	0.21	33.7	30.6	17.0	0.21	16.8	0.20	98.9	37.9	72.7
X-2 gr 11-2	316	0.10	0.16	36.2	26.7	17.0	0.21	16.7	0.18	97.3	33.1	72.5
X-2 gr 11-3	317	0.10	0.21	38.6	24.0	16.5	0.21	17.2	0.18	97.1	29.4	73.7
X-2 gr 11-4	318	0.10	0.20	36.7	25.5	17.0	0.21	16.9	0.20	96.8	31.8	73.3
X-2 gr 11-5	319	0.10	0.26	37.2	23.4	18.7	0.20	16.2	0.19	96.2	29.7	70.6
X-2 gr 12-1	320	0.08	0.20	36.1	27.0	17.1	0.20	17.2	0.21	98.1	33.4	74.1
X-2 gr 12-2	321	0.08	0.22	35.7	27.5	16.9	0.19	17.2	0.18	98.0	34.0	74.1
X-2 gr 12-3	322	0.10	0.23	37.7	24.0	17.8	0.19	17.2	0.18	97.3	29.9	73.6
X-2 gr 12-4	323	0.11	0.30	34.6	26.2	18.7	0.19	16.3	0.20	96.6	33.7	71.3
X-2 gr 13-1	324	0.09	0.25	27.4	37.6	17.4	0.24	15.8	0.23	99.0	47.9	70.5
X-2 gr 13-2	325	0.11	0.24	27.6	37.5	17.6	0.22	15.9	0.23	99.3	47.7	70.5
X-2 gr 13-3	326	0.12	0.22	28.9	35.6	17.7	0.25	15.9	0.20	98.9	45.3	70.4
X-2 gr 13-4	327	0.12	0.20	32.9	30.7	17.4	0.21	16.5	0.18	98.3	38.5	71.9
X-2 gr 13-5	328	0.10	0.19	36.7	26.9	16.9	0.18	17.4	0.22	98.6	32.9	74.2
X-2 gr 13-6	329	0.12	0.25	39.3	22.9	16.9	0.18	17.9	0.18	97.8	28.1	75.6
X-2 gr 14-1	330	0.12	0.23	35.0	28.9	17.2	0.20	17.1	0.18	99.0	35.6	73.3
X-2 gr 14-2	331	0.10	0.25	33.8	29.2	17.3	0.21	16.9	0.20	97.9	36.7	73.3
X-2 gr 14-3	332	0.07	0.27	33.7	28.8	17.5	0.19	16.4	0.20	97.1	36.5	71.7
X-2 gr 14-4	333	0.08	0.27	38.9	22.5	17.2	0.16	17.3	0.21	96.6	28.0	74.2
X-2 gr 15-1	334	0.11	0.21	28.1	35.2	17.6	0.23	15.5	0.22	97.2	45.6	70.1
X-2 gr 15-2	335	0.12	0.23	32.1	31.5	17.2	0.18	16.1	0.22	97.7	39.7	70.8
X-2 gr 15-3	336	0.10	0.24	34.4	28.4	17.0	0.19	16.3	0.23	96.9	35.6	71.5
X-2 gr 15-4	337	0.07	0.20	36.7	26.0	16.7	0.18	17.2	0.23	97.3	32.2	74.3
X-2 gr 15-5	338	0.06	0.25	38.9	22.9	17.5	0.17	17.1	0.20	97.0	28.3	73.1
X-2 gr 16-1	339	0.05	0.31	29.2	33.6	17.8	0.21	15.4	0.23	96.9	43.6	69.5
X-2 gr 16-2	340	0.06	0.27	28.0	34.3	17.8	0.23	15.3	0.18	96.2	45.2	69.6
X-2 gr 16-3	341	0.09	0.21	36.5	25.7	16.8	0.17	16.5	0.19	96.1	32.1	72.2
X-2 gr 16-4	342	0.10	0.21	39.5	22.8	17.4	0.16	17.7	0.20	98.2	27.9	74.8
X-2 gr 17-3	345	0.11	0.23	34.9	28.5	17.6	0.19	16.9	0.23	98.6	35.4	72.6
X-2 gr 17-4	346	0.13	0.21	39.5	23.0	17.6	0.21	17.6	0.28	98.5	28.1	74.3
	av 343-344	0.11	0.24	30.9	33.0	17.8	0.24	16.4	0.23	98.9	41.7	71.6
	std	0.02	0.06	0.1	0.4	0.1	0.00	0.1	0.00			

Table A-IV Composition of Cr-spinel from Dagmálafell (Continued).

Comment	No.	SiO_2	TiO_2	Al_2O_3	Cr_2O_3	FeO	MnO	MgO	NiO	Total	Cr#	Mg#
X-2 gr 18-1	347	0.13	0.20	29.1	35.0	17.7	0.26	15.9	0.21	98.6	44.6	70.6
X-2 gr 18-2	348	0.12	0.24	29.6	34.6	17.9	0.22	16.2	0.23	99.1	43.9	71.3
X-2 gr 18-3	349	0.14	0.24	31.1	32.0	17.7	0.22	16.3	0.26	97.9	40.8	71.7
X-2 gr 18-4	350	0.13	0.29	33.4	29.1	18.0	0.22	16.7	0.26	98.0	36.8	72.5
X-2 gr 19-1	351	0.10	0.23	32.6	30.9	17.6	0.23	16.5	0.25	98.5	38.8	71.9
X-2 gr 19-2	352	0.05	0.23	36.6	27.0	16.8	0.17	17.2	0.26	98.3	33.1	73.7
X-2 gr 19-3	353	0.07	0.27	38.8	24.3	16.3	0.15	17.8	0.22	97.9	29.6	75.4
X-2 gr 19-4	354	0.07	0.21	39.6	23.3	16.2	0.16	17.9	0.26	97.6	28.3	75.9
X-2 gr 20-1 lo lft	355	0.09	0.27	38.1	24.1	16.2	0.14	17.6	0.23	96.8	29.8	75.5
X-2 gr 20-2	356	0.09	0.22	37.0	26.5	16.4	0.18	17.1	0.24	97.6	32.4	73.4
X-2 gr 20-3	357	0.07	0.26	33.4	30.6	16.6	0.18	16.9	0.26	98.3	38.1	73.3
X-2 gr 20-4 up rgt	358	0.15	0.24	37.1	25.3	17.2	0.19	16.8	0.24	97.2	31.4	72.6
X-2 gr 21-1	359	0.07	0.27	37.7	25.0	16.5	0.17	17.5	0.25	97.4	30.8	74.9
X-2 gr 21-2	360	0.09	0.26	34.9	28.3	16.6	0.17	17.1	0.22	97.7	35.2	73.9
X-2 gr 21-3	361	0.09	0.24	38.9	23.1	16.4	0.17	17.5	0.24	96.6	28.5	74.9
X-2 gr 21-4	362	0.10	0.27	38.8	23.2	16.8	0.17	17.1	0.22	96.7	28.6	73.5
X-2 gr 22-1	363	0.10	0.24	35.4	27.6	17.8	0.20	15.7	0.21	97.2	34.4	68.7
X-2 gr 22-2	364	0.09	0.27	36.0	26.6	17.8	0.22	16.3	0.23	97.6	33.1	70.8
X-2 gr 22-3	365	0.08	0.27	33.7	29.4	17.8	0.18	16.1	0.23	97.7	36.9	70.5
X4 crl 1 gr 1-1	402	0.08	0.42	24.8	39.1	20.3	0.23	15.3	0.15	100.3	51.4	67.7
X4 crl 1 gr 1-2	403	0.08	0.40	24.6	39.4	20.8	0.21	15.3	0.11	100.8	51.8	67.4
X4 crl 1 gr 1-3	404	0.06	0.45	25.0	39.2	20.2	0.21	15.4	0.16	100.6	51.3	67.9
X4 crl 1 gr 1-4	405	0.10	0.24	36.3	27.9	17.4	0.18	17.2	0.15	99.5	34.1	72.7
X4 crl 1 gr 1-5	406	0.11	0.29	36.9	26.7	17.8	0.18	17.5	0.18	99.6	32.6	73.5
X4 crl 1 gr 2-1	407	0.10	0.25	29.3	36.3	17.6	0.21	16.2	0.18	100.1	45.4	70.7
X4 crl 1 gr 2-2	408	0.12	0.24	27.6	38.3	17.9	0.23	15.9	0.19	100.4	48.3	69.6
X4 crl 1 gr 2-3	409	0.11	0.29	27.1	38.8	17.8	0.23	15.8	0.18	100.3	49.0	69.7
X4 crl 1 gr 2-4	410	0.10	0.33	34.4	30.9	18.1	0.22	16.8	0.18	101.0	37.6	70.9
X4 crl 1 gr 2-6	412	0.11	0.25	33.5	31.7	17.5	0.22	16.5	0.20	99.9	38.8	70.9
X4 crl 1 gr 3-1	413	0.11	0.27	26.0	40.6	18.2	0.27	15.3	0.19	101.0	51.1	67.5
X4 crl 1 gr 3-2	414	0.14	0.27	26.1	41.0	17.9	0.25	15.2	0.20	101.1	51.3	67.0
X4 crl 1 gr 3-3	415	0.11	0.27	26.2	40.0	18.1	0.27	15.3	0.19	100.5	50.6	67.9
X4 crl 1 gr 3-4	416	0.12	0.26	34.0	30.8	17.4	0.21	16.6	0.20	99.5	37.8	71.2
X4 crl 1 gr 3-5	417	0.08	0.23	39.8	25.0	17.0	0.18	18.0	0.21	100.4	29.7	74.3

Table A-IV Composition of Cr-spinel from Dagmálafell (Continued).

Comment	No.	SiO_2	TiO_2	Al_2O_3	Cr_2O_3	FeO	MnO	MgO	NiO	Total	Cr#	Mg#
X4 crl 1 gr 4-5	422	0.13	0.22	38.8	25.1	17.4	0.19	16.9	0.25	99.1	30.3	71.5
X4 crl 1 gr 4 p 1-4	av 418-421	0.10	0.24	34.9	30.3	17.4	0.20	16.8	0.21	100.1	36.8	71.5
	std	0.02	0.01	0.3	0.5	0.1	0.02	0.2	0.02			
X4 crl 1 gr 5-4	426	0.12	0.23	34.5	29.5	17.6	0.23	15.9	0.21	98.3	36.5	69.2
X4 crl 1 gr 5-5	427	0.12	0.22	36.5	27.3	17.5	0.22	16.3	0.23	98.3	33.4	70.1
X4 crl 1 gr 5 p 1-3	av 423-425	0.14	0.24	29.8	35.5	18.2	0.24	15.2	0.23	99.6	44.4	66.9
	std	0.01	0.01	0.3	0.4	0.0	0.01	0.1	0.01			
X4 crl 3 gr 1 p 1-4	av 428-431	0.13	0.29	28.0	38.0	16.5	0.26	16.1	0.27	99.5	47.7	71.0
	std	0.01	0.03	0.1	0.1	0.2	0.02	0.1	0.02			
X4 crl 3 gr 2 p 1-4	av 432-435	0.12	0.26	27.3	39.3	17.0	0.23	16.6	0.22	101.1	49.2	72.4
	std	0.01	0.01	0.3	0.1	0.2	0.01	0.1	0.02			
X4 crl 3 gr 3 p 1-4	av 436-439	0.11	0.22	27.1	39.4	15.9	0.21	16.7	0.21	99.9	49.4	74.0
	std	0.01	0.02	0.4	0.8	0.2	0.00	0.3	0.03			
X4 crl 3 gr 4 p 1-4	av 440-443	0.11	0.23	27.2	39.6	16.3	0.22	16.5	0.21	100.4	49.3	72.4
	std	0.03	0.02	0.4	0.5	0.2	0.01	0.1	0.03			
X4 crl 3 gr 5 p1-4	av 444-447	0.13	0.27	27.2	39.0	16.1	0.23	16.3	0.20	99.5	49.0	72.0
	std	0.00	0.02	0.1	0.3	0.2	0.01	0.2	0.02			
X10 crl 1 gr 1-4	451	0.10	0.24	31.4	34.3	17.8	0.19	16.2	0.15	100.3	42.3	70.0
X10 crl 1 gr 1-5	452	0.09	0.19	36.4	27.4	17.4	0.16	16.9	0.18	98.7	33.5	72.1
X10 crl 1 gr 1 p 1-3	av 448-450	0.10	0.28	28.1	38.2	18.0	0.23	15.7	0.14	100.7	47.7	68.5
	std	0.01	0.04	0.1	0.3	0.2	0.01	0.0	0.01			
X10 crl 1 gr 2-4	456	0.11	0.22	34.0	31.5	17.5	0.20	16.7	0.14	100.4	38.3	70.9
X10 crl 1 gr 2-7	459	0.03	0.19	33.3	32.0	17.6	0.14	16.6	0.09	100.0	39.2	71.3
X10 crl 1 gr 2 p1-3	av 453-455	0.09	0.30	28.0	38.4	18.0	0.22	15.6	0.17	100.7	47.9	68.1
	std	0.01	0.02	0.1	0.1	0.1	0.02	0.1	0.02			
X10 crl 1 gr 3-4	463	0.07	0.17	35.8	29.7	17.3	0.19	17.0	0.08	100.2	35.7	72.0
X10 crl 1 gr 3-5	464	0.06	0.14	35.7	27.8	17.5	0.18	16.7	0.08	98.2	34.3	71.9
X10 crl 1 gr 3 p 1-2	av 460-462	0.06	0.25	33.3	32.4	17.4	0.18	16.4	0.08	100.1	39.5	70.4
	std	0.00	0.02	0.2	0.5	0.0	0.00	0.0	0.01			
X10 crl 1 gr 5-4	471	0.18	0.28	39.3	24.5	18.6	0.17	16.4	0.18	99.7	29.5	68.9
X10 crl 1 gr 5-5	472	0.13	0.25	35.4	29.9	17.7	0.16	16.4	0.19	100.0	36.1	69.7
X10 crl 1 gr 5 p 1-2	av 469-470	0.09	0.29	28.9	37.5	18.2	0.21	15.3	0.15	100.7	46.5	66.7
	std	0.01	0.01	0.4	0.0	0.2	0.01	0.1	0.00			

Table A-IV Composition of Cr-spinel from Dagmálafell (Continued).

Com .ent	No.	SiO_2	TiO_2	Al_2O_3	Cr_2O_3	FeO	MnO	MgO	NiO	Total	Cr#	Mg#
X10 crl 1 gr 6-3	475	0.10	0.23	31.2	34.2	18.2	0.20	15.8	0.14	100.2	42.3	68.6
X10 crl 1 gr 6-4	476	0.10	0.30	31.5	33.2	18.4	0.19	15.7	0.19	99.5	41.4	68.2
X10 crl 1 gr 6 p 1-2	av 473-474	0.09	0.27	29.0	37.1	18.2	0.20	15.4	0.16	100.4	46.1	67.2
	std	0.01	0.00	0.1	0.0	0.2	0.01	0.5	0.02			
X10 crl 1 gr 7 p 1-3	av 477-479	0.12	0.27	30.3	35.0	18.5	0.19	15.9	0.18	100.5	43.6	69.0
	std	0.00	0.05	0.2	0.2	0.2	0.01	0.2	0.02			
X10 crl 1 gr 8 p 1-4	av 480-483	0.11	0.24	30.2	35.3	18.1	0.19	16.1	0.18	100.5	44.0	69.8
	std	0.01	0.03	0.4	0.8	0.3	0.02	0.1	0.02			
X10 crl 1 gr 9 p 1-4	av 484-487	0.11	0.23	30.5	35.2	18.2	0.21	15.9	0.21	100.6	43.7	69.1
	std	0.02	0.01	0.5	0.7	0.2	0.03	0.2	0.03			
X10 crl 1 gr 10 p 1-5	av 488-492	0.10	0.26	30.7	35.4	18.0	0.19	16.0	0.14	100.8	43.7	69.0
	std	0.01	0.02	0.5	0.8	0.1	0.03	0.2	0.02			

Table A-V Composition of Cr-spinel from Dagmálafell micronodules and inclusions in Diopside.

Comment	No.	SiO_2	TiO_2	Al_2O_3	Cr_2O_3	FeO	MnO	MgO	NiO	Total	Cr#	Mg#
X-6 gr 1 p 1-5	av 155-159	0.09	0.46	28.1	32.7	20.9	0.21	15.4	0.14	97.9	43.9	68.4
	std	0.02	0.03	0.2	0.3	0.3	0.03	0.1	0.01			
X-6 gr 2 p 1-5	av 160-164	0.07	0.50	28.2	33.1	21.0	0.21	15.3	0.15	98.4	44.0	67.7
	std	0.01	0.03	0.1	0.3	0.3	0.01	0.2	0.02			
X-6 gr 3 p 1-5	av 165-169	0.08	0.50	27.5	32.8	20.9	0.23	15.4	0.16	97.6	44.4	68.8
	std	0.03	0.03	0.4	0.3	0.1	0.01	0.2	0.02			
X-6 gr 4 p 1-5	av 170-174	0.08	0.51	27.5	32.9	20.6	0.22	15.5	0.15	97.5	44.5	69.4
	std	0.02	0.01	0.2	0.4	0.2	0.01	0.1	0.02			
X-6 gr 5 p 1-5	av 175-179	0.08	0.42	29.4	32.3	20.2	0.22	15.2	0.17	98.0	42.4	67.3
	std	0.01	0.04	0.2	0.4	0.7	0.01	0.4	0.02			
X-6 gr 6 p 1-5	av 180-184	0.08	0.28	29.3	33.6	18.7	0.22	15.4	0.15	97.6	43.5	68.8
	std	0.02	0.08	1.4	1.5	0.7	0.03	0.7	0.02			
X-6 gr 7 p 1-5	av 185-189	0.08	0.25	32.3	31.2	17.0	0.18	16.8	0.17	98.0	39.3	73.4
	std	0.01	0.03	1.3	1.5	0.2	0.01	0.3	0.03			
X-6 gr 8 p 5	194	0.56	0.71	29.8	27.9	26.1	0.25	13.1	0.18	98.6	38.6	57.3
X-6 gr 8 p 1-4	av 190-193	0.12	0.27	32.0	30.3	18.9	0.21	15.7	0.19	97.6	38.8	69.0
	std	0.02	0.03	0.1	0.2	0.7	0.01	0.5	0.03			
X-6 gr 9 p 4	198	0.09	0.25	32.9	29.2	19.2	0.19	15.6	0.18	97.7	37.3	68.8
X-6 gr 9 p 5	199	0.12	0.28	33.5	28.9	19.0	0.25	16.1	0.18	98.4	36.7	70.2
X-6 gr 9 p 1-3	av 195-197	0.07	0.32	31.4	31.8	17.4	0.20	16.8	0.17	98.1	40.5	73.3
	std	0.01	0.02	0.2	0.4	0.3	0.00	0.2	0.02			
X-6 gr 10 p 1-5	av 200-204	0.10	0.47	29.0	32.6	19.1	0.22	16.1	0.18	97.7	43.0	71.2
	std	0.01	0.03	0.2	0.4	0.3	0.02	0.3	0.02			
X-6 gr 11 p 1-5	av 205-209	0.09	0.48	27.6	32.0	22.1	0.23	14.9	0.17	97.5	43.7	66.8
	std	0.01	0.02	0.2	0.4	0.1	0.01	0.2	0.01			
X-6 crl 1 gr 1 p 1-4	av 212-215	0.09	0.43	27.7	33.3	20.8	0.22	15.2	0.15	97.9	44.7	67.9
	std	0.02	0.03	0.4	0.3	0.1	0.02	0.2	0.01			
X-6 crl 1 gr 2 p 1-4	av 216-219	0.09	0.37	29.0	33.3	19.3	0.19	15.7	0.16	98.1	43.6	69.6
	std	0.01	0.04	0.3	0.2	0.6	0.01	0.3	0.01			
X-6 crl 1 gr 3 p 1-4	av 220-223	0.08	0.45	28.8	33.4	20.1	0.22	14.5	0.15	97.7	43.7	64.9
	std	0.01	0.05	0.2	0.2	0.2	0.02	0.6	0.03			

Table A-V Composition of Cr-spinel from Dagmálafell micronodules and inclusions in Diopside (Continued).

Comment	No.	SiO_2	TiO_2	Al_2O_3	Cr_2O_3	FeO	MnO	MgO	NiO	Total	Cr#	Mg#
X-6 crl 1 gr 4 p 1-4	av 224-227	0.07	0.48	28.6	33.0	20.0	0.23	14.2	0.17	96.8	43.6	64.4
	std	0.01	0.03	0.1	0.2	0.2	0.01	0.2	0.01			
X-6 crl 1 gr 5 p 1-4	av 228-231	0.07	0.41	29.1	33.5	18.9	0.23	14.8	0.17	97.2	43.6	66.3
	std	0.01	0.03	0.2	0.3	0.1	0.00	0.4	0.02			
X-6 crl 1 gr 6 p 1-4	av 232-235	0.08	0.44	28.1	33.3	20.0	0.23	15.7	0.14	98.0	44.3	69.7
	std	0.01	0.05	0.4	0.3	0.5	0.02	0.2	0.03			
X-6 crl 1 gr 7 p 1-4	av 236-239	0.08	0.38	28.9	33.4	18.9	0.20	16.0	0.17	98.0	43.6	71.0
	std	0.01	0.01	0.2	0.2	0.1	0.02	0.2	0.02			
X-6 crl 1 gr 8 p 1-4	av 240-243	0.06	0.38	29.1	33.6	18.4	0.23	16.2	0.16	98.1	43.7	71.6
	std	0.02	0.05	0.4	0.1	0.2	0.00	0.1	0.01			
X-6 crl 1 gr 9 p 1-4	av 244-247	0.06	0.45	28.0	33.6	19.7	0.23	15.7	0.16	97.9	44.6	69.9
	std	0.02	0.02	0.2	0.2	0.2	0.02	0.2	0.02			
X-6 crl 1 gr 10 p 1-4	av 248-251	0.07	0.51	24.1	37.5	20.9	0.26	14.6	0.17	98.0	51.1	66.2
	std	0.01	0.02	0.1	0.3	0.1	0.02	0.1	0.03			
X-6 crl 1 gr 11 p 1-4	av 252-255	0.08	0.49	23.0	38.7	20.4	0.25	14.5	0.11	97.5	53.0	66.5
	std	0.02	0.01	0.3	0.1	0.0	0.03	0.1	0.01			
X3 crl 1 gr 2-1	375	0.07	0.16	35.1	31.3	16.9	0.22	16.4	0.24	100.4	37.4	70.2
X3 crl 1 gr 2-2	376	0.06	0.18	34.3	31.6	16.9	0.19	16.6	0.19	100.0	38.2	71.3
X3 crl 1 gr 2-3	377	0.06	0.15	34.8	31.5	16.8	0.18	16.5	0.20	100.1	37.8	70.4
X3 crl 1 gr 2-4	378	0.07	0.17	35.4	30.5	16.5	0.19	17.1	0.15	100.1	36.6	72.7
X3 crl 1 gr 2-5	379	0.07	0.18	29.6	36.7	16.2	0.22	16.4	0.22	99.5	45.4	71.9
X3 crl 1 gr 2-6	380	0.08	0.25	36.0	29.7	16.8	0.18	17.6	0.18	100.8	35.6	73.8
X3 crl 1 gr 2-7	381	0.08	0.25	29.8	36.5	16.7	0.19	16.6	0.20	100.2	45.1	72.1
X3 crl 1 gr 3 p 1-4	av 382-385	0.07	0.26	26.6	40.6	17.5	0.23	16.1	0.18	101.5	50.6	70.1
	std	0.01	0.02	0.4	0.7	0.8	0.02	0.7	0.03			
X3 crl 2 gr 1 p 1-5	av 387-391	0.07	0.36	25.0	40.9	18.6	0.22	15.3	0.16	100.6	52.3	67.7
	std	0.02	0.09	0.4	1.5	2.8	0.02	1.7	0.03			
X3 crl 2 gr 2 p 1-5	av 392-396	0.09	0.41	30.5	31.7	22.1	0.21	15.1	0.16	100.2	41.1	65.7
	std	0.01	0.02	0.3	0.3	0.2	0.01	0.2	0.02			
X3 crl 2 gr 3 p 1-5	av 397-401	0.08	0.47	25.5	40.4	18.3	0.24	16.0	0.15	101.2	51.5	69.9
	std	0.01	0.05	0.4	0.8	0.8	0.02	0.3	0.02			